CANADA

DEPARTMENT OF
ENERGY, MINES AND RESOURCES
MINES BRANCH
OTTAWA

CRYSTAL GROWTH PART III: THE SULPHIDES OF COBALT, IRON, AND NICKEL

LEONARD G. RIPLEY

MINERAL SCIENCES DIVISION

JANUARY, 1972

Research Report R 237

Price $1.25

Available by mail from Information Canada, Ottawa,
and at the following Information Canada bookshops:

HALIFAX
1735 Barrington Street

MONTREAL
1182 St. Catherine Street West

OTTAWA
171 Slater Street

TORONTO
221 Yonge Street

WINNIPEG
393 Portage Avenue

VANCOUVER
657 Granville Street

or through your bookseller

Price: $1.25 Catalogue No. M38-1/237

Price subject to change without notice

Information Canada
Ottawa, 1972

Mines Branch Research Report R237

CRYSTAL GROWTH
PART III:
THE SULPHIDES OF COBALT, IRON, AND NICKEL

by

Leonard G. Ripley

ABSTRACT

This report deals with an applied research project to explore the various methods of preparing and growing single crystals of twenty-two different sulphides of cobalt, iron, and nickel.

Five growth procedures have been utilized. They are: chemical vapour transport, vapour transport, flux growth, hydrothermal growth, and a modified "melt-and-anneal" method.

The main conclusions are that:

(i) the melt-and-anneal method is ideal for the high-temperature form of nickel monosulphide (α-NiS), and for pentlandite ($Fe_{0.5}Ni_{0.5})_9S_8$;

(ii) the iodine vapour transport is a good method for preparing monoclinic pyrrhotite ($Fe_{1-x}S$), cattierite (CoS_2), pyrite (FeS_2), and vaesite (NiS_2);

(iii) the hydrothermal growth procedure will produce marcasite (FeS_2), greigite (Fe_3S_4), and bravoite ($Fe_{0.5}Ni_{0.5})S_2$;

(iv) the flux growth, using $PbCl_2$ as the flux, has produced cattierite (CoS_2), pyrite (FeS_2), and vaesite (NiS_2), but the crystals contained approximately 1% Pb as inclusions of $PbCl_2$; all attempts to eliminate this problem have been unsuccessful.

---

*Research Scientist, Physical Chemistry Group, Mineral Sciences Division, Mines Branch, Department of Energy, Mines and Resources, Ottawa, Canada.

Sulphide Research Contribution No. 47.

Direction des mines
Rapport de recherches R237

LA CROISSANCE DES CRISTAUX
III^{e} PARTIE:
LES SULFURES DE COBALT, DE FER ET DE NICKEL

par

Leonard G. Ripley*

RÉSUMÉ

Ce rapport traite d'un projet de recherche appliquée pour étudier les différentes méthodes de préparation et de croissance des monocristaux de vingt-deux différents sulfures de cobalt, de fer et de nickel.

On a utilisé cinq procédés de croissance: le transport chimique en phase vapeur, le transport en phase vapeur, la croissance par la méthode des fondants, la croissance hydrothermique et une méthode modifiée de "fondre-et-recuire".

Les principales conclusions sont les suivantes:

(i) la méthode "fondre-et-recuire" est idéale pour la forme du monosulfure de nickel (α-NiS) à haute température et pour la pentlandite $(Fe_{0.5}Ni_{0.5})_9S_8$;

(ii) le transport en phase vapeur de l'iode est une bonne méthode pour préparer la pyrrhotite monoclinique ($Fe_{1-x}S$), la cattiérite (CoS_2), la pyrite (FeS_2) et la vaesite (NiS_2);

(iii) le procédé de croissance hydrothermique produira la marcassite (FeS_2), la greigite (Fe_3S_4) et la bravoite $(Fe_{0.5}Ni_{0.5})S_2$;

(iv) la croissance par la méthode des fondants, utilisant $PbCl_2$ comme fondant, a produit la cattiérite (CoS_2), la pyrite (FeS_2) et la vaesite (NiS_2) mais les cristaux contenaient à peu près 1% de Pb en tant qu'inclusions de $PbCl_2$; tous les essais pour éliminer ce problème n'ont pas réussi.

---

*Chercheur scientifique, Groupe de la chimie physique, Division des sciences minérales, Direction des mines, ministère de l'Énergie, des Mines et des Ressources, Ottawa, Canada.

Contribution de recherches sur les sulfures No. 47.

CONTENTS

LIST OF FIGURES

List of Figures Continued - Pages

LIST OF TABLES

List of Tables Continued - Pages

List of Tables Continued - Pages

List of Tables Continued - Pages

List of Tables Continued - Pages

INTRODUCTION

The work of the present author in the crystal-growth aspects of the Mineral Sciences Division Sulphide Research Programme is being described in an intended five-part series of Research Reports.

Part I (R235) is "Background to Crystal Growth" (1), and includes a review of the experimental techniques available and the various growth procedures actually used in this programme.

Part II (R236) is a comprehensive report on the growth of zinc sulphide crystals and is entitled "The Growth of Zinc Sulphide Crystals" (2).

This present report is Part III, and will deal with "The Sulphides of Cobalt, Iron, and Nickel". This subject relates to the second main class of compounds included in the scope of the crystal-growing programme.

This group of sulphides has attracted considerable attention. The main interest has been for identification and characterization purposes; for the study of their chemical, mineralogical, and physical properties; and, more recently, for the examination of their electrical properties.

The preparation of these sulphides has been accomplished by the use of several methods. A direct combination of the elements concerned, if heated under the right conditions, will often produce the desired product. However, this procedure usually yields a cluster of very small single crystals. If a large single crystal is required for some specific study, then a special growth procedure is necessary. Both the direct-combination approach and any crystal-growing technique are dependant on the thermal stability of the desired sulphide.

Twenty-two sulphide species are included within the scope of this study. Each is listed in Table 1, along with its formula, mineral name, and crystal system. The mineral name, Godlevskite, has recently been approved (3).

TABLE 1

Nomenclature of the Sulphides Included in This Study

Type of Sulphide	Formula	Mineral Name	Crystal System
Monosulphides (a)	$Co_{1-x}S$	Jaipurite	Hexagonal
	FeS	Mackinawite (b)	Tetragonal
	FeS	Troilite (b)	Hexagonal
	$Fe_{1-x}S$	Pyrrhotite (b)	Monoclinic and Hexagonal
	α-$Ni_{1-x}S$	High-temperature Millerite (b)	Hexagonal
	β-$Ni_{1-x}S$	Millerite (b)	Hexagonal
	α-Ni_7S_6	High-temperature Godlevskite (b)	-
	β-Ni_7S_6	Godlevskite (b)	-
	$(Ni, Fe)_{1-x}S$	Ferrous α-NiS (b)	Hexagonal
	$(Fe, Ni)_9S_8$	Pentlandite (b)	Cubic
	Co_9S_8	Cobaltian-Pentlandite	Cubic
Intermediate-Sulphides	Fe_3S_4	Greigite (b)	Cubic
	Fe_3S_4	Smythite (b)	Rhombohedral
	Co_3S_4	Linnaeite	Cubic
	Ni_3S_4	Polydymite	Cubic
	$FeNi_2S_4$	Violarite (b)	Cubic
Disulphides	CoS_2	Cattierite (b)	Cubic
	NiS_2	Vaesite (b)	Cubic
	FeS_2	Pyrite (b)	Cubic
	FeS_2	Marcasite (b)	Orthorhombic
	$(Co, Fe)S_2$	Cobaltian-bravoite (b)	Cubic
	$(Ni, Fe)S_2$	Nickelian-bravoite (b)	Cubic

(a) This general term will be used to describe compounds with the composition $MS_{(1\pm x)}$, where x is < 0.20.

(b) These species were requested for various research projects within the Mineral Sciences Division Sulphide Research Programme.

The need for single crystals of many of these sulphides arose from the desire to study some of their physical properties. One of the stipulated requirements, imposed by the potential users of the crystals, was that the crystals should be at least a cubic centimetre in size in order that they could be cut so as to be suitable for specific physical measurements. However, many useful measurements have been obtained, in spite of the fact that the largest crystals grown (in the present study) were only a few millimetres in size, and those in only a few cases.

Chemical and physical analysis of the products have played a vital role in this study, as was the case with ZnS (2), and are reported in context. The analyses were performed in the laboratories of the Mineral Sciences Division, Mines Branch, as detailed in Table 2.

The analytical results in some instances have differed from the anticipated phase-structures and also from the calculated formula obtained by the ratio of metal to sulphur determined gravimetrically. In those cases in which single crystals were analysed, no unpredicted results occurred. However, when the sample was a mixture of two or more compounds, segregation could have occurred making a random selection of an analytical sample unrepresentative of the whole product. This latter condition was often caused through disproportionation when some products were being cooled to room temperature.

Many of the techniques and growth procedures described previously (1, 2) were applied in this present study.

STABILITY OF COBALT, IRON, AND NICKEL SULPHIDES

The temperature-composition equilibrium diagrams for the cobalt-sulphur, iron-sulphur, nickel-sulphur, iron-nickel-sulphur, and iron-cobalt-sulphur systems have been studied by a number of investigators, among whom are: Rosenqvist (4), Hansen and Anderko (5), Clark and Kullerud (6), Elliott (7), Klemm (8, 9) Naldrett, Craig and Kullerud (10), Uda (11),

TABLE 2

Methods of Analysis of Cobalt, Iron, and Nickel Sulphides and the Analysts of the Mineral Sciences Division Involved

Method of Analysis	Analyst
Atomic-Absorption Spectrophotometric	The present author.
Chemical	Miss E. Mark The present author.
Differential Thermal	Mr. R.H. Lake
Electrical Resistance Measurements	Dr. G. Springer* Mr. T.M. Baleshta
Electron Microprobe	Dr. D.C. Harris Mr. D.R. Owens
Hardness Measurements and Bond Energies	Dr. E.H. Nickel
Infra-red Absorption Spectra	Dr. A.H. Gillieson Mr. D.M. Farrell
Neutron-Activation	Mr. C. McMahon
Semi-Quantitative Spectrochemical	Mr. D.P. Palombo
Thermoelectric Power	Dr. M. Townsend Mr. J.R. Tremblay
X-Ray Diffraction (Powder)	Mr. E.J. Murray
X-Ray Fluorescence	Mrs. D.J. Reed
X-Ray Precession Camera	Mr. J.F. Rowland

The above-mentioned personnel were all members of the staff of the Mineral Sciences Division, Mines Branch, Department of Energy, Mines and Resources, at the time of their involvement with this project.

*Former N.R.C. Postdoctorate Fellow, assigned to the Mines Branch.

Taylor (12), Shewman and Clark (13), Kullerud and Yund (14), Kuznetsov, Sokolova, Palkina, and Popova (15), and others.

One of the main objectives of the above studies was to determine the fields of thermal stability of the related compounds. However, the term stability has several connotations; it may refer to;

(i) Melting point.

(ii) Crystal phase changes, i.e., transition temperatures.

(iii) Equilibrium temperature - The temperature at which the partial pressure of one component is equal to one atmosphere; in the present cases, the sulphur partial pressure.

(iv) Disproportionation - Some compounds are stable at a certain range of temperature and will disproportionate into two other compounds if the temperature is raised or lowered from the stable range.

(v) Metastability - Some compounds can be formed in a state where the free energy exceeds that required for its most stable state; when this condition persists indefinitely, a metastable state exists.

For convenience, the presentation of the relevant phase-equilibrium data is divided into two parts: the two-component systems, and the three-component systems.

(a) Two-Component Sulphide Systems

There have been several phase-equilibrium diagrams published by the above-mentioned investigators, (4) to (15). Representative diagrams of the cobalt-sulphur, iron-sulphur, and nickel-sulphur systems are shown in Figures 1, 2, and 3, respectively. The source of these diagrams is also given. A study of these diagrams reveals some similarities and several differences.

It is seen that, whereas iron was shown to form only a monosulphide and a disulphide, cobalt and nickel form both of these, as well as a M_3S_4 compound and several other compounds that contain less sulphur than the monosulphide. In general, the stability of the different sulphides decreases in the sequence iron-cobalt-nickel, and the composition of the most stable sulphide shifts toward the lower sulphur contents.

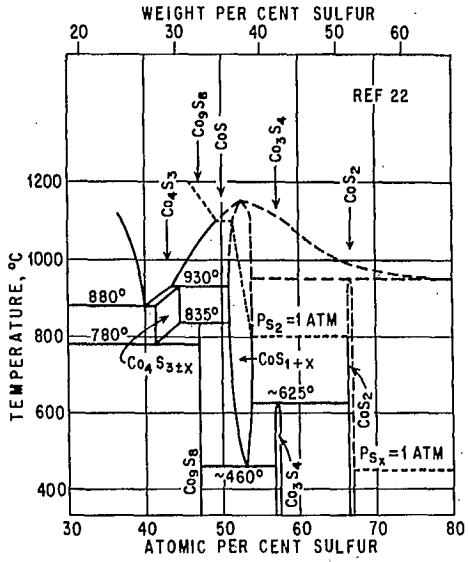

Figure 1. - The Cobalt-Sulphur System According to Hansen and Anderko (5).

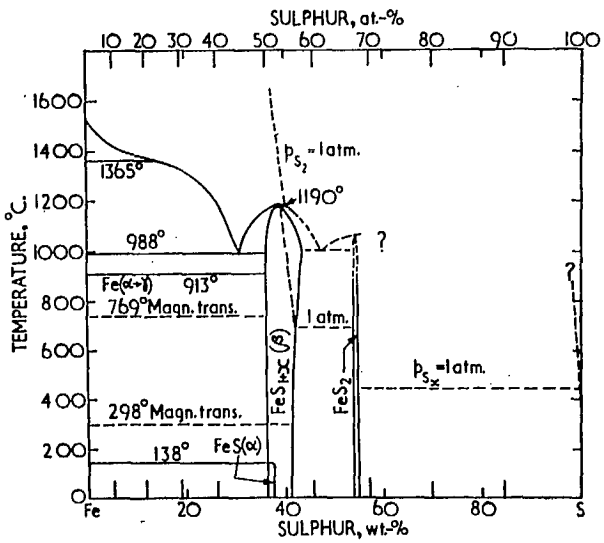

Figure 2. - The Iron-Sulphur System According to Rosenqvist (4).

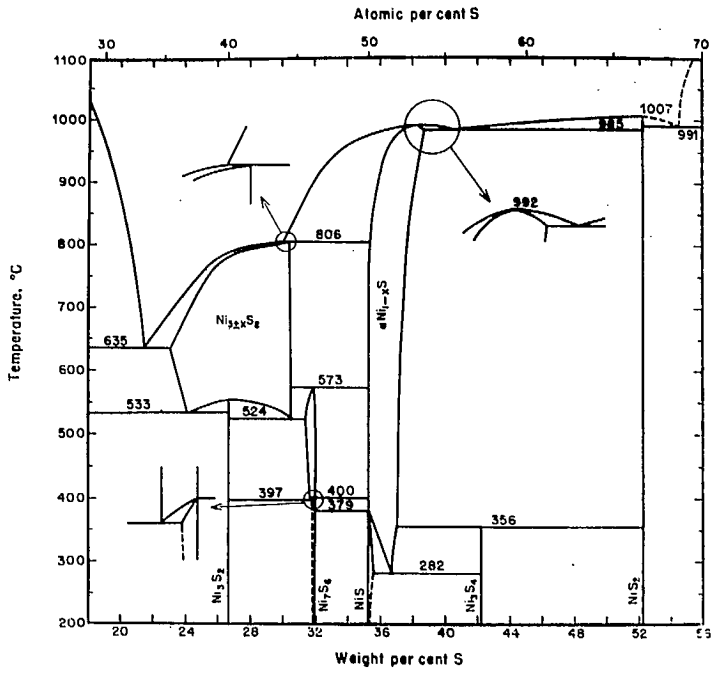

Figure 3. - The Nickel-Sulphur System According to Kullerud and Yund (14).

Additional information is given in Figures 1 and 2 where the temperature-composition relationship at 1 atmosphere sulphur pressure is shown as a dotted line. However, it was desirable to know the decomposition temperature of various compositions in the FeS - FeS_2 system, i.e., the temperature at which sulphur is just starting to evolve when the sample is being heated in an evacuated capsule.

To achieve this information, synthetic Fe:xS mixtures were sealed in evacuated silica capsules and annealed at 500°C for several days to achieve equilibrium. These products, in their capsules, were then heated slowly from room temperature, and the temperature at which there was evidence of free sulphur being evolved was recorded; this temperature has been plotted against composition in Figure 4 (see page 11).

A visual comparison of the dotted line shown in Figure 2 with the results given in Figure 4 indicates that the decomposition temperature is approximately 200°C lower than the equilibrium temperature at 1 atmosphere sulphur pressure for all compositions from FeS to FeS_2.

The decomposition temperatures of the cobalt and nickel sulphide systems were not similarly explored, but the relevant information can be calculated from Rosenqvist's thermodynamic study of the iron, cobalt, and nickel sulphides (4).

It is well known that each of the three sulphide systems includes a rather stable monosulphide that forms solid solutions with excess sulphur. Since these monosulphides have a composition that is non-stoichiometric, their formulae are often shown in one of two ways, i.e. MS_{1+x} or $M_{1-x}S$. The latter formula is preferred for the reasons discussed in the following paragraphs.

When Hägg and Sucksdorf (16) investigated various samples, containing different iron to sulphur ratios, by relating the cell dimensions with the density of the material, it was demonstrated that the variations in the composition were due to vacancies in the iron sites in the structure and not due to excess sulphur. Therefore, the formula should be written $Fe_{1-x}S$, which indicates a metal deficiency.

Similarly, in the case of nickel monosulphide, Arnold and Kullerud (quoted in reference 14) found that the variable composition of this monosulphide was due to vacancies in the nickel sites in the structure $Ni_{1-x}S$.

The present author assumes that the cobalt monosulphide is analogous to iron and nickel in forming the structure of $Co_{1-x}S$. Kuznetsov, Sokolova, Palkina, and Popova, (15) describe the monosulphides of cobalt as unilateral imperfect solid solutions of sulphur in CoS, with vacancies in the positions of cobalt; however, they used the formula CoS_{1+x} and not $Co_{1-x}S$.

The range of the composition of these monosulphides has been determined by several of the above-mentioned investigators. It is observed in Figures 1, 2, and 3, that the boundaries of the monosulphides are temperature-composition dependant, but, for the clarification of the range and formula of the monosulphides, Table 3 was compiled from the phase diagrams and other data of Rosenqvist (4).

TABLE 3

Range of Composition of the Monosulphides

Lowest Sulphur		Highest Sulphur	
Formula	Temperature	Formula	Temperature
$Co_{0.96}S$	~ 700°C	$Co_{0.85}S$	~ 800°C
$Fe_{1.00}S$	~ 980°C	$Fe_{0.86}S$	~ 700°C
$Ni_{1.00}S$	~ 400°C	$Ni_{0.92}S$	~ 500°C

Therefore, if the calculated ratio of metal to sulphur yields a formula lying within the above limits, it should be written $M_{1-x}S$; however, if it yields a formula which lies outside these limits, the form $MS_{1\pm x}$ should be used.

Since no cell-dimension determinations or density measurements were made on the monosulphides of this report, the formula of $M_{1-x}S$ will be used when the metal : sulphur ratio present (in the various experiments of this report) are in the above ranges. These formulae give only the gross M:S ratio and in no way imply that these materials are single-phased.

The non-stoichiometric monosulphides have the fundamental crystal lattice of the NiAs-type ($a = 3.+$ Å and $c = 5.+$ Å). However, some cobalt and iron monosulphides have a superstructure, based on the NiAs-type cell, but have dimensions that are multiples of the above values.

The solid-solution of the cobalt monosulphides has been reported by Kuznetsov, Sokolova, Palkina, and Popova (15) to have two different structures: the basic structure for the composition range $Co_{0.94}S$ to $Co_{0.98}S$, and a superstructure for the composition range $Co_{0.85}S$ to $Co_{0.94}S$*. Both of these structures are quenchable.

*The A.S.T.M. X-ray diffraction patterns of these structures were the basis of identification of the monosulphides of this report.

The crystallography of pyrrhotite, the solid solution of iron monosulphide, has been studied by many workers. The following two groups of authors have published recently:

(1) Morimoto, Nakazawa, Nishiguchi, and Tokonami (17) who described five different structures for pyrrhotite, one for each of the following compositions : FeS - hexagonal ; $Fe_{11}S_{12}$ - hexagonal ; $Fe_{10}S_{11}$ - orthorhombic ; Fe_9S_{10} - hexagonal ; and Fe_7S_8 - monoclinic. All of these structures are superstructures and all are stable at room temperature.

(2) Nakazawa and Morimoto (47) described three synthetic pyrrhotites that were found to be stable in the temperature range 100 to 300°C; all of these were quenchable, and have superstructures.

The nickel monosulphides have been studied by Kullerud and Yund (14). The high-temperature form (α-$Ni_{1-x}S$) was shown to be a solid solution whose basic lattice parameters change gradually and linearly with composition.

Cobalt, iron, and nickel also form disulphides. It is known that these disulphides deviate only slightly from the stoichiometric composition. Therefore, the range of solid solubility with the disulphides is much smaller than with the monosulphides. These disulphides have a cubic crystal structure that is referred to as the pyrite structure.

The phase diagram for the lower-temperature region of the iron-sulphur system is shown in Figure 5; this diagram was published by Taylor (12). Although this diagram shows the regions of stability of several additional iron-sulphur compounds, especially the pyrrhotites, it does not indicate the exact field for the two Fe_3S_4 compounds, greigite and smythite. Greigite is shown, tentatively, as stoichiometric Fe_3S_4 and as being stable up to 75°C; whereas, smythite is shown, tentatively, as a shaded area with an average composition of Fe_9S_{11} ($\sim Fe_{3.27}S_4$) and with an undefined maximum thermal stability level. The composition of smythite was obtained by microprobe analyses of smythites from the Silverfields Mines, Cobalt, Ontario.

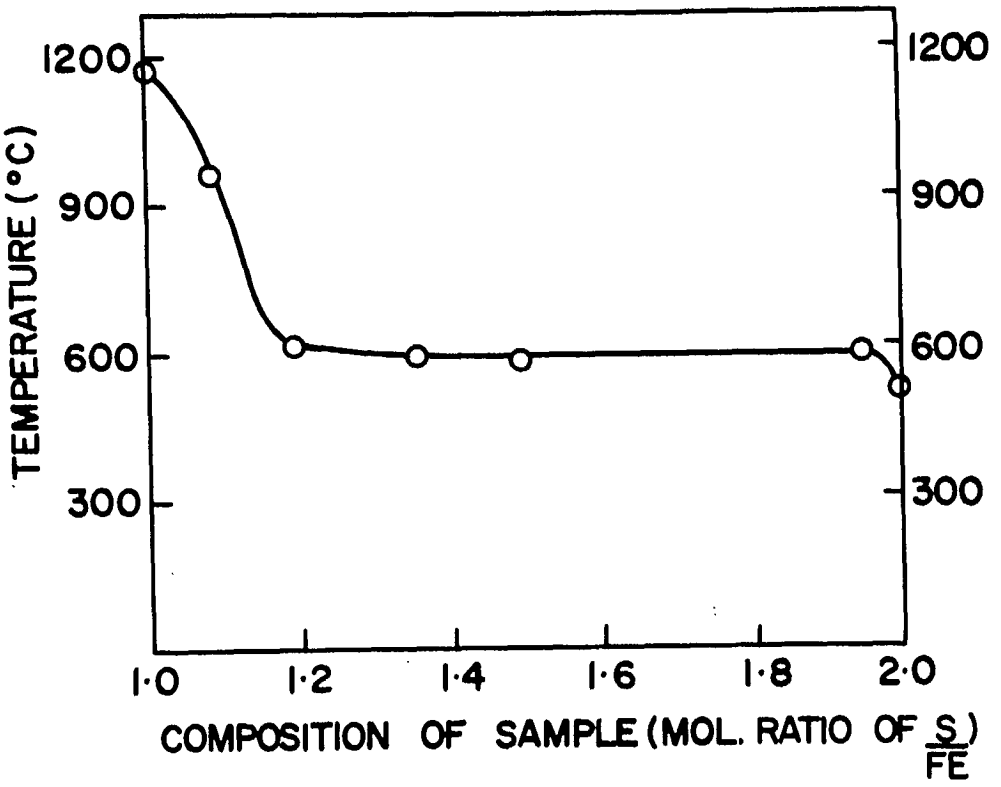

Figure 4. - Visually-Observed Decomposition Temperatures of a Partial Iron-Sulphur System.(These compositions were heated in evacuated quartz capsules).

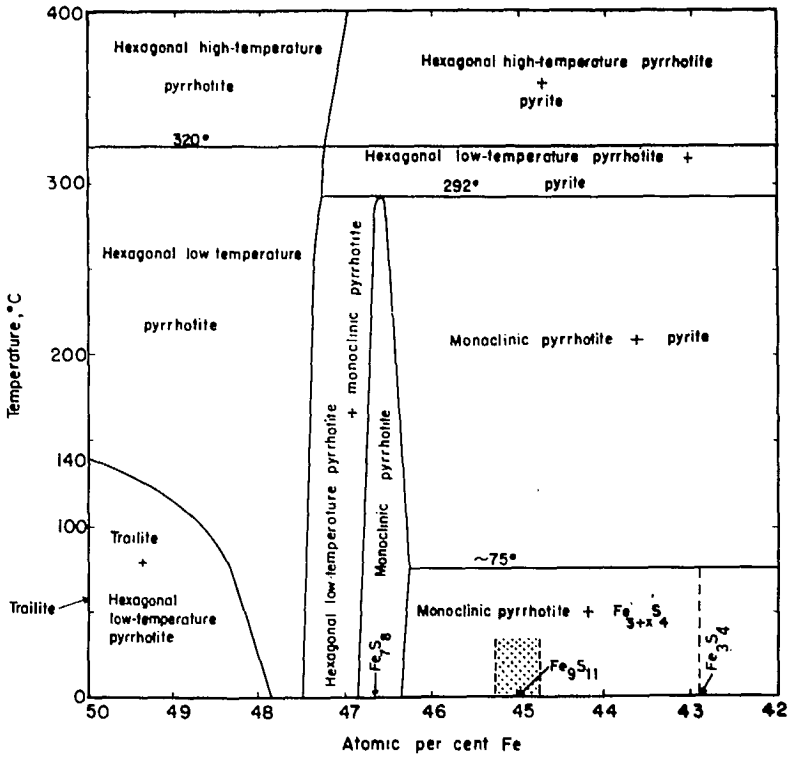

Figure 5. - A Portion of the Iron-Sulphur System at Low Temperature According to Taylor (12).

In the original work of Skinner, Erd, and Grimaldi (18), who discovered greigite in a natural deposit, it was stated that naturally-occurring greigite could be heated to 238°C for 165 hours without any decomposition. However, when it was heated at 282°C for 148 hours, some change had occurred. Uda (11) described his synthetic greigite as being stable at 190°C, and stated that it would decompose to tetragonal or to hexagonal FeS with some free sulphur at temperatures below or above this temperature, respectively. Therefore, it was necessary to quench from 190°C to avoid contamination by tetragonal FeS formed during cooling.

Smythite was originally discovered in a natural deposit by Erd, Evans, and Richter (19), who stated that naturally-occurring smythite was unchanged when it was heated at 200°C for a month, but was changed completely to pyrrhotite when it was heated at 400°C for 18 hours. Rickard (48), who prepared synthetic smythite in an aqueous solution at room temperature and in the absence of air, did not describe the stability of his product per se, except to state that, for X-ray diffraction analysis, a wet sample was sealed in a capillary to avoid any alteration of the product by drying or oxidation.

Mackinawite, FeS, is not shown on Figure 5. Ward (49) described mackinawite as a sulphide richer in iron than troilite, FeS, and stated that it can be represented by a formula near $Fe_{1.06}S$; however, the presence of other metals could affect the composition. Ward also stated that mackinawite decomposes at about 140°C.

It is also noted that Figure 2 does not indicate a field for the polymorph of pyrite, marcasite (FeS_2), which has an orthorhombic crystal structure. Buerger (50) stated that marcasite is not stoichiometric in that it is sulphur-deficient, i.e., FeS_{2-x}, whereas, pyrite is stoichiometric FeS_2. The chemical analyses of naturally-occurring pyrite and marcasite, as shown in Table 64, agree with the above statement; the calculated formula of pyrite and of marcasite were found to be $FeS_{2.00}$ and $FeS_{1.92}$, respectively. The transition temperature of marcasite, as listed in "The Handbook of Chemistry and Physics" (21), is 450°C; however, recent differential thermal analysis in the Mines Branch laboratories of naturally-occurring marcasite failed to show

any different thermal behaviour by comparison with naturally-occurring pyrite, when heated at 12 deg/min up to 750°C. Allen, Crenshaw, Johnston, and Larsen (20) showed that marcasite formed hydrothermally at temperatures of 100° to 300°C; the latter was their maximum working temperature. However, the higher temperatures resulted in a greater quantity of pyrite being formed simultaneously, compared with the formation of essentially pure marcasite at 100°C.

(b) Three-Component Sulphide Systems

The three-component systems $Fe_x Ni_y S_z$ are shown in part in Figure 6. The region of stability of the monosulphides, $(Fe_{1-y}Ni_y)_{1-x}S$, extends over a broad band from $Ni_{0.92}S$ to $Ni_{1.00}S$ in the Ni-S binary system (i.e., no Fe) and increases uniformly as the iron content is increased until the limits, $Fe_{0.86}S$ to FeS, are reached in the Fe-S binary system (i.e., no Ni). It should be mentioned that both boundaries of the $(Fe_{1-y}Ni_y)_{1-x}S$ solid-solution area curve gently through a maximum of slightly higher sulphur values than the mean of the end members.

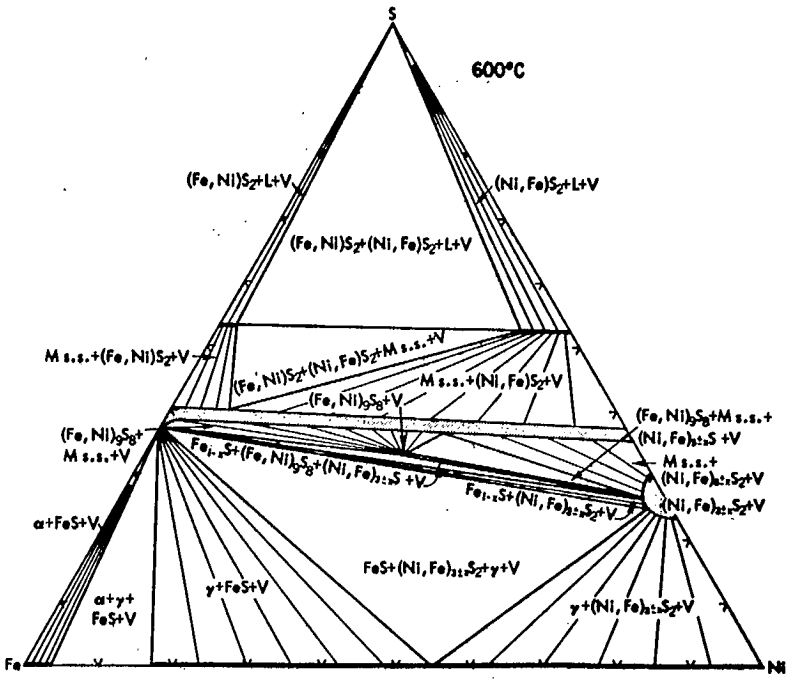

Figure 6. - The 600°C Isothermal Section of the Condensed System Fe-Ni-S According to Kullerud (52).

Pentlandite, $(Fe,Ni)_9S_8$, is shown as a stable zone in which the iron, nickel, and sulphur contents can vary over a small range. This variation results in a solid-solution formation. Kullerud (22) reported that pentlandite decomposes at 610 ± 2°C into $(Fe,Ni)_{1-x}S$, some hexagonal pyrrhotite, and to a high-temperature non-quenchable phase, equivalent to $Ni_{3\pm x}S_2$ in the pure Ni-S system, but containing some iron.

The 300°C isothermal section of the same condensed system published by Craig (23) is shown in Figure 7. This figure shows another compound, $FeNi_2S_4$ - violarite, which has a maximum thermal stability of 461 ± 3°C.

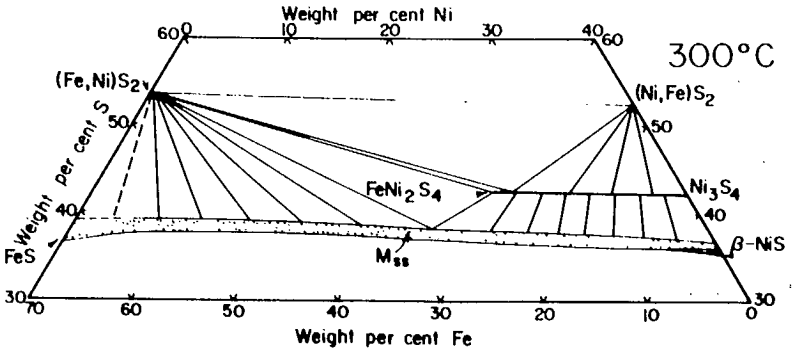

Figure 7. - The 300°C Isothermal Section of the Condensed System Fe-Ni-S According to Craig (23).

The FeS_2-NiS_2 system is shown in some detail in Figure 8. The compound bravoite, FeS_2:NiS_2, is shown to be stable only at temperatures below 137°C. Originally, Clarkand Kullerud (6) had presented this information in two diagrams based on a demarcation line of 200°C. But, for convenience, they are here combined into one diagram.

Clark and Kullerud (6) were unable to prepare bravoite in a dry synthesis at 200°C over 250 days, with a grinding part-way through the heating period. However, they were able to prepare bravoite in a hydrothermal system at temperatures of 131°C and below, and, for a good crystalline bravoite, a heating period of 12 or more days was required. These same researchers (6) studied the thermal breakdown of naturally-occurring bravoite in the presence of excess sulphur; no breakdown occurred at 450°C even after 10 days of heating. However, there was a partial breakdown at 463°C after 11 days. Also, during this study, it was observed that the cell edge of bravoite is the mean of the two end members, pyrite and vaesite. Further, it was stated that bravoite has been always found associated with pyrite and not with vaesite.

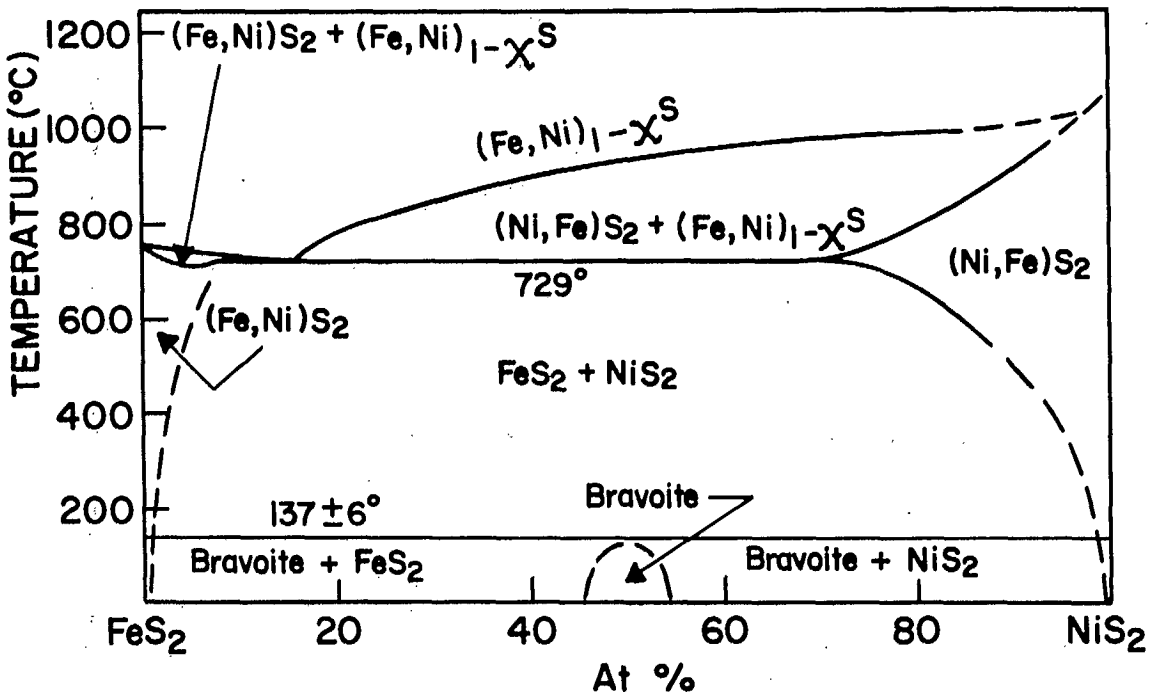

Figure 8. - The FeS_2-NiS_2 System According to Clark and Kullerud (6).

In order to present the FeS_2-CoS_2 system, some of Klemm's data (8, 9), and some data from Figures 1 and 2 were combined to give a probable diagram for this system, as shown in Figure 9.

The solid solutions involving CoS_2 and FeS_2 are apparent in Figure 9; however, to complete the low-temperature portion of the system, in a way analogous to that presented for the Fe-Ni-S system in Figure 8, it would be necessary to assess the stability range of a cobaltic bravoite compound, $FeS_2 . CoS_2$.

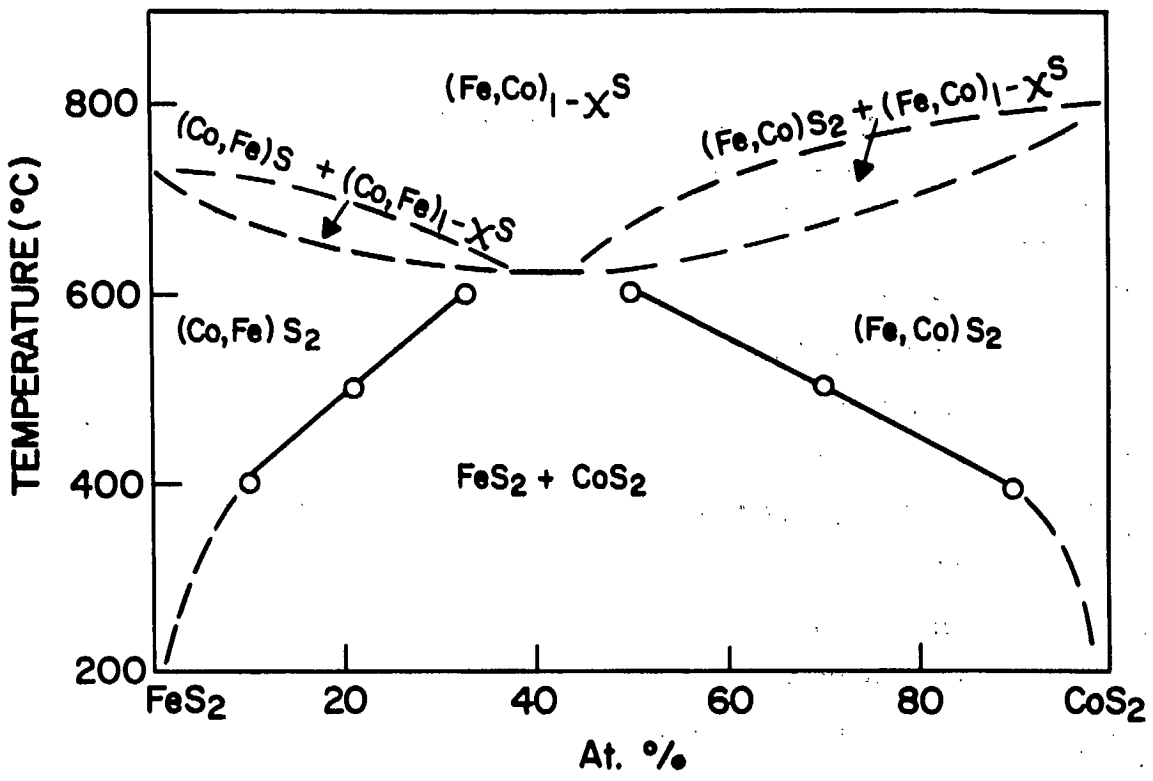

Figure 9. - The FeS_2-CoS_2 System, Compiled from Various Sources.

The data on the stabilities of the various sulphides of cobalt, iron, and nickel, that have been presented in the above Figures and in the comments pertaining to them, have been compiled in tabular form in Table 4. The footnotes refer to the type of thermal stability being described. The values quoted may not agree with other published data; however, they do indicate the general stability within experimental error.

The thermal stability of the various sulphides, listed in Table 1, plays a very definite role in controlling their preparation.

TABLE 4

Stability Range of Various Sulphides

Formula	Mineral Name	Stability Range (°C)
$Co_{1-x}S$	Jaipurite	460 - 1000 (g)
FeS	Mackinawite	R.T. - 140 (c)
FeS	Troilite	R.T. - 1175 (b)
$Fe_{1-x}S$	Pyrrhotite	R.T. - 1175 (f)
α-$Ni_{1-x}S$	High-Temperature Millerite	379 - 806 (e)
β-$Ni_{1-x}S$	Millerite	R.T. - 379 (c)
α-Ni_7S_6	High-Temperature Godlevskite	400 - 573 (e)
β-Ni_7S_6	Godlevskite	R.T. - 400 (c)
$(Ni,Fe)_{1-x}S$	Ferrous Nickel Sulphide	379 - 806 (d)
$(Fe,Ni)_9S_8$	Pentlandite	R.T. - 610 (a)
Co_9S_8	Cobaltian Pentlandite	R.T. - 835 (a)
Fe_3S_4	Greigite, and Smythite	R.T. - $\sim$ 200 (a)
Co_3S_4	Linnaeite	R.T. - 625 (a)
Ni_3S_4	Polydymite	R.T. - 350 (a)
$FeNi_2S_4$	Violarite	R.T. - 460 (a)
CoS_2	Cattierite	R.T. - 800 (f)
NiS_2	Vaesite	R.T. - 780 (f)
FeS_2	Pyrite	R.T. - 698 (f)
FeS_2	Marcasite	R.T. - 450 (c)
$(Co,Fe)S_2$	Cobaltian-Bravoite	Not given
$(Ni,Fe)S_2$	Nickelian-Bravoite	R.T. - 137 (a)

R.T. = Room Temperature.
(a) = Disproportionation.
(b) = Melting Point.
(c) = Transition.
(d) = Transition to Melting Point.
(e) = Transition to Disproportionation.
(f) = At one atmosphere sulphur pressure.
(g) = Disproportionation to Melting Point.

SOURCE OF MATERIALS

No commercial sources of cobalt, iron, and nickel sulphides were used in this study. Two naturally-occurring compounds, which were obtained by a heavy-liquid separation from their ores, pyrite and marcasite, the two crystal polymorphs of FeS_2, were utilized only in some preliminary experiments. Therefore, it was necessary to synthesize all the sulphides listed in Table 1, either from the elements or from relevant compounds.

The source and the manufacturers' quoted purity of the elements and compounds used in the preparation and/or crystal-growth of the sulphides are shown in Table 5. The semi-quantitative spectrochemical analysis of the powder samples of cobalt and nickel, the millings of iron, and of the lead chloride flux material, are shown in Table 6a. These results show that the main impurity in the cobalt and nickel is a little iron, while the iron millings and the lead chloride are of good quality. The analysis of the high-purity sulphur is shown in Table 6b.

TABLE 5

The Source and Purity of the Elements and Compounds Used in Crystal Growing

Element or Compound	Physical Form	Source	% Purity (Suppliers' Data)
Co	Powder	Fisher	None given (b)
Co	Plate	---	99.9
Co	Wire	Koch-Light	99.99
Fe	Millings	British Chemical Standard	~ 99.93 (a) (b)
Ni	Powder	Sherritt-Gordon	~ 99.5 (a) (b)
Ni	Wire	Koch-Light	99.99
S	Powder	ASARCO	99.999 (c)
$PbCl_2$	Powder	Matheson, Coleman and Bell	99.0 (b)
$Fe_2(SO_4)_3 \cdot 7.6H_2O$	Powder	Mallinckrodt	Reagent grade
$Fe(NH_4)_2(SO_4)_2 \cdot 6H_2O$	Crystal	Nichols	Reagent grade
$Na_2S.9H_2O$	Crystal	Fisher	Reagent grade
H_2S	Gas	Matheson	98.5
HCl	Gas	Matheson	99.0
I_2	Crystal	Anachemia	~ 99.9 (a)

(a) = Derived by subtracting the total quoted impurities from 100%.
(b) = Additional analyses are in Table 6a.
(c) = Additional analyses are in Table 6b.

TABLE 6a

Analysis of Some Metals and of Lead Chloride Used in Crystal Growing

Element or Compound	Physical Form	Semi-Quantitative Spectrochemical Analysis (% by weight)						
		Mn	Si	Fe	Mo	Cu	Ni	Co
Co	Powder	0.01	N.D.	0.2	N.D.	N.D.	N.D.	P.C. (a)
Fe	Millings	0.03	0.07	P.C.	0.1	N.D.	N.D.	N.D. (a)
Ni	Powder	N.D.	N.D.	0.4	N.D.	0.03	P.C.	N.D. (a)
$PbCl_2$	Powder	N.D.	0.006	N.D.	0.02	0.01	N.D.	N.D. (b)

(a) = Internal Report MS-AC 71-126.
(b) = Internal Report MS-AC 71-88.

N.D. = Not detectable.
P.C. = Principal constituent.

TABLE 6b

Analysis of Special High-Purity "ASARCO" Sulphur*

Source of Analysis	Na	Cl	Mg	Cu	O_2
	(In ppm)				
ASARCO (a)	1	1	N.D.	-	-
Mineral Sciences Division	N.D. (b)	-	80 (b)	400 (b)	55 (c)

*Special high-purity sulphur obtained from American Smelting and Refining Company (ASARCO). This sulphur was labelled 99.999 +%, Lot 5-64-1.

(a) = In addition to the above elements, the following elements were reported as being not detectable by spectrographic means: Sb, Tl, Mn, Pb, Sn, Si, Cr, Fe, Ni, Bi, Al, Ca, In, Cd, Zn, Ag.

(b) = Internal Report MS-AC 68-649. Semi-quantitative Spectrographic Analysis; in addition to the above, the following elements were reported as being not detectable: Ba, Mn, Mo, Sb, W, Pb, Sn, Cr, Nb, Ta, Fe, Bi, Al, In, Ca, V, Zr, Ti, Ni, Co, Sr.

Note: 400 ppm Cu (0.04%) is a somewhat high figure in view of the 99.999% purity of this sulphur, claimed by the manufacturer.

(c) = Internal Report MS-AC 68-642. Neutron-activation analysis.

PURIFICATION OF METAL POWDERS

The following metal powders were purified by a hydrogen reduction to remove oxygen:

1. Cobalt powder (Fisher Scientific).
2. Iron millings (British Chemical Standards).
3. Nickel powder (Sherritt-Gordon).

The results are shown in Table 7.

TABLE 7

Hydrogen Reduction of Metal Powders to Remove Oxygen

Metal	Temperature (°C)	Time (min)	$\%O_2$ (calc.)(a)
Cobalt	650	90	0.17
Iron	800	120	0.16
Iron	900	120	0.18
Nickel	900	90	0.19

(a) = Calculated from weight loss.

The above value for oxygen in the nickel powder agrees with the value of 0.19% that was obtained by Sherritt-Gordon.

PREPARATION OF SULPHIDE MATERIAL

The synthesis of the sulphides of cobalt, iron, and nickel has been accomplished by one of two main approaches, viz., either through the direct combination of the reactants, or through a special growth procedure.

Some useful references pertaining to previous studies in which sulphides were prepared by direct combination of the elements, are shown in Table 8.

TABLE 8

References to Previous Direct-Combination Preparations of Cobalt, Iron, and Nickel Sulphides

Formulae	References	
CoS_x, FeS_x, NiS_x	Rosenqvist	(4)
CoS_2, FeS_2, NiS_2	Klemm	(8) (9)
CoS_2	Morris, Johnson, and Wold	(24)
$(Co_{1-x}Fe_x)S_x$	Gallagher, MacChesney, and Sherwood	(25)
$(Fe_xCo_{1-x})S_2$; $(Co_xNi_{1-x})S_2$	Bouchard	(26)
NiS_x system	Kullerud and Yund	(14)
Fe-Ni-S system	Clark and Kullerud	(6)
	Naldrett, Craig, and Kullerud	(10)
FeS_2-NiS_2 system	Clark and Kullerud	(6)

Some references pertinent to growth procedures of several of the sulphide compounds involved in this study are shown in Table 9.

TABLE 9

References to Previous Growth Procedures for Cobalt, Iron, and Nickel Suphides

Growth Procedure	Formulae	References	
Vapour Transport	$Ni_{1-x}S$	Gamondes and Laffitte	(27)
Chemical Vapour Transport	$Ni_{1-x}S$	Gamondes and Laffitte	(27)
	CoS_2, FeS_2, NiS_2	Bouchard	(28)
Direct Combination and Anneal	Low-temperature $Fe_{1-x}S$	Taylor	(51)
Melt - Bridgman technique	FeS to $Fe_{1-x}S$	Kamigaichi, Hihara, Tazaki and Hirahara	(29)
		Hirahara and Murakami	(30)
Melt - Slow-cool technique	NiS	Tsubokawa	(31)
Flux - $PbCl_2$ as flux	CoS_2, FeS_2, NiS_2	Wilke, Schultze and Töpfer	(32)

In the present study, attempts were made to prepare all the sulphides listed in Table 1 by both the direct-combination procedure and by one of four different growth procedures. Each of these systems will now be described in detail.

(a) Preparation of Sulphides by Direct Combination

This general technique has been further subdivided into four main methods:

1. Hydrogen Sulphide Reaction

In this method, a metal or a salt of a metal was heated in a stream of hydrogen sulphide. Oxygen was removed as water at the same time as a monosulphide was formed. Representative results are shown in Table 10 for the reaction with the metals. The results obtained when a salt of a metal was used, as shown in Table 11, are for iron compounds only, as neither cobalt nor nickel compounds were used. It is obvious from the results given in Tables 10 and 11 that neither stoichiometric monosulphides nor the disulphides (pyrite) were obtained by the hydrogen sulphide treatment.

It is observed that, in the case of cobalt, Expts. #354 and #489, the calculated ratio of cobalt to sulphur was approximately 1:1; however, the X-ray diffraction analysis showed them to be mixtures of $Co_{1-x}S$ and Co_9S_8. The explanation is that CoS disproportionates on cooling; this fact is observed in Figure 1. In addition,it has been found that some uncertainty still exists in the X-ray diffraction patterns of the $Co_{1-x}S$ sulphides. The recent work of Kuznetsov, Sokolova, Palkina, and Popova (15) has provided some diffraction patterns that have been accepted by A.S.T.M. However, the difficulty appears to be due to the rapid disproportionation of $Co_{1-x}S$, when x is small (see Figure 1 for additional data).

TABLE 10

The Heating of Cobalt, Iron, or Nickel Metals in Hydrogen Sulphide

Expt. No.	Metal	Temperature (°C)	Time (hr)	Calculated Gross Composition (a)	Phase Present (b)	X-ray Report No.
354	Cobalt	1100	1	$Co_{0.96}S$	$Co_{1-x}S$, Co_9S_8 (c)	68-0419
489	Cobalt	865	1	$Co_{0.89}S$	-	-
489 (d)	Cobalt	1140	1	$CoS_{0.97}$	Co_9S_8, $Co_{1-x}S$ (c)	69-11
754	Cobalt	1100	1	$CoS_{0.99}$	Not Analysed	-
765	Cobalt	950	0.5	$CoS_{0.98}$	Not Analysed	-
356	Iron	1200	3	$Fe_{0.92}S$	Hexagonal Pyrrhotite	70-34
368	Iron	984	4	$Fe_{0.91}S$	Hexagonal Pyrrhotite	68-0759
353	Nickel	805	3	$Ni_{0.98}S$	α-NiS	68-0382
362	Nickel	900	1.5	Ni_7S_6	α-NiS and unidentified minor	68-0438
487	Nickel	815	4	$Ni_{0.96}S$	α-NiS	69-03
604	Nickel	800	2	$NiS_{0.89}$	α-NiS (e)	69-799
621	Nickel	800	4	$Ni_{0.96}S$	α-NiS	69-872
753	Nickel	850	0.5	$NiS_{0.88}$	Not Analysed	-
766	Nickel	900	0.5	$NiS_{0.73}$	Not Analysed	-

(a) = Based on the weight change of the metal going to MS_x.
(b) = By X-ray diffraction analysis; the products are listed in decreasing order of abundance.
(c) = Also a trace constituent that has not been identified.
(d) = This represents additional treatment of the same sample.
(e) = No minor constituent was observed in the sample analysed.

TABLE 11

Preparation of Sulphides by Heating an Iron Compound in Hydrogen Sulphide

Expt. No.	Iron Compound	Temperature (°C)	Time (hr)	Calculated Gross Composition (a)	Analysis by X-ray Diffraction
436	Fe_3O_4	500-700	10	$FeS_{1.83}$	Major-pyrite (b) Minor-pyrrhotite
443	$FeCl_3 \cdot 6H_2O$	300	13	$FeS_{1.83}$	Not Analysed
459	$Fe_2(SO_4)_3 \cdot 7.6H_2O$	400	4	$FeS_{1.94}$	Pyrite (c)

(a) = Calculated ratio of M:S in product, based on the assumed iron content in the starting material.
(b) = X-ray Diffraction Report Number 68-1048.
(c) = X-ray Diffraction Report Number 68-1156.

Nickel monosulphides containing a nickel-to-sulphur ratio that is slightly nickel-rich, see Expts. #362 and #604, where the calculated ratio was equivalent to Ni_7S_6, gave an X-ray diffraction pattern that showed them to be predominantly α-$Ni_{1-x}S$. The explanation is that these samples had been heated at temperatures above the maximum stability temperature for Ni_7S_6, which is shown to be 575°C in Figure 3, and also, that the cooling rate had been too fast for the formation of Ni_7S_6 when the samples were cooled; however, a minor amount of unidentified material was detected in Expt. #362.

The iron samples, Expts. #356 and #368, showed the calculated ratio of iron to sulphur to be in the pyrrhotite range; this was confirmed by the X-ray diffraction analysis. Figure 2 shows that $Fe_{1-x}S$ does not disproportionate on cooling.

It has been found that these resulting monosulphides of cobalt, iron, and nickel, were useful as starting materials in crystal-growing procedures, since the ratio of metal to sulphur could be easily calculated from the gain in weight of the sample.

In an attempt to form pentlandite*, $Ni_{4.5}Fe_{4.5}S_8$, a metallic charge of equal atomic proportions of nickel and iron was heated in hydrogen-sulphide. Initial heating at 800 to 1000°C for five hours gave a product that had a calculated gross composition of $Ni_1Fe_1S_2$. However, when this product was heated in helium at 900°C for two hours, the resultant product had a calculated gross composition of $Ni_1Fe_1S_{1.79}$, i.e., essentially pentlandite. The X-ray diffraction report, #69-104, showed the composition to be predominantly pentlandite (a -10.11 Å), with a minor amount of pyrrhotite.

The "a" value of the above pentlandite agrees with the expanded "a" value of Knop, Huang, and Woodhams (33), who found that, when naturally-occurring pentlandite from Creighton Mine, Sudbury, Ontario, had been crushed to -100 mesh and annealed in vacuo at 200°C for 53 hours, there was an irreversible expansion of the "a" value from 10.044 ± 0.001 Å to 10.105 ± 0.001 Å.

---

*Expt. #493B, not shown in any table.

2. Sintering of the Metal with Stoichiometric Sulphur

This procedure involved heating one or more of the metals with a calculated amount of sulphur, in an evacuated silica capsule, to yield the sought-after sulphide. This procedure has the advantage that controlled quantities of the reactants can be heated for as long as desired without any possible loss. In this method the product is not melted, but is sintered instead.

The conditions used to prepare a number of two-component sulphides are shown in Table 12. The calculated composition of the product was obtained gravimetrically, based on the weight change of the metal to the compound MS_x. In these cases when excess elemental sulphur was present after the heating period, it was removed by a CS_2 leaching prior to the calculation; the leached samples were Expts. 476, 244, 320, 444, 463 and 473.

The results of X-ray diffraction analyses of many of the products listed in Table 12 are shown in Table 13. A few comments on these results should be made at this time.

(i) The cobalt-sulphur experiments gave a mixture of compounds which was probably caused by disproportionation on cooling.

(ii) Some of the iron-sulphur experiments gave unexpected results. Expts. #245 and #837 gave products that had a gradation of composition from one end to the other end of the sintered mass. The end that had been heated at a slightly higher temperature was shown, by X-ray diffraction analysis, to be principally pyrrhotite with a minor amount of pyrite, while the opposite end was found to be principally pyrite with a minor amount of pyrrhotite. These analyses imply that the ratio of pyrite to pyrrhotite is temperature-dependent, and that the slight temperature gradient had resulted in this partial segregation.

Expt. #463 presented an anomaly in that the calculated composition of $FeS_{1.75}$ was shown by X-ray diffraction analysis to be totally pyrite. It is assumed that the portion of Expt. #463 submitted for analysis must not have been representative of the whole sample, and that equilibrium had not been attained in the sample.

(iii) The nickel-sulphur experiments gave results that were similar to those of the cobalt-sulphur samples in that the products were mixtures of compounds, which were probably the result of disproportionation.

The present study showed that sulphur combines readily with cobalt, iron, and nickel when heated at temperatures above 500°C to form metallic-appearing products in all metal:sulphur ratios up to approximately $MS_{1.95}$. However, at 300°C, the rate of reaction is extremely slow; for example, it was not possible to prepare Ni_3S_4 from finely-divided nickel powder and sulphur, even though the intermediate product was ground once during the heating period. In general, most of the products were mixtures of two or more sulphides. The rate of combination of $MS_{1.95}$ compositions with sulphur to yield stoichiometric MS_2 was extremely slow, even when a large excess of sulphur was present.

The preparation of only two three-component sulphides was attempted by this method; these results are shown in Table 14. The analysis confirms that the sought-after sulphides are not stable at the temperature employed, and that they disproportionated in accordance with the data presented earlier.

It is evident that the direct-combination procedure will yield some useful products, especially the monosulphides. However, the procedure fails, under the conditions described, to produce the intermediate sulphide, Fe_3S_4, or the stoichiometric disulphides CoS_2, FeS_2 and NiS_2. Both cobalt and iron appear to form a nearly-stoichiometric disulphide, while nickel formed a mixture of monosulphide and disulphide.

Although several compounds can be formed by this procedure, it has been found that, in order to achieve better-quality products, these compounds can be obtained by a "melt-and-anneal" growth procedure, which will be described later in this report (see page 35).

3. Melting of the Sulphide

If a substance has a congruent melting point, this physical property can be used to advantage for growing crystals of this material.

Two variations of this general procedure are in the modes of cooling that cause nucleation and subsequent crystal growth. The first way is a slow

TABLE 12

Conditions Used for Direct Combination of Cobalt, Iron, and Nickel with Sulphur

Expt. No.	Metal	Metal:Sulphur Ratio	Temperature (°C)	Time (days)	Calculated Gross Composition
836	Cobalt	1:1.05	800	6	$Co_{0.95}S$
823	Cobalt	1:1.13	800	6	$Co_{0.885}S$
476	Cobalt	1:3	620	9	$CoS_{1.946}$ (a)
71	Iron	1:1	900	1	FeS
630	Iron	1:1.03	1190	0.5	$Fe_{0.97}S$
268	Iron	1:1.1	1000	0.1	$Fe_{0.91}S$
837	Iron	1:1.25	600	3	$FeS_{1.25}$
245	Iron	1:1.33	190	85	Fe_3S_4
258	Iron	1:1.5	480	5	Fe_2S_3
269	Iron	1:1.95	510	2	$FeS_{1.95}$
244	Iron	1:2	400	60	$FeS_{1.99}$ (a)
320	Iron	1:3	700	8	$FeS_{1.74}$ (a)
444	Iron	1:3	740	15	$FeS_{1.98}$ (a)
463	Iron	1:3	600	12	$FeS_{1.75}$ (a)
430	Nickel	1:0.857	380	15	Ni_7S_6
800	Nickel	1:1.002	800	12	$Ni_{0.998}S$
473	Nickel	1:3	620	9	Ni_3S_4 (a)

(a) = See text for details of this calculation.

TABLE 13

X-Ray Diffraction Analyses of the Two-Component Sulphides Described in Table 12

Expt. No.	Calculated Gross Composition	Phases Present	X-Ray Diffraction Report No.
836	$Co_{0.95}S$	Co_9S_8 and β-$Co_{0.966}S$	71-848
823	$Co_{0.885}S$	$Co_{1-x}S$ (several)	71-809
476	$CoS_{1.946}$	Cattierite and Linnaeite	69-35
71	FeS	Pyrrhotite	65-0528
630	$Fe_{0.97}S$	Not Analysed (b)	-
268	$Fe_{0.91}S$	Not Analysed	-
837	$FeS_{1.25}$	Pyrrhotite and minor of Pyrite (a) Pyrite and minor of Pyrrhotite (a)	71-845 71-846
245	Fe_3S_4	Pyrite and minor of Pyrrhotite (a) Pyrrhotite and minor of Pyrite (a)	68-0057 68-0058
258	Fe_2S_3	Pyrite and Pyrrhotite	70-80
269	$FeS_{1.95}$	Not Analysed	-
244	$FeS_{1.99}$	Not Analysed	-
320	$FeS_{1.74}$	Pyrite and Pyrrhotite	68-0465
444	$FeS_{1.98}$	Pyrite	68-1113
463	$FeS_{1.75}$	Pyrite (a)	68-1220
430	Ni_7S_6	Shiny material Ni_7S_6 Dull material α-NiS	68-1129 68-1130
800	$Ni_{0.998}S$	Not Analysed	-
473	Ni_3S_4	Vaesite and α-NiS	69-34

(a) = See the text for special comments. (b) = Used for thermoelectric power studies.

TABLE 14

Direct Combination of Iron and Nickel with Sulphur to Form Three-Component Sulphides

Expt. No.	Sulphide Attempted	Temperature (°C)	Time (days)	Calculated Gross Composition (a)	Phases Present (b)
458	$(Ni_{0.5}Fe_{0.5})_9S_8$	640	20	As planned.	Hot zone: (c) Pyrrhotite and a minor amount of Pentlandite (a = 10.11Å) Cold zone: (d) Pentlandite (a = 10.11Å) and a minor amount of Pyrrhotite
608	$(Ni_{0.5}Fe_{0.5})S_2$	650		$(Ni_{0.5}Fe_{0.5})S_{1.58}$	Light grey material: (e) Pyrite and a minor amount of Pyrrhotite Dark grey material: (f) Vaesite and a minor amount of α-NiS

(a) = Calculations are based on the weight change of metals to $M_1M_2S_x$.
(b) = By X-ray diffraction analysis.
(c) = X-ray diffraction Report Number 68-1218.
(d) = X-ray diffraction Report Number 68-1219.
(e) = X-ray diffraction Report Number 69-765.
(f) = X-ray diffraction Report Number 69-776.

cooling of the molten material through the freezing point. The second procedure, developed by Bridgman (34), requires a bullet-shaped container that is migrated downward in a vertical furnace, causing the pointed tip to be cooled first. While this movement is maintained, a crystal will develop and seed the balance of the melt.

The Bridgman technique was used by Kamigaichi, Hihara, Tazaki, and Hirahara (29) and by Hirahara and Murakami (30) to grow pyrrhotites, $Fe_{1-x}S$, while Tsubokawa (31) used the slow-cooling method to prepare $Fe_{1-x}S$. In the present study, the Bridgman technique was not used.

However, a "melt-and-quench" method was applied to several iron and nickel sulphides, as shown in Table 15. The X-ray diffraction analyses of these products are shown in Table 16. Experiment #495 showed that some of the FeS_2 had dissociated at the range of temperature employed and that the excess sulphur pressure had not eliminated this dissociation. It was also observed that α-$Ni_{1-x}S$ has an incongruent melting point of about 990°C.

A method that is often used to prevent the loss of volatile components from compounds that dissociate, or from their melts, is the technique of Liquid Encapsulation (35). Usually, an inert liquid (e.g., B_2O_3) is used as a liquid seal over the dissociating compound. A high pressure must be maintained over the liquid B_2O_3. During the present study, in Expt. #676, it was found that the application of liquid encapsulation, under a helium atmosphere at one atmosphere pressure, failed to prevent disproportionation during the melting of α-$Ni_{1-x}S$.

After assessing this method, it is assumed that, if a slower rate of cooling of annealing were applied to the troilite and pyrrhotite samples, better crystalline products might have been obtained.

4. Melt-and-Anneal Technique (Coalescence)

By way of contrast, a technique that produced good crystalline material without the use of B_2O_3, involved a two-step approach. Firstly, nickel monosulphide, contained in a silica capsule, was melted and cooled three times; this yielded a uniform melt and some free sulphur. The second

TABLE 15

Melting of Some Iron, Nickel, and Iron-Nickel Sulphides

Expt. No.	Nutrient	Atmosphere	Temperature (°C)	Calculated ratio of M:S in product (a)
339	Iron	$H_2S \sim 1$ Atm (b)	1200	$Fe_{1.10}S$
450	Synthetic $FeS_{1.1}$	$H_2S \sim 1$ Atm (c)	1200	$Fe_{0.93}S$
451	Synthetic $FeS_{1.1}$	He ~ 1 Atm (c)	1200	$Fe_{1.01}S$
455	Synthetic $FeS_{1.1}$	$H_2S \sim 1$ Atm (c)	1200	$Fe_{0.93}S$
495	Natural-Occurring FeS_2	S ~ 1 Atm (c)	1000 then down to 740	$FeS_{1.53}$
676	NiS (d)	He ~ 1 Atm (e)	950	$Ni_{1.05}S$
490	Synthetic (f) $(Ni,Fe)_9S_8$	He ~ 1 Atm (b)	900	$(Ni,Fe)_9S_8$

(a) = Based on the weight change of the metal going to MS_x.
(b) = Open system with a flowing atmosphere.
(c) = Closed system with the sulphur pressure held at 1 atm by temperature control of the coldest part of the capsule.
(d) = See sample #675 in Table 17.
(e) = B_2O_3 was used for liquid encapsulation in an open system under controlled helium pressure.
(f) = See sample #458 in Table 14.

TABLE 16

X-Ray Diffraction Analyses of Melt-Produced Iron, Nickel, and Iron-Nickel Sulphides

Expt. No.	Phases Present	X-Ray Diffraction Report No.
339	Major: FeS (troilite) Minor: α-Fe	68-0285
450	Pyrrhotite	68-1118
451	FeS (troilite)	68-1122
455	Not analysed	---
495	Pyrrhotite and Pyrite	69-45
676	Not analysed	---
490	Major: Pentlandite (a = 10.11 Å) Minor: Pyrrhotite	69-10

step was to anneal this product at 800°C for several days; this resulted in all the sulphur being absorbed and in a crystalline product being formed. If the nickel:sulphur ratio was nickel-rich compared with the composition of the stable stoichiometric monosulphide, then a second phase of a nickel-rich sulphide was deposited at the warmer end of the billet. This second phase was involved in only a small portion of the over-all billet. The remainder of the billet, whether it was α-$Ni_{1-x}S$ or $(Ni_yFe_z)_{1-x}S$, was very useful for thermoelectric power experiments.

In Table 9, there is a reference to Taylor's preparation of low-temperature pyrrhotite (51) involving the reaction of iron and sulphur at 700°C, then annealing at temperatures between 75°C and 290°C for several weeks. This low-temperature annealing of pyrrhotite was not attempted in this present study.

The preparation of several cobalt, iron, and nickel monosulphides by the melt-and-anneal procedure is shown in Table 17. The X-ray diffraction analyses of these products are shown in Table 18.

The preparation of Co_9S_8, Expt. #853, required a long annealing period of 27 days at 700 to 775°C. After annealing for 9 days and a subsequent 13 days, traces of Co_3S_4 were still present but had decreased in amount after the second heating period and had disappeared after the third heating period of 5 days. The preparation of Co_3S_4, Expt. #854, presented no problems.

The preparation of pyrrhotite, Expt. #803, failed to produce only one product; a troilite-type substance was also present.

When the nickel:sulphur ratio was slightly sulphur-rich by comparison with the 1:1 stoichiometry, only one product was obtained. However, when the ratio was either 1:1 or slightly nickel-rich by comparison with the 1:1 stoichiometry, the end of the billet that was at the slightly lower temperature during the annealing showed only one phase, α-$Ni_{1-x}S$, and represented about 90% of the total mass, whereas the other end of the billet, which was probably only a fraction of a degree warmer during the annealing, was shown by electron microprobe analyses (see Table 72) to be a mixture

of phases, $Ni_{1-x}S$, Ni_7S_6, and Ni_3S_2. This condition arises due to disproportionation of the nickel-rich monosulphides on annealing. The preparation of β-NiS, α-Ni_7S_6, and β-Ni_7S_6, in Expts. #851, #850, and #852, respectively, caused no problems. The nickel:sulphur ratio of Expts. #631, #632, and #684, are outside the composition range of the monosulphides (see Table 3); they are therefore shown as $NiS_{1\pm x}$.

Ten samples of $(Ni_{1-x}Fe_x)S$ were also prepared by the melt-and-anneal procedure as shown in Table 19. The X-ray diffraction analyses of some of the samples are shown in Table 20. There was some disproportionation in Expt. #674 on cooling; the minor constituent, which was reported as being unidentified, had a pattern that was close to the A.S.T.M. Card No. 17-201, namely $Fe_{0.906}S$. Expt. #822 yielded a product containing only one detectable phase, pentlandite. Three of the samples contained Fe^{57}-enriched iron; this non-radioactive isotope of iron is very useful in Mössbauer experiments.

Most of the products from Tables 17 and 19 have been used for thermo-electric and other electrical studies in the Mineral Sciences Division; some results of this work have been published (see References 36, 37, 38, and 39).

5. Two-Stage Process

When Craig (23) attempted to prepare violarite, $FeNi_2S_4$, by direct combination of the elements, it was found that pyrite, vaesite, and the monosulphide were formed; regrinding with long periods of annealing failed to yield very much violarite. However, the successful preparation of violarite was achieved by a two-stage process; the first stage was to prepare the monosulphide FeS.2NiS at a temperature of 500° to 700°C; the second stage involved grinding the monosulphide and reacting it with additional sulphur at a much lower temperature of 200° to 300°C for several days.

In the present study, this general procedure was tried, not only in the preparation of violarite, but in the synthesis of polydymite, greigite, smythite, and of marcasite; the conditions used are shown in Table 21.

(Continued on page 48)

TABLE 17

Conditions Used in Melt-and-Annealing of Some Cobalt, Iron, and Nickel Sulphides

Expt. No.	Metal	Metal:Sulphur Ratio	Annealing Temperature (°C)	Time (days)	Calculated Gross Composition
853	Cobalt	1:0.888	775, later 700	27	Co_9S_8
854	Cobalt	1:1.333	575	11	Co_3S_4
803	Iron	1:1.01	1050	10	$Fe_{0.99}S$
850	Nickel	1:0.857	500	12	Ni_7S_6
852	Nickel	1:0.857	350	17	Ni_7S_6
597	Nickel	1:1	775	3	NiS
624	Nickel	1:1	815	0.25	NiS
631	Nickel	1:0.975	850	10	$NiS_{0.975}$
632	Nickel	1:0.99	850	10	$NiS_{0.99}$

(Continued on page 42)

TABLE 18

X-Ray Diffraction Analyses of Melt-and-Annealed Sulphides

Expt. No.	Phases Present	X-Ray Diffraction Report No.
853	Co_9S_8	72-015
854	Linnaeite a = 9.40 Å	71-957
803	Major - Monoclinic Pyrrhotite Minor - Troilite type ?	71-545 71-545
850	α-Ni_7S_6	71-941
852	β-Ni_7S_6	71-948
597	α-NiS	69-678
624	Not Analysed (a)	---
631	α-NiS (a)	71-488
632	Not Analysed (a)	---

(Continued on page 43)

TABLE 17 (Concluded)

Expt. No.	Metal	Metal:Sulphur Ratio	Annealing Temperature (°C)	Time (days)	Calculated Gross Composition
633	Nickel	1:1	850	10	NiS
634	Nickel	1:1.01	850	10	$Ni_{0.99}S$
635	Nickel	1:1.025	850	10	$Ni_{0.975}S$
675	Nickel	1:1	750	0.25	NiS
684	Nickel	1:1.07	700	11	$NiS_{1.07}$
793	Nickel	1:1	850	8	NiS
840	Nickel	1:1.015	800	7	$Ni_{0.985}S$
851	Nickel	1:1.015	300	14	$Ni_{0.985}S$
855	Nickel	1:1.333	340	10	Ni_3S_4

TABLE 18 (Concluded)

Expt. No.	Phases Present	X-Ray Diffraction Report No.
633	Not Analysed (a)	---
634	Not Analysed (a)	---
635	α-NiS	71-489
675	Used for melting under B_2O_3 (b)	---
684	Prepared as an analytical standard (c)	---
793	α-NiS	71-144
840	α-NiS	71-854
851	β-NiS (Millerite)	71-963
855	α-NiS and NiS_2	71-958

Notes: (a) = Used for thermoelectric power studies.
(b) = See sample #676 in Table 15.
(c) = Used as a standard in chemical and electron-microprobe work.

TABLE 19

Conditions Used for Melting and Annealing of Three-Component Sulphides

Expt. No.	Sulphide Attempted	Annealing Temperature (°C)	Time (days)
673	$(Ni_{0.99}Fe_{0.01})S$	850	10
698	$(Ni_{0.98}Fe_{0.02})S$	850	9
699	$(Ni_{0.97}Fe_{0.03})S$	850	9
686	$(Ni_{0.95}Fe_{0.05})S_{1.07}$	700	16
685	$(Ni_{0.90}Fe_{0.10})S_{1.07}$	700	16
674	$(Ni_{0.50}Fe_{0.50})S$	850	16
740 (a)	$(Ni_{0.99}Fe_{0.01})S$	800	6
751 (a)	$(Ni_{0.98}Fe_{0.02})S$	850	10
799 (a)	$(Ni_{0.96}Fe_{0.04})S$	840	12
822	$(Ni_{0.5}Fe_{0.5})_9S_8$	590	12

(a) = The iron was Fe^{57}-enriched to contain ~ 90% Fe^{57}.

Notes: (i) All of these products were either rough or grey at one end of the billet, visually indicating that some disproportionation had occurred.

(ii) These sulphides were submitted for thermoelectric power experiments.

TABLE 20

X-Ray Diffraction Analyses of Melt-and-Annealed Three-Component Sulphides

Expt. No.	Phases Present	X-Ray Diffraction Report No.
673	Not Analysed	---
698	Not Analysed	---
699	α-NiS	71-532
686	α-NiS	71-531
685	Not Analysed	---
674	Major - Pentlandite (a = 10.09 Å) and α-Fe Minor - Unidentified (see text)	71-530 71-530
740	Not Analysed	---
751	α-NiS and a small trace of Pyrrhotite	72-068
799	α-NiS	71-529
822	Pentlandite (a = 10.09 Å)	71-825

TABLE 21

Conditions Used in the Two-Stage Preparation of Some Sulphides

Expt. No.	Sought-after Sulphide	Nutrients	Temperature (°C)	Time (days)
835	Fe_3S_4	3FeS and S	190	22
839	Fe_3S_4	$3FeS_{1.25}$ and 0.25 S	190	12
841	Fe_3S_4	FeS_2 (pyrite) and Fe (a)	230	10
842	Fe_3S_4	FeS_2 (marcasite) (b) and Fe (a)	230	15
838	FeS_2 (marcasite)	$FeS_{1.25}$ and 0.75 S	300-400	36
865	Ni_3S_4	3 NiS and S	300	8
834	$FeNi_2S_4$	$FeNi_2S_3$ and S	300	29
861	$FeNi_2S_4$	$FeNi_2S_{3.18}$ and 0.82 S	300	7
868	$Fe_{0.97}Ni_{2.03}S_4$	$Fe_{0.97}Ni_{2.03}S_{3.11}$ and 0.89 S	425	21

(a) = The Fe was placed at the opposite end of the tube from the FeS_2.
(b) = This marcasite was a naturally-occurring sample containing a few per cent of pyrite.

TABLE 22

X-Ray Diffraction Analyses of the Two-Stage-Prepared Sulphides

Expt. No.	Phases Present	X-Ray Diffraction Report No.
835	Orthorhombic pyrrhotite and pyrite	71-899
839	Monoclinic pyrrhotite and a minor amount of pyrite	71-855
841	Pyrite	71-860
842	Marcasite and some pyrite	71-868
838	Pyrite and a minor amount of pyrrhotite	71-933
865	Millerite, polydymite, and α-NiS	72-041
834	Violarite (a = 9.45 Å), α-NiS, and some unidentified material	72-001
861	Violarite (a = 9.44 Å), α-NiS	72-023
868	Violarite (a = 9.44 Å), and α-NiS, and sl. trace of pyrite	72-082

Note: The analyses of Expts. #841 and #842 refer to the FeS_2 end of the tube.

The X-ray diffraction analyses of the products are shown in Table 22, which indicates that none of the desired sulphides was produced. The interpretation of these results appears to be that, in the case of violarite, Expts. #834 and #861, and of polydymite, Expt. #865, the rate of reaction is extremely slow at 300°C, which is the maximum permissible temperature in order to avoid disproportionation; therefore, a longer period of annealing may prove successful. An attempt to prepare a nickel-rich violarite, which is stable to approximately 460°C (23), was made in Expt. #868. The X-ray diffraction analysis showed that some α-NiS was present; this suggests that a longer period of annealing than that used in Expt. #868 is necessary. There is only a slight difference in the "a" value of the lattice between polydymite and violarite, as was shown by Craig (23), who reported that the cell dimensions of polydymite and violarite were $a = 9.489 \pm 0.003$ Å and $a = 9.465 \pm 0.003$ Å, respectively. Therefore, it is necessary to measurethis parameter and, by means of the "a" value, determine the presence and quantity of violarite in the sample.

The dry approach to the synthesis of marcasite, Expt. #838, produced pyrite preferentially, even in the temperature range where marcasite is stable, which suggests that marcasite is a metastable form of FeS_2. (Marcasite was successfully prepared by the hydrothermal technique, to be described later in this report.) The preparation of greigite and smythite was attempted by two approaches. The first by synthesis with pyrrhotite and sulphur, Expts. #835 and #839, which failed since only part of the nutrients were used up and pyrite appears as the only new product formed, indicating that the intermediate sulphides of iron may be metastable. (Greigite, and smythite to a much smaller degree, were successfully prepared by the hydrothermal technique, also to be described later.) The second approach, Expts. #841 and #842, was through an anticipated degradation reaction involving pyrite or marcasite, as shown in the following equation:

$$3FeS_2 + 2Fe^\circ \rightarrow Fe_3S_4 + 2FeS \qquad \text{(Eq. 1)}$$

Pyrite and marcasite were heated at a temperature of 230°C in an attempt to volatilize some sulphur which would then react with metallic iron located at the opposite end of the quartz capsule. The metallic iron was separated from the MS_2 by quartz wool and was heated at a higher temperature than that of the MS_2 zone. Unfortunately, it was found that the sulphur vapour pressure over pyrite or marcasite at 230°C was too low to give a significant rate of reaction. A calculation of the sulphur vapour pressure at this temperature, using Rosenqvist's data (4), showed it to be $\sim 1 \times 10^{-19}$ atm.

(b) Preparation of Sulphides by Growth Procedures

Four growth procedures have been used in this study. They will be discussed in turn.

(1) Vapour Transport (V.T.)

This technique relies on the sublimation of the sulphide from the warm zone of a sealed capsule tothe colder zone, as shown in Figure 10.

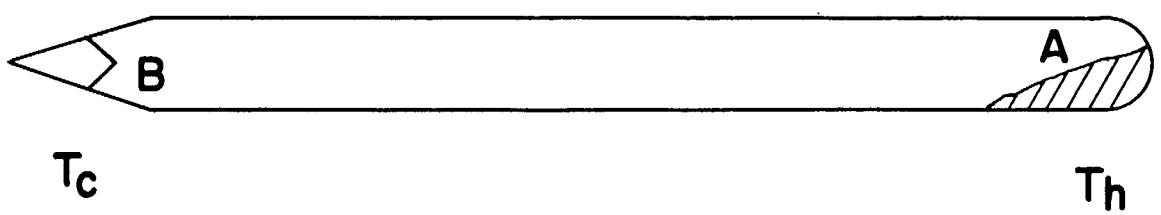

Figure 10. - Schematic Arrangement for Vapour Transport*

In Table 9, it is seen that Gamondes and Laffitte (27) reported the transfer of α-$Ni_{1-x}S$ from a nutrient temperature of 700 to 800°C to a growth

*The symbols T_h and T_c, used in this and subsequent diagrams, refer to the hot and cold zones of the tube, respectively. The difference between T_h and T_c is the temperature gradient.

temperature of 600 to 650°C, over a one-to-two-week period. When this experiment was tried in the present study, only an extremely minute amount of α-$Ni_{1-x}S$ had sublimed from 800°C with a 200-deg C temperature gradient, even after nineteen days. However, it was assumed that the difference between the two experimental results was probably due to a variation in the excess-sulphur concentrations.

The conditions used in the above experiment, and with several other sulphides, are shown in Table 23. At the conclusion of several of the experiments, there was excess sulphur (in the growth zone) which was leached by CS_2 from the transported product prior to the calculation of the growth rate. The X-ray diffraction analyses of these samples are shown in Table 24.

The mode of the vapour transport reaction is apparent from the monosulphide experiments, Expts. #820, #817, and #641, which indicated that, when the sulphur:metal ratio is approximately 1:1, very little transport occurred; however, the sulphur-rich monosulphide of iron was sublimed. Therefore, the vapour pressure of the sulphide, which obviously varies directly with the sulphur content, must be high enough to cause a significant rate of sublimation at the temperature used. A further clue is observed from Expt. #817, in which the transported and untransported materials were hexagonal pyrrhotite. In all the disulphide experiments, Expts. #819, #815, and #818, there was excess sulphur present in the growth zone at the conclusion of the experiments. This indicates that a dissociation had occurred; and, since one of the untransported products was a monosulphide of the $M_{1-x}S$ type, it is reasonable to assume that the key to the sublimation of all sulphides is the monosulphide. Therefore, it is assumed that the sublimation of the disulphides is via the sequence of the following three equations:

$$(1-x)MS_2 \rightarrow M_{1-x}S + \frac{(1-2x)}{2} S_2 \uparrow \quad \text{(dissociation)} \qquad \text{(Eq. 2)}$$

$$M_{1-x}S\,(\text{solid}) \rightleftarrows M_{1-x}S(\text{vapour}) \quad \text{(sublimation)} \qquad \text{(Eq. 3)}$$

$$M_{1-x}S\ (\text{vapour}) + \frac{(1-2x)}{2}\ S_2 \rightarrow (1-x)\ MS_2 \quad (\text{association}) \quad (\text{Eq. 4})$$

Based on the results obtained in Tables 23 and 24, it appears that the vapour transport technique has a limited application in the growth of crystals of cobalt, iron, and nickel sulphides.

(2) Chemical Vapour Transport (C.V.T.)

This procedure is based on a reversible chemical reaction occurring in a closed system. Usually, a halogen or a halogen compound is used to generate an intermediate volatile compound*. Two of the most often used reactions are as follows:

$$RS + 2HCl \rightleftarrows RCl_2 + H_2S \quad (\text{Eq. 5})$$

$$RS + I_2 \rightleftarrows RI_2 + 1/2\ S_2 \quad (\text{Eq. 6})$$

From Table 9, it is seen that Bouchard (28) applied this technique to the growth of FeS_2, CoS_2, and NiS_2. He used chlorine as the carrier.

In the present study, three different carriers have been used, viz., HCl, I_2, and Br_2. The tube design and the overall chemical reaction for this technique are shown in Figure 11.

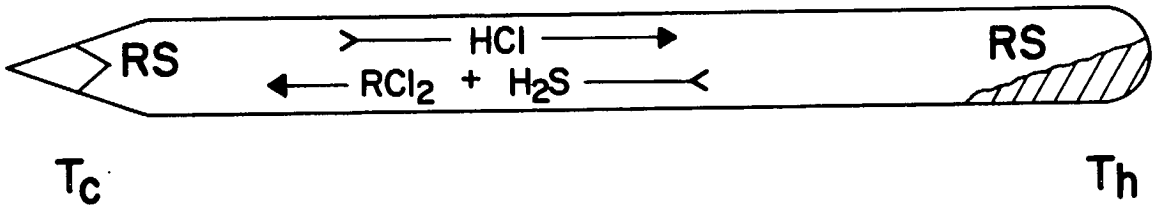

Figure 11. - Schematic Arrangement for Chemical Vapour Transport.

*Usually 5 mg/cm^3 of iodine, or 0.5 atm. pressure at R.T. of HCl gas, are employed.

TABLE 23

Condition Used for V. T. of Cobalt, Iron, and Nickel Sulphides

Expt. No.	Nutrient	Nutrient Temperature (°C)	Growth Temperature (°C)	Growth Rate (mg/hr)	Time (days)
819	$CoS_{2.053}$ (a)	789	400	0.099	14
820	FeS (b)	1150	1000	No Growth	4
817	$Fe_{0.910}S$	900	750	0.043	9
815	FeS_2 (c)	730	400	0.069	18
641	$Ni_{0.969}S$	800	600	No Growth	19
818	$NiS_{2.10}$ (a)	760	400	0.554	11

(a) = Excess sulphur present.
(b) = Troilite.
(c) = Naturally-occurring.

TABLE 24

X-Ray Diffraction Analyses of V. T. -Grown Cobalt, Iron, and Nickel Sulphides

Expt. No.	Phases Present	X-Ray Diffraction Report No.
819	Trans : Cattierite	71-804
	Untrans : $Co_{1-x}S$ and a minor amount of Co_9S_8	71-805
820	Not Analysed	---
817	Trans : Hexagonal Pyrrhotite	71-872
	Untrans : Hexagonal Pyrrhotite	71-873
815	Trans : Pyrite	71-792
	Untrans : Pyrite and Monoclinic Pyrrhotite	71-793
641	Not Analysed	---
818	Trans : Vaesite	71-794
	Untrans : Vaesite and α-NiS	71-795

Note: Trans = Transported Product, and Untrans = Untransported Product.

Although the silica capsule was pointed in the growth zone to enchance single-crystal growth, as described in Part I (1), this design did not result in the growth of any large single crystals of the sulphides included in the present report because many crystals tended to grow along the tube walls in the growth zone and not primarily at the tip of the tube, as was the case with ZnS (2).

Since the rate of growth was very slow - much slower than was observed for ZnS - the migration technique of moving the capsule slowly through the furnace to aid nucleation and growth was not advantageous; instead, a static temperature-gradient was preferred.

The conditions used to transport the monosulphides of cobalt, iron, and nickel are shown in Table 25. The X-ray diffraction analyses of the products are shown in Table 26.

The cobalt and nickel monosulphide nutrients were transported, but the products were a mixture of the desired monosulphide along with one or more other sulphides. The sulphur-rich pyrrhotites were readily transported by one of several carriers.

The quantity of transported $Fe_{1-x}S$ varied with the value of x. When the value of x was low, i. e., essentially stoichiometric FeS, extremely little transport occurred with either HCl or I_2, but, when x was approximately 0. 1, the rate of transport varied in an ascending order with the sequence HCl, I_2, and Br_2, i. e., bromine appears as the best carrier.

The transport problem of various $Fe_{1-x}S$ compositions was studied further when an attempt was made to transport FeS, troilite, with iodine (see, Expt. #774, Table 25). The transported product was soluble in methanol and was found to be sulphur-free but contained the same weight of iron as corresponds to the weight loss of the nutrient. Therefore, it must be assumed that all the original sulphur was retained by the nutrient residue; a calculation of the Fe:S ratio of the untransported residue shows it to be $Fe_{0.912}S$. This indicates that the following reaction has occurred:

$$FeS + xI_2 \rightarrow Fe_{1-x}S + xFeI_2 \uparrow \qquad \text{(Eq. 7)}$$

Also, as no $Fe_{1-x}S$ had been transported at the temperatures used in Expt. #774, it appears that the threshold value for x in $Fe_{1-x}S$, at which pyrrhotitic material can be transported, must be temperature-dependent, and that this critical condition was not satisfied.

The above results suggest that the mode of chemical vapour transport of the monosulphides could be as follows:

$$MS + xI_2 \rightarrow M_{1-x}S + xMI_2\uparrow \qquad \text{(Eq. 8)}$$

$$M_{1-x}S + (1-x)I_2 \rightleftarrows (1-x)\,MI_2 + 1/2\,S_2 \qquad \text{(Eq. 9)}$$

Transport is possible only if the iodine concentration and the reaction temperature are such that Equation 8 goes to completion, leaving some iodine for the chemical vapour transport as shown in Equation 9.

This phenomenon explains the situation which existed at the time of writing Part II of this series of reports, dealing with ZnS. It was stated therein that (FeS + ZnS) would not transport with iodine, but that ($FeS_{1.08}$ + ZnS) was transported. The explanation appeared to be that the FeS was absorbing all the free sulphur, as shown in the following equations:

$$xZnS + xI_2 \rightleftarrows xZnI_2 + (\tfrac{x}{2})\,S_2 \qquad \text{(Eq. 10)}$$

$$(1-x)\,FeS + (\tfrac{x}{2})\,S_2 \rightarrow Fe_{1-x}S \qquad \text{(Eq. 11)}$$

$$xZnS + (1-x)\,FeS + xI_2 \rightarrow xZnI_2 + Fe_{1-x}S \qquad \text{(Eq. 12)}$$

The value of x is dependent on two conditions; firstly, on the kinetics of Equation 10, to supply sufficient elemental sulphur, i.e., the concentration of the iodine and the temperature of this reaction; and secondly, on the partial pressure of sulphur over $Fe_{1-x}S$, which was shown to be temperature-dependent (see Figure 4). Therefore, if the iodine concentration and/or the

TABLE 25

Conditions Used for C. V. T. of Cobalt, Iron, and Nickel Monosulphides

Expt. No.	Carrier	Nutrient	Nutrient Temperature (°C)	Growth Temperature (°C)	Growth Rate (mg/hr)	Time (days)
811	I_2	CoS	850	550	0.91	7
805	I_2	$Co_{0.99}S$	850	700	No Growth	1
806	I_2	$Co_{0.88}S$	850	550	1.00	6
243	HCl	FeS	900	900→ 825 (a)	No Growth	5
254	HCl	FeS	800	800→ 725 (a)	No Growth	5
275	I_2	FeS	900	650	No Growth	8
774	I_2	$Fe_{0.998}S$	700	635	No Growth	3
821	I_2	$Fe_{0.998}S$	1000	650	2.80	3
816	I_2	$Fe_{0.95}S$	800	650	0.33	5
646	I_2	$Fe_{0.925}S$	800	680	0.34	11
643	Br_2	$Fe_{0.925}S$	800	680	1.00	18
426	HCl	$Fe_{0.91}S$	980	970→ 960 (a)	0.06	10
642	I_2	$Ni_{0.96}S$	800	550	0.22	20
648	Br_2	$Ni_{1.04}S$	800	700	0.28	13

(a) = A migration of the sample capsule was undertaken, causing the growth temperature to decrease gradually over this temperature range.

TABLE 26

X-Ray Diffraction Analyses of C. V. T. -Grown Cobalt, Iron, and Nickel Monosulphides

Expt. No.	Phases Present	X-Ray Diffraction Report No.
811	Trans = β-$Co_{0.91}S$, Co_9S_8, and (a) Untrans	71-612 71-613
805	Not Analysed	---
806	Trans = β-$Co_{0.91}S$, and a minor of CoS_2 Untrans = β-$Co_{0.91}S$	71-642 71-636
243	Not Analysed	---
254	Not Analysed	---
275	Not Analysed	---
774	Not Analysed	---
821	Trans = Monoclinic Pyrrhotite Untrans = Hexagonal Pyrrhotite	71-775 71-776
816	Trans Untrans = Hexagonal Pyrrhotite	71-634 71-635
646	Trans = Hexagonal Pyrrhotite (b)	70-33
643	Trans Untrans = Hexagonal Pyrrhotite	70-16 70-17
426	Trans Untrans = Pyrrhotite	68-1059 68-1060
642	Trans = α-NiS and Ni_3S_4 (Polydymite, a = 9.56 Å)	70-78
648	Trans = α-NiS and (c) Untrans = Ni_3S_2 (Heazelwoodite type ?), and Millerite	70-67 70-68

Note: Trans = Transported Product and Untrans = Untransported Product.
(a) and (c) = These are two different unidentified substances.
(b) This material has the same X-ray diffraction pattern as the nutrient, Expt. #356 - Table 10; therefore, it is assumed to have the same composition, $Fe_{0.92}S$.

temperature of the reaction were of such values as to cause the partial pressure of sulphur over $Fe_{1-x}S$ to be too low, then no transport of elemental sulphur to the cold end of the reaction tube could take place. Hence, Equation 10 could not reverse to deposit ZnS crystals at the cold end of the tube.

The intermediate sulphides were the next group to be attempted by an iodine transport. A synthetic mixture of iron and sulphur was prepared to yield Fe_2S_3 (see Expt. #258, Table 12). When this material was transported with iodine (see Expt. #662), as shown in Tables 27 and 28, pyrite was the growth product. Synthetic mixtures of $M_3:S_4$ for cobalt, iron and nickel were prepared in silica tubes with iodine and subjected to a growth transport under the conditions shown in Table 27. Whenever there was excess sulphur (in the growth zone) at the conclusion of the experiment, it was leached with CS_2 from the transported product before the calculation of the growth rate. The X-ray diffraction analyses of the products obtained in Table 27 are shown in Table 28. In all cases the disulphide was the transported product; the untransported product was a mixture of sulphides, the composition of which was dependent on the experimental conditions such as composition of the nutrient, temperatures, and time.

The conditions used for C. V. T. growth when the nutrients contained enough sulphur to yield the equivalent of stoichiometric MS_2, and, in some cases, sulphur in excess of MS_2, are shown in Tables 29, 31, and 33, for CoS_2, FeS_2, and NiS_2, respectively. At the conclusion of several of the experiments, there was excess sulphur (in the growth zone) which was leached with CS_2 from the transported product before the calculation of the growth rate. The results of the X-ray diffraction analyses are shown in Tables 30, 32, and 34, for CoS_2, FeS_2, and NiS_2, respectively.

The results obtained with the above series were similar to those shown in Table 28, the attempted intermediate sulphide growth experiments, in the following respects:

(i) The growth product was the disulphide.

(ii) The untransported residues were a mixture of the disulphide and the monosulphide.

(Continued on page 66)

TABLE 27

Conditions Used for Attempted C. V. T. Growth of Cobalt, Iron, and Nickel Intermediate Sulphides

Expt. No.	Metal	M:S ratio	Carrier	Nutrient Temperature (°C)	Growth Temperature (°C)	Growth Rate (mg/hr)	Time (days)
669	Cobalt	3:4	I_2	1000	780	0.29	7
344	Iron	3:4	I_2	715	625	Tube not opened	17
662	Iron	2:3	I_2	768	638	0.61	7
681	Nickel	3:4	I_2	900	680	0.22	7

Note: Crystals had grown in Expt. #344, but the tube was not opened.

TABLE 28

X-Ray Diffraction Analyses of the Attempted C. V. T. Growth Products of the Intermediate Sulphides

Expt. No.	Phases Present	X-Ray Diffraction Report No.
669	Transported Product = Cattierite	70-206
	Untransported Product = Linnaeite and Co_9S_8	70-207
344	Good-looking crystals of pyrite, but not analysed	---
662	Transported Product = Pyrite	70-230
	Untransported Product = Hex. Pyrrhotite and minor amount of Pyrite	72-007
681	Transported Product = Vaesite	70-365
	Untransported Product = α-NiS and Vaesite	70-356

TABLE 29

Conditions Used for C. V. T. of Cobalt Disulphide

Expt. No.	Carrier	Nutrient	Nutrient Temperature (°C)	Growth Temperature (°C)	Average Growth Rate (mg/hr)	Time (days)
365 (a)	I_2	CoS_2 (re-growth of flux-grown Expt. #350)	715	690		20
			815 (b)	790		21
			815 (b)	755	0.33	71
405	I_2	CoS + S (no excess S)	800	740		20
			850 (b)	790		10
			850 (b)	750	0.19	8
552	HCl	$CoS_{1.85}$ + S (1Mole S excess)	700	525		5
			800 (b)	400	No Growth	8
561 (a)	I_2	$CoS_{1.85}$ + S (1 Mole S excess)	800	500	No Growth	10
587 (a)	I_2	Co + 2S + slight excess sulphur	810	775		15
			910 (b)	865	No Growth	16
606	I_2	Co + 2S + slight excess sulphur	790	752		34
			840 (b)	800		18
			865 (b)	818	0.22	12

(a) = A quartz wool plug was used in these experiments.
(b) = Additional heating at these temperatures, and the corresponding growth temperatures.

TABLE 30

X-Ray Diffraction Analyses of C.V.T.-Grown Cobalt Disulphide

Expt. No.	Phases Present	X-Ray Diffraction Report No.
365	Transported Product = Cattierite Untransported Product = Cattierite	72-013 72-014
405	Transported Product = Cattierite	68-0943
552	No growth	---
561	No growth	---
587	Very little growth	---
606	Transported Product = Cattierite Untransported Product = Cattierite, Linnaeite, and an unidentified substance	69-896 60-897

TABLE 31

Conditions Used for C.V.T. of Iron Disulphide

Expt. No.	Carrier	Nutrient	Nutrient Temperature (°C)	Growth Temperature (°C)	Average Growth Rate (mg/hr)	Time (days)
343	I_2	FeS_2 (re-growth of flux-grown Expt. #319)	715	615	Tube not opened	20
396	I_2	$FeS_{1.1}$ + 0.9S	715	630		11
			750	665		7
			750	620	0.39	50
407	I_2	$FeS_{1.1}$ + 0.9 S	705	455	Tube not opened	26
428	I_2	FeS + S + H_2S (a)	715	630	No Growth	13
445	HCl	$FeS_{1.09}$ + 0.91 S	685	610	Tube not opened	46
414	I_2	$FeS_{1.1}$ + 0.9 S + slight excess S	432	408	0.016	12
519	HCl	FeS_2 + 1 Mole S in excess (regrowth of Expt. #444)	675	500		20
			700 (b)	525	Tube not opened	23
611	I_2	$FeS_{1.08}$ + 0.92 S + slight excess S	719	668		22
			730 (b)	679		10
			760 (b)	660	0.47	14
645	Br_2	FeS_2 (regrowth of Expt. #611)	250	195	No growth	13
862	I_2	FeS_2 (naturally-occurring)	750	610	0.44	6

(a) = Pressure of H_2S was 0.34 atm at room temperature.

(b) = Additional heating at these temperatures, with the corresponding growth temperatures.

Note: No wool plugs were used in any of these experiments.

TABLE 32

X-Ray Diffraction Analyses of C. V. T. -Grown Iron Disulphide

Expt. No.	Phases Present	X-Ray Diffraction Report No.
343	Good-looking crystals, not analysed	---
396	Transported Product = Pyrite Untransported Product, not analysed	68-0945
407	Good-looking crystals, not analysed	---
428	Transported Product = Sulphur (a) Untransported Product = Pyrite and a trace of Pyrrhotite	--- 68-1066
445	Good-looking crystals, not analysed	---
414	Transported Product = Unidentified substance (b) Untransported Product = FeS_2 + Pyrrhotite (minor)	68-0935 68-0938
519	Good-looking crystals, not analysed	---
611	Transported Product = Pyrite Untransported Product = Pyrrhotite + minor amount of Pyrite	69-898 69-899
645	No transported Product	---
862	Transported Product = Pyrite Untransported Product = Pyrrhotite and Pyrite	72-027 72-028

(a) = Determined by chemical analysis.
(b) = This product was probably a CS_2-insoluble form of sulphur.

TABLE 33

Conditions Used for C. V. T. of Nickel Disulphide

Expt. No.	Carrier	Nutrient	Nutrient Temperature (°C)	Growth Temperature (°C)	Average Growth Rate (mg/hr)	Time (days)
364(a)	I_2	NiS_2 (re-growth of flux grown Expt. #342)	715	690		20
			620 (b)	590		13
			815 (b)	790		21
			815 (b)	755	0.05	58
404	I_2	NiS + S	800	740		19
		(no excess S)	850 (b)	750	1.46	8
551	HCl	NiS + S	700	525		5
		+ 1 mole excess S	800 (b)	400	No Growth	13
563	I_2	NiS_2 + excess S (from Expt. #551)	800	500	Tube not opened	13
588 (a)	I_2	Ni + 2S + slight excess S	800	785		15
			885 (b)	865		6
			910 (b)	870	No Growth	10
605	I_2	NiS + S + slight excess	790	760		34
			840 (b)	815	1.76	17

(a) = A quartz wool plug was used in these experiments.
(b) = Additional heating at these temperatures, with the corresponding growth temperatures.

TABLE 34

X-Ray Diffraction Analyses of C. V. T. -Grown Nickel Disulphide

Expt. No.	Phases Present	X-Ray Diffraction Report No.
364	Transported Product = Vaesite and a trace of an unidentified substance	68-0952
	Untransported Product = Vaesite and a minor amount of α-NiS	68-0953
404	Transported Product = Vaesite	68-0944
551	No growth	---
563	Very small crystals, not analysed	---
588	No growth	---
605	Transported Product = Vaesite	69-866

(iii) At the conclusion of these experiments there was excess sulphur in the growth zone. It was assumed that, during the cooling period after the growing period had been terminated, some of the residual excess sulphur could have recombined with the untransported nutrient; however, it was general to find some of the excess sulphur in the elemental form.

The above results indicate that the mode of chemical vapour transport of nutrients that contain a metal to sulphur ratio of 1:1.33 to 1:2 + a, could be as follows:

$$(1-x)MS_y \rightarrow M_{1-x}S + \frac{(y-xy-1)}{2} S_2 \quad \text{(dissociation)} \qquad \text{(Eq. 13)}$$

$$M_{1-x}S + (1-x)I_2 \rightleftarrows (1-x)MI_2 + 1/2\, S_2 \quad \text{(transport)} \qquad \text{(Eq. 14)}$$

$$M_{1-x}S\,(\text{trans}) + \frac{(1-2x)}{2} S_2 \rightarrow (1-x)\, MS_2\,(\text{association}) \qquad \text{(Eq. 15)}$$

It is observed from the tables showing the conditions used in vapour transport and the chemical vapour transport that no extensive study of the effects of the growth parameters, such as the range of nutrient temperature, the magnitude of temperature gradients, sulphur partial pressure, and presence of foreign gases, were undertaken. However, it is seen that the growth rate when iodine was used as the carrier, is generally three to eight times larger for the growth of $Fe_{1-x}S$, CoS_2, FeS_2, and NiS_2, than is produced by vapour transport under the same general conditions.

With the limited number of experiments involving excess sulphur over the requirement for MS_2, the results were inconclusive; but, in general, excess sulphur tended to impede the growth reactions.

Plugs of loosely-packed quartz wool were placed next to the nutrient in some of the experiments. Their purpose was to prevent dusting of the sample during the preparation step and in the growth step. In the latter step, particles of the nutrient sticking to the tube in the growth zone would act as

unwanted additional nucleation sites. In the limited number of experiments involving these plugs, it was found that they tended to impede, and in some cases prevent, the growth reaction. It is possible that the variation in this effect may have been due to the degree of compactness of the plugs, which could vary considerably. These findings are opposite to those found in ZnS (2) growth reactions, which were described as occurring by diffusion; therefore, the transport of cobalt, iron, and nickel sulphides would appear to be principally by the convection process.

The growth products were composed of a large number of small crystals, 3 mm^3 and less in size, that had grown along the wall of the silica capsule in the growth zone. The FeS_2 crystals were larger than those of either CoS_2 or NiS_2, when grown at the same temperature and for the same time. Iodine was a successful carrier for all three disulphides, but HCl was successful only with FeS_2. The reason for this is, undoubtedly, the high boiling point of $CoCl_2$ and the high sublimation point of $NiCl_2$, which are 1049°C and 973°C, respectively; whereas $FeCl_2$ sublimed at the growth temperature used in most of the experiments. A low-temperature transport of FeS_2, Expt. #645, was undertaken using Br_2, with the objective of growing marcasite; however, no transport occurred.

As noted above, the growth products were composed of a large number of small crystals. None of the conditions used seemed to control this rampant nucleation. Bouchard (28), in his preparation of the disulphides using a chlorine transport, described a method of cycling by reversing the temperature of the nutrient and the growth zones; in this way only the large crystals would survive. He used periods of 16 hours and 8 hours per day during the initial days, for the transport and for the reverse transport, respectively. This procedure has not been utilized in the present study.

3. Flux Growth

Fluxing involves changing from a one-component to a two-component system and, thereby the lowering of the melting point; alternatively, it can be considered as the dissolution of the nutrient in a molten salt. When

the temperature of the fusion mixture is lowered, the dissolved nutrient is deposited as crystals.

The majority of fluxes used in crystal growing are low-melting halides. A mixture of two or more salts often forms a eutectic that has a lower melting point than that of either of the end members.

A useful reference is "Kristallisation,von Disulfiden aus Schmelzlösengen", by K.-Th. Wilke, D. Schultze and K. Töpfer (32); this paper describes the growth of the metal disulphides having the pyritic structure from a lead chloride flux in sealed silica capsules, under an atmosphere of sulphur vapour.

In the present investigation, four fluxes were used. In the growth experiments involving the following fluxes : $PbCl_2$, 50 NH_4Cl : 50 LiCl, and 59 LiCl : 41 KCl, the reactions were contained within evacuated and sealed quartz capsules. In the growth experiments involving $SnCl_2$ as flux, the reaction was performed in an open quartz boat using a controlled atmosphere and in a constant-pressure system.

The sealed capsule, as shown in Figure 12, is placed in an oblique position in a furnace; this keeps the molten salt C at the rounded end of the tube. If the crystals are grown in an atmosphere of excess sulphur, then the pressure in the tube (and over the molten salt) is controlled by the temperature at D, the coldest part of the tube. The letters A and B show the location of the undissolved nutrient and the growing crystals, respectively.

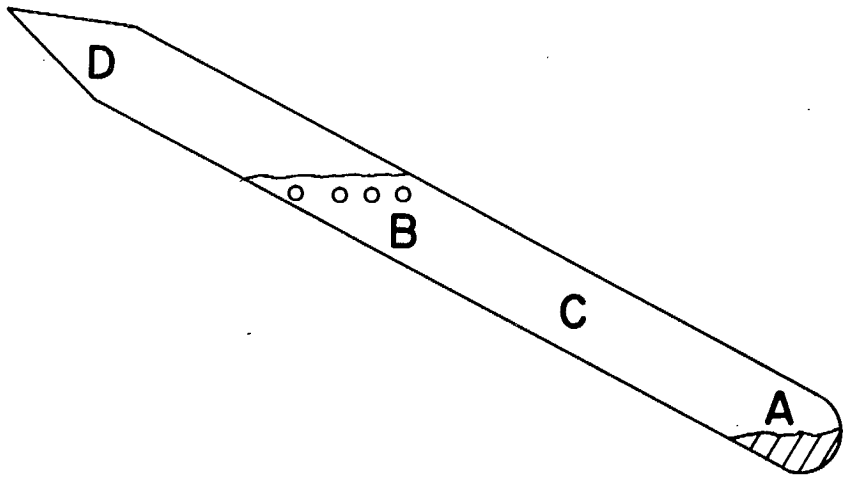

Figure 12. Schematic Arrangement for Flux Growth.

The usual procedure is to heat the silica capsule to a temperature about 250 °C above the melting point of the flux and, after holding the temperature constant for several hours to ensure maximum solubility, the tube is cooled stepwise (1 to 6 °C per hr) for several hours during the day, followed by a constant-temperature period during the night. This cooling cycle is repeated several times until the melting point of the flux is reached. After cooling more rapidly to room temperature, the tube is then cut open with a diamond saw. The frozen salt mixture is leached from the crystals with water or acid, the choice depending on the nature of the crystal and the flux involved.

The flux growth studies will be presented in four parts.

(i) $PbCl_2$-Flux Growths with Two-Component Systems

The procedure followed in the present study was similar to that used by K.-Th.Wilke et al. (32) and good single crystals of CoS_2, FeS_2, and NiS_2, having the pyrite structure, were prepared.

The nutrients were prepared in the ratio of 1 mole of metal to 3 moles of sulphur or 1 mole of the monosulphide to 2 moles of sulphur; i.e., excess sulphur was used in all cases.

The nutrient was combined with the $PbCl_2$ flux in the ratio of 1 mole of nutrient to 2-plus moles of flux in a quartz tube (13 mm I.D.) and sealed under a vacuum.

Crystal growth was achieved by controlling the rate of cooling, either manually or automatically with a programmed controller. In the former case, the flux mixture was heated to 750°C, then cooled step-wise at 5 °C each hour for several hours during the daytime, followed by a constant period overnight. This cooling cycle was repeated several times until a temperature of 520°C was reached, and then the tube was cooled rapidly to room temperature. Alternatively, the automatic programmed controller permitted a constant cooling rate of 0.5 to 6 °C per hour throughout the experiment.

The flux was removed from the crystals by leaching with a hot acidic solution, then with hot water, and finally with methanol.

(Continued on page 76)

TABLE 35

Conditions Used for Flux ($PbCl_2$)-Growth of Cobalt Disulphide

Expt. No.	Ratio of Flux to Nutrient	Nutrient (mole ratios)	Starting Temperature (°C)	Cooling Rate (°C per hr)	Time (days)
350	2.43:1	Co powder and 3 S	750	5 (a)	4
609	2.56:1	Co plate and 3 S	700	5 (a)	12
687	2.93:1	Co wire and 3 S	550	static	8
754	5.63:1	CoS and 2 S	750	0.5 (b)	21

(a) = Manually controlled.
(b) = Programmed controller used.

TABLE 36

X-Ray Diffraction Analyses of Flux ($PbCl_2$)-Grown Cobalt Disulphide

Expt. No.	Phases Present	X-Ray Diffraction Report No.
350	Cattierite	68-0429
609	Cattierite	69-837
687	Major product = Linnaeite	70-463
	Minor product = $Co_{1-x}S$ type	70-463
754	Cattierite	71-224

TABLE 37

Conditions Used for Flux ($PbCl_2$)-Growth of Iron Disulphide

Expt. No.	Ratio of Flux to Nutrient	Nutrient (mole ratios)	Starting Temperature (°C)	Cooling Rate (°C/hr)	Time (days)
319	2:1	Fe and 3 S	770	5 (a)	3
332	2:1	Fe and 3 S	750	5 (a)	5
438	2.6:1	Fe and 3 S	750	5 (a)	9
679	2.8:1	Fe and 3 S	740	1 (b)	10

(a) = Manually controlled.
(b) = Programmed controller used.

TABLE 38

X-Ray Diffraction Analyses of Flux ($PbCl_2$)-Grown Iron Disulphide

Expt. No.	Phases Present	X-Ray Diffraction Report No.
319	Pyrite	68-0130
332	Not Analysed	---
438	Not Analysed	---
679	Not Analysed	---

Note: See Table 74 for the electron-microprobe analysis of samples #332, #438, and #679.

TABLE 39

Conditions Used for Flux ($PbCl_2$)-Growth of Nickel Disulphide

Expt. No.	Ratio of Flux to Nutrient	Nutrient (mole ratios)	Starting Temperature (°C)	Cooling Rate (°C/hr)	Time (days)
342	2.04:1	Ni powder and 3 S	750	5 (a)	5
610	3.07:1	NiS and 2 S	700	5 (a)	11
683	2.76:1	Ni wire and 3 S	750	1 (b)	14
753	4.97:1	Ni wire to NiS and 2 S	750	0.5 (b)	21

(a) = Manually controlled.
(b) = Programmed controller used.

TABLE 40

X-Ray Diffraction Analyses of Flux ($PbCl_2$)-Grown Nickel Disulphide

Expt. No.	Phases Present	X-Ray Diffraction Report No.
342	Grey material = Vaesite	69-12
	Yellow material = α-NiS and Polydymite	69-13
610	Major product = Vaesite	69-838
	Minor product = α-NiS	69-838
683	Incomplete reaction, not analysed	---
753	Crystals = Vaesite	72-076
	Lumpy material = Vaesite, α-NiS, and a trace of unidentified material	71-115

The product was composed of many crystals 3 mm^3 or less in size. The crystal phase(s) were identified by X-ray diffraction analysis.

The experimental conditions used for growth of the disulphides of cobalt, iron, and nickel are shown in Tables 35, 37, and 39, respectively. The results of the X-ray diffraction analyses are in Tables 36, 38, and 40, respectively.

Additional analyses, to be presented later, include X-ray fluorescence which showed some lead to be present in all the samples tested, (see Table 76). The electron microprobe has proved that the lead is in the form of inclusions of $PbCl_2$ (see Table 74).

Originally, (1), it had been hoped that, if the rate of cooling could be controlled at a constant and somewhat slower rate than was possible by the manual approach, this problem could have been eliminated. However, when the most recent disulphides, obtained through slow cooling using the programmed controller, were analysed for lead, using an atomic-absorption spectrophotometric technique, the following lead values were found, as shown in Table 41.

TABLE 41

Lead Analysis by Atomic-Absorption Spectrophotometry of Some Disulphides

Expt. No.	Disulphide	Lead (%)
754(a)	CoS_2	1.46
679 (b)	FeS_2	0.99
753 (c)	NiS_2	1.16

(a) = See Table 35.
(b) = See Table 37.
(c) = See Table 39.

(ii) Partial Phase Diagrams of the MS_2 - $PbCl_2$ Systems

In order to ascertain the reason for the lead inclusions, a partial phase-diagram study of the FeS_2 - $PbCl_2$ system was undertaken. Five mixtures of crushed FeS_2 (obtained from a previous experiment) with an equivalent molar amount of sulphur were added to $PbCl_2$ in a silica tube and sealed under a vacuum. The capsules were heated at 750°C for 24 hours and then air-quenched. The solidus and liquidus temperatures were determined visually as the capsule was heated slowly at 4 °C per min. The visibility of the melting phenomenon was obscured somewhat by the dark-coloured solutions also partly by the sulphur vapour.

The results shown in Figure 13 indicate that the liquidus temperature is constant at a figure of about 610°C over the FeS_2 concentration range of 10 to 50 mol %. This means that, on cooling a flux mixture in this range of concentration, the crystals of FeS_2 would not form above 610°C. The shape of the liquidus curve in Figure 13 indicates that the rate of precipitation, or crystal growth, would be very rapid after cooling to just below 610°C. The net result is that some entrapment of the $PbCl_2$ flux would certainly occur. However, it is anticipated that, by careful control of the cooling from 610 to 500°C, and with periods of constant temperature, larger crystals, with less entrapped $PbCl_2$, might be achieved in the future.

A comparison of the CoS_2 - $PbCl_2$, FeS_2 - $PbCl_2$, and the NiS_2 - $PbCl_2$ systems is shown in Figure 14. Additional points for the CoS_2 - $PbCl_2$ and NiS_2 - $PbCl_2$ systems were not obtained due to the limited amount of the CoS_2 and NiS_2 materials on hand. However, the results indicate that the liquidus temperatures, at the concentration tested, form a decreasing sequence in the order: iron, cobalt, nickel. It is assumed that the overall curves would follow the same pattern as the FeS_2 - $PbCl_2$ curve.

The conclusions of this study are, firstly, that crystals of CoS_2 and NiS_2 would not form above 560°C and 540°C, respectively. This fact explains the smaller size and the greater lead entrapment compared with the corresponding FeS_2 crystals and, secondly, that, even

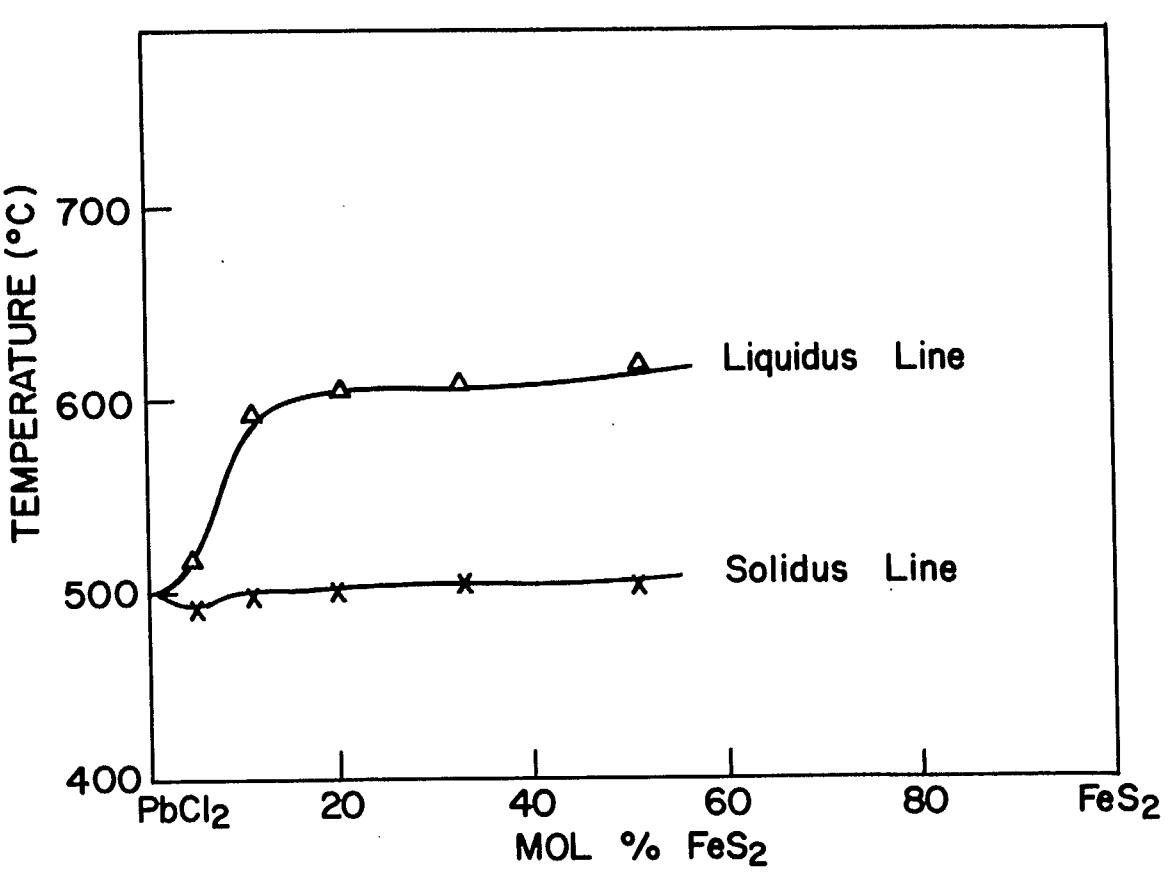

Figure 13. - Partial Phase Diagram of the $PbCl_2$ - FeS_2 system.

with further control of the cooling temperatures, there is less possibility of success in obtaining larger and purer crystals with CoS_2 and NiS_2 than with FeS_2.

(iii) $PbCl_2$ -Flux Growths with Three-Component Systems

An attempt was made to prepare bravoite $(Ni_{0.5}Fe_{0.5})S_2$ and cobaltian pyrite $(Co_{0.7}Fe_{0.3})S_2$ by the flux-growth technique. Since these compounds are analogous to pyrite, a similar growth approach, using a $PbCl_2$ flux, was explored. The experimental conditions are shown in Table 42, and the X-ray diffraction analyses of these products are shown in Table 43.

A partial explanation of the results obtained on Expt. #598 is found by referring to Figure 8, in which Clark and Kullerud (6) showed that bravoite is stable up to only 137°C. However, because a minor amount of bravoite was

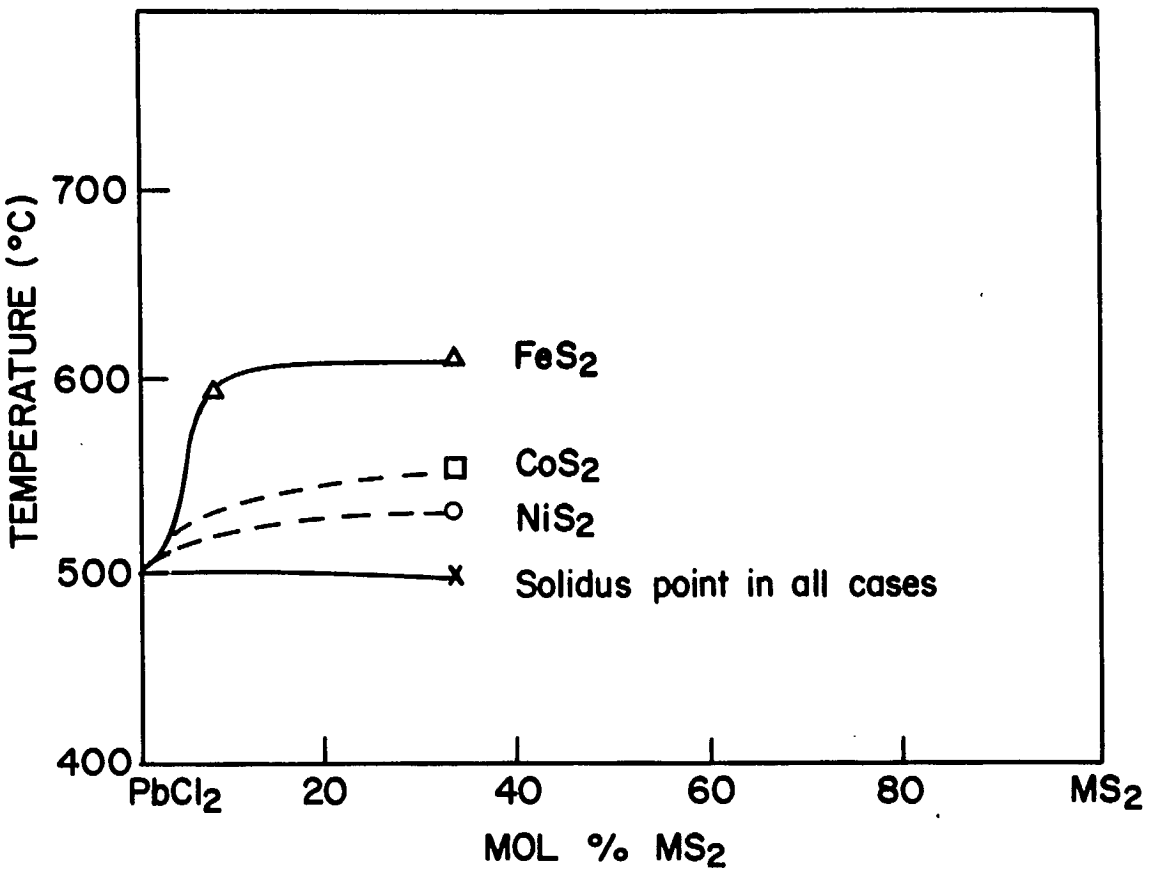

Figure 14. - Comparison of the Partial Phase Diagrams of the FeS_2-$PbCl_2$, CoS_2-$PbCl_2$, and NiS_2-$PbCl_2$ Systems.

obtained in Expt. #598, it indicates that bravoite can be formed at a much higher temperature than 137°C. The explanation of this fact might be similar to Klemm's conclusion to his investigations, viz., "that most bravoites are merely zoned or statistic mixtures of the natural-limit solid solutions which lie close to the points of the triangular diagram". Therefore, it would appear that the bravoite in Expt. #598 is probably a solid solution of the phases FeS_2 and NiS_2.

The electron-microprobe analyses of Expt. #598 and #603 will be given in Table 75 (see page 130).

(iv) Other Fluxes

In order to avoid flux-metal contamination, like-metal chloride fluxes were considered, e.g., $FeCl_2$ for FeS_2; $CoCl_2$ for CoS_2; and $NiCl_2$ for NiS_2.

TABLE 42

Conditions Used for Flux ($PbCl_2$)-Growth of $(Ni_{0.5}Fe_{0.5})S_2$ and $(Co_{0.7}Fe_{0.3})S_2$

Expt. No.	Nutrient (mole ratios)	Starting Temperature (°C)	Cooling Rate (°C/hr)	Time (days)
598	(1Ni : 1Fe) : 3 S	750	5 to 640°C (a)	7
603	(7Co : 3Fe) : 3 S	700	5 to 500°C (a)	10

(a) = Manually controlled

TABLE 43

X-Ray Diffraction Analyses of Flux ($PbCl_2$)-Grown $(Ni_{0.5}Fe_{0.5})S_2$ and $(Co_{0.7}Fe_{0.3})S_2$

Expt. No.	Phases Present	X-Ray Diffraction Report No.
598	Golden material = Major : Pyrite Minor : Bravoite and an unidentified substance	69-744
	Blackish material = Vaesite and a trace of an unidentified substance	69-745
603	Large crystal = Linnaeite and unidentified substance	69-795
	Small crystals = Linnaeite and an unidentified substance	69-796
	Fines = Linnaeite and an unidentified substance	69-794

Note: The unidentified substance in 69-794 is similar to that in 69-796, but it is different from that in 69-795.

The application of these chlorides was precluded by two factors: (1), they are very hygroscopic and would require special drying procedures in an HCl atmosphere, and (2), the possibility that the solubility of the sulphides in the chlorides would be too low to allow crystal growth by this procedure (private communication from A.H. Webster, Physical Chemistry Group, Mineral Sciences Division).

The growth of FeS_2 crystals by the use of three other fluxes was explored briefly. The chief advantage in using these fluxes was their low melting points. Stannous chloride ($SnCl_2$) has a melting point of 246°C. Boorman (40) quotes the work of Delarue (41), who used two low-melting salt systems: (i), KCl-LiCl (eutectic at 358°C; 41 mole percent (KCl), and (ii), NH_4Cl-LiCl (eutectic at 267°C; 50 mole percent NH_4Cl).

The experimental conditions are shown in Table 44 and the X-ray diffraction analyses of these products are shown in Table 45. In the case of $SnCl_2$, where the system was open, the reaction must have been as given in Equation 16:

$$FeS_2 + 2SnCl_2 \rightarrow 2SnS + FeCl_3\uparrow + 1/2Cl_2\uparrow \qquad \text{(Eq. 16)}$$

Although the experiment failed to produce FeS_2, it did yield SnS, herzenbergite.

The salt mixture $50NH_4Cl$: 50LiCl, (see Expt. #599), gave a good yield of pyrite. It was anticipated that, at a melt temperature of 300°C, marcasite (FeS_2) might have been produced but none was detected by X-ray diffraction analysis.

The value of the third flux, 59LiCl : 41KCl, was not determined because, in the first sample, Expt. #502, natural pyrite was used as the nutrient, thereby making it impossible to determine if there was a growth product or only the nutrient present after the growth run. In the second sample, Expt. #525, the tube blew up due to excessive sulphur vapour pressure.

The application of the fluxes $SnCl_2$ and $50NH_4Cl$: 50LiCl for the growth of β-Ni_7S_6, which has a range of temperature stability from room temperature to 379°C, was unsuccessful. Stannous chloride, when heated

TABLE 44

Conditions Used for Miscellaneous Flux Growth of Iron Disulphide

Expt. No.	Flux	Nutrient (mole ratios)	Temperature (°C)	Cooling Programme	Time
500A	$SnCl_2$	FeS_2 (a)	390	(b)	1 hour
500B	$SnCl_2$	FeS_2 (a)	420	(b)	1 hour
599	$50NH_4Cl$: 50LiCl	Fe and 3 S	300	(c)	6 days
502	59LiCl : 41KCl	FeS_2 (a)	400	(d)	10 days
525	59LiCl : 41KCl	Fe and 3 S	685	(e)	< 1 day

(a) = Naturally-occurring pyrite.
(b) = The temperature was held constant over the time interval recorded above and then decreased quickly to room temperature.
(c) = Manually controlled, 5°C decrease in temperature in the early morning and again the late afternoon, followed by a few days at constant temperature; this cycle was repeated several times.
(d) = The temperature was held constant for 7 days and then decreased manually at the rate of 10°C (once each day) for the remaining 3 days.
(e) = The tube blew up.

TABLE 45

X-Ray Diffraction Analyses of Miscellaneous Flux Growths of Iron Disulphides

Expt. No.	Phases Present	X-Ray Diffraction Report No.
500A	Pyrite and a small amount of iron chloride	69-59
500B	SnS_2 (Herzenbergite)	69-62
599	Pyrite	69-738
502	Pyrite	69-137
525	Tube blew up	---

to 380°C and cooled slowly to 220°C over a period of three hours, failed to dissolve any of a piece of solid Ni_7S_6 (55 mg). Similarly, $50NH_4Cl$: 50LiCl, when heated to 315°C and cooled slowly to 265°C over a period of six days, failed to dissolve any of the same piece of solid Ni_7S_6 (55 mg).

The full potential of these low-melting salt systems was not assessed by any partial phase-diagram studies as was done with $PbCl_2$. However, due to their attractive low melting points, these fluxes merit more detailed investigation in the future.

4. Hydrothermal Growth

Hydrothermal crystallization is defined as the use of an aqueous solvent under high temperature and pressure to increase the solubility of the substance to be grown to a level that causes single crystals to be deposited at the coldest part of the system.

Some useful references to previous hydrothermal studies are shown in Table 46.

The majority of the hydrothermal experiments in the present study were conducted in Pyrex tubing, 8 mm I. D. with walls 3 mm thick. The length of the sealed tubes varied from 15 to 30 cm. In all cases, the solutions filled 60% to 70% of the available volume of the tubes at room temperature.

TABLE 46

References to Previous Hydrothermal Growth Studies

Compounds Grown	References	
Pyrite and Marcasite (FeS_2)	Allen, Crenshaw, Johnston, and Larsen	(20)
Pyrite (FeS_2)	Barnard	(42)
Mackinawite (FeS)	Evans, Milton, Chao, Adler, Mead, Ingram, and Berner	(43)
Greigite (Fe_3S_4)	Uda	(11)
Smythite (Fe_3S_4)	Rickard	(48)

The charged tube was cooled in an ice bath, and sealed while being pumped with a water aspirator; the pressure was ~10 mm Hg. These tubes could be heated safely to about 250°C but, for protection against a possible explosion that could result from a failure of the sealed tube, an iron-pipe jacket was used to enclose the glass tube during the heating stage. However, these protective jackets have the disadvantage that rapid quenches of the enclosed tube are precluded because of the time-delay required to cool the protective jackets. This condition was found to be particularly detrimental in the greigite preparations.

The presentation of the results obtained from the growth experiments is made difficult due to the variety of nutrients used, the overall conditions employed, and also by the fact that most growth products were mixtures of sulphides. However, the results will be presented on the basis of the nutrients used and on the acidic condition of the nutrient medium.

(i) Metallic Iron in Aqueous Hydrogen Sulphide

Berner (44) described a procedure for preparing mackinawite, a tetragonal form of FeS. The formation is based on the following equation:

$$Fe^{o} + H_2S_{aq} \xrightarrow{R.T.} FeS + H_2\uparrow \qquad \text{(Eq. 17)}$$

During the present study, this experiment was allowed to run for sixty hours; the reaction tube was then opened and the resultant solution was filtered. The dried product was composed of both coarse and fine particles. X-ray diffraction analyses showed both fractions to be similar in composition, as shown in Table 47.

These results show that mackinawite did form, but that it was contaminated with at least three other materials. No attempt was made to remove these contaminants because, in order to achieve this separation, it would have been necessary to have more information on the exact chemical and physical properties of mackinawite.

TABLE 47

X-Ray Diffraction Analysis of a Mackinawite Preparation

Particle Size	Phases Present	X-Ray Diffraction Report No.
Coarse	Mackinawite, FeS Pyrrhotite, $Fe_{1-x}S$ Trace of α-Fe Trace of an unidentified material	68-0145
Fine	Mackinawite, FeS Pyrrhotite, $Fe_{1-x}S$ Trace of α-Fe Trace of an unidentified material	68-0146

(ii) Ferrous and/or Ferric Iron in Aqueous Sodium Sulphide

Several experiments were made using either a ferrous or a ferric iron solution with aqueous sodium sulphide; the conditions used for growth and the X-ray diffraction analyses are shown in Tables 48 and 49.

A second group of experiments was conducted involving a mixture of both ferrous and ferric iron solutions with aqueous sodium sulphide; the conditions used for growth and the X-ray diffraction analyses are shown in Tables 50 and 51.

In some cases, crystals of calcite were added in an attempt to seed the solution, with the objective of obtaining rhombohedral crystals of smythite, (Fe_3S_4). However, the results indicate that the calcite served no useful purpose under the conditions used.

Rickart (48) used ferrous carbonate and sodium sulphide under various acidic conditions to obtain smythite; unfortunately, ferrous carbonate was not available in the present investigation.

The growth products are recorded in the order of abundance, as indicated by the X-ray diffraction analysis. The size of all the products obtained hydrothermally, except marcasite (see Figure 22), was very much less than 1 mm^3.

A study of Tables 49 and 51 shows that seven different sulphides were formed, but always as mixtures of two or more sulphides.
It can be deduced that:

(1) ferrous iron yielded pyrrhotite, pyrite, and greigite;

(2) ferric iron yielded pyrite and marcasite;

(3) mixtures of ferrous and ferric iron gave varying combinations of pyrite, pyrrhotite, troilite, marcasite, greigite, and smythite.

Some of the important variables appear to be:

(1) the length of the heating time : some sulphides do not survive long heating times, e.g., greigite;

(2) the growth temperature : the thermal stability of some sulphides required careful temperature control at a definite range, e.g., greigite, which appears to form at both room temperature and 190° $\pm$ ~10°C.

(Continued on page 92)

TABLE 48

Conditions Used for Hydrothermal Growth Involving Ferrous or Ferric Iron with Aqueous Na_2S

Expt. No.	Fe^{++} (a) (moles)	Fe^{+++} (b) (moles)	$S^{=}$ (c) (moles)	H_2O (ml)	Fe:S	Temperature (°C)	Time (hr)
313A	0.00045	---	0.0006	6.0	1:1.33	190	48
313B	0.00045	---	0.0006	6.0	1:1.33	250	70
313C	0.00045	---	0.0006	6.0	1:1.33	160	70
330A	0.0003	---	0.0004	4.0	1:1.33	R.T.	144
330B	0.0003	---	0.0004	4.0	1:1.33	190	1
331A (d)	0.0003	---	0.0004	4.0	1:1.33	190	< 0.5
331B (d)	0.0003	---	0.0004	4.0	1:1.33	R.T.	144
465	---	0.0009	0.0006	6.0	1:0.67	190	192
831	0.00255	---	0.00383	5.0	1:1.5	190	288
832	---	0.0024	0.0048	5.0	1:1.99	190	288
858	0.0015	---	0.0020	5.0	1:1.34	190 (e)	1
867	0.0005	---	0.0007	8.0	1:1.42	190 (e)	288
876	0.0044 (f)	---	0.0079	5.0 (g)	1:1.8	R.T.	67

(a) = The salt $Fe(NH_4)_2(SO_4)_2 \cdot 6H_2O$ was used.
(b) = The salt $Fe_2(SO_4)_3 \cdot 7.6\,H_2O$ was used.
(c) = The salt $Na_2S \cdot 9H_2O$ was used.
(d) = Calcite was used as a seed crystal.
(e) = After heating, this product was quenched as quickly as possible in ice water.
(f) = The salt $FeSO_4 \cdot 7H_2O$ was used.
(g) = Dilute HCl was added dropwise to achieve a pH of ~ 6.

TABLE 49

X-Ray Diffraction Analyses of Hydrothermal Growth Involving Ferrous or Ferric Iron with Aqueous Na_2S

Expt. No.	Phases Present	X-Ray Diffraction Report No.
313A	Hexagonal Pyrrhotite and an unidentified substance	68-0020 68-0059
313B	Monoclinic Pyrrhotite and Pyrite	68-0026 68-0060
313C	Hexagonal Pyrrhotite and an unidentified substance	68-0051 68-0079
330A	Sulphur	68-0193
330B	Hexagonal Pyrrhotite	68-0194
331A (a)	Tube blew up	---
331B (a)	Sulphur	68-0200
465	Metallic-looking material = Pyrite, Hematite, Marcasite White material = $FeSO_4 \cdot H_2O$	68-1191 68-1190
831	Pyrite, Spinel (a = 8.32 Å), and some Pyrrhotite	71-851
832	Pyrite, Pyrrhotite, and some Marcasite	71-852
858	Greigite, and a trace of Pyrrhotite	71-953
867	Pyrite, Marcasite, and a trace or Greigite	72-070
876	Greigite, Pyrite, and some Sulphur	72-113

(a) = Calcite was used as a seed crystal. Note: The products are recorded in order of abundance.

TABLE 50

Conditions Used for Hydrothermal Growth Involving Ferrous and Ferric Iron with Aqueous Na_2S

Expt. No.	Fe^{++} (a) (moles)	Fe^{+++} (b) (moles)	$S^{=}$ (c) (moles)	H_2O (ml)	Fe:S	Temperature (°C)	Time (hr)
464	0.0003	0.0003	0.0006	6.0	1:1	190	24
466 (d)	0.0003	0.0003	0.0006	6.0	1:1	190	192
478A	0.00026	0.00024	0.0005	5.0	1:1	190	144
478B	0.00026	0.00024	0.0005	5.0	1:1	190	3
478C	0.00026	0.00024	0.0005	5.0	1:1	R.T.	144
492A (d)	0.00026	0.00024	0.0005	5.0	1:1	190	216
492B	0.00026	0.00024	0.0005	5.0	1:1	190	216
507A	0.0004	0.0001	0.0010	4.5	1:2	190	360
507B (d)	0.0004	0.0001	0.0010	4.5	1:2	190	360
507C (d)	0.0005	0.00012	0.0010	5.0	1:1.6	190	360
507D (d)	0.0006	0.00015	0.0010	5.5	1:1.33	190	360
507E	0.0006	0.00015	0.0010	5.5	1:1.33	190	360
833	0.0013	0.00195	0.0058	5.0	1:1.78	190	288

(a) = The salt $Fe(NH_4)_2(SO_4)_2 \cdot 6H_2O$ was used.

(b) = The salt $Fe_2(SO_4)_3 \cdot 7.6H_2O$ was used.

(c) = The salt $Na_2S \cdot 9H_2O$ was used.

(d) = Calcite was used as a seed crystal.

TABLE 51

X-Ray Diffraction Analyses of Hydrothermal Growth Involving Ferrous and Ferric Iron with Aqueous Na_2S

Expt. No.	Phases Present	X-Ray Diffraction Report No.
464	Pyrrhotite, and Pyrite	68-1162
466 (a)	Greigite, Pyrite, and Pyrrhotite	68-1189
478A	Pyrite, and Pyrrhotite	68-1233
478B	Pyrite, Troilite, and Marcasite	68-1234
478C	Sulphur	68-1235
492A (a)	Pyrite, and Pyrrhotite	69-29
492B	Pyrite, Pyrrhotite, and Greigite	69-30
507A	Pyrite, Pyrrhotite, and Greigite	69-159
507B (a)	Pyrite, Pyrrhotite, and Greigite	69-160
507C (a)	Pyrrhotite, Pyrite, Greigite, and Smythite	69-161
507D (a)	Pyrrhotite, Pyrite, Greigite, and Smythite	69-162
507E	Pyrite, Pyrrhotite, Greigite, and Smythite	69-163
833	Spinel (a = 8.32 Å), Pyrrhotite, and Pyrite	71-853

(a) = Calcite used as a seed crystal.

Note: The products are recorded in order of abundance; the presence of smythite was more distinct in X-ray patterns 69-161 and 69-162 than in 69-163.

(3) Quenching; using greigite as an example, rapid quenching is essential to prevent disproportionation during cooling.

An attempt to dissolve pyrrhotite away from greigite showed that both of these sulphides are quite soluble in cold, dilute hydrochloric acid.

(iii) Ferric, or Ferrous-and-Ferric, Iron in 0.2N H_2SO_4 Medium

Two groups of nutrients were prepared in 0.2 N sulphuric acid, one group involved ferric sulphate, the other a mixture of ferrous and ferric sulphates. The addition of aqueous sodium sulphide in the crystal-growth experiments still left the resulting growth-medium slightly acidic.

The conditions of the hydrothermal growth when the first nutrient was used, i.e., ferric sulphate alone, are shown in Table 52. The X-ray diffraction analyses of these experiments are shown in Table 53.

The main product was marcasite, with the impurities being sulphur and a white material that was identified as $FeSO_4.H_2O$. This latter impurity was easily removed by leaching with hot water. Pyrite was also present in some products. The bulk of the marcasite formed as segments of a thin metallic-looking ribbon ($5 \times 5 \times < 1$ mm). These segments could be easily picked from the growth product, leaving the other impurities behind.

The conditions of the hydrothermal growth when the nutrient was a mixture of ferrous and ferric sulphates, are shown in Table 54. The X-ray diffraction analyses are shown in Table 55. The main growth product was pyrite, with varying amounts of pyrrhotite, as well as smaller amounts of marcasite or greigite.

A comparison of the two groups of nutrients indicates that the ferric sulphate alone was more useful, since an isolatable product, marcasite, was obtained.

(iv) Ferrous and/or Ferric Iron in 3.0N H_2SO_4 Medium

All three types of nutrient: ferrous sulphate, ferric sulphate, and a mixture of ferrous and ferric sulphates, were prepared in 3.0N sulphuric acid. The addition of aqueous sodium sulphide in the crystal growth experiments did not affect the acidity appreciably.

The conditions of the hydrothermal growth are shown in Table 56. The X-ray diffraction analyses, as shown in Table 57, indicated that there was no growth product other than sulphur in two of the three experiments; the third experiment was terminated by an explosion.

(v) Iron or Nickel Sulphides in a Strong Acid Medium

In this section of the study, the nutrients were either iron or nickel sulphides, placed in silica tubes with various acid concentrations. The experimental conditions for the hydrothermal growth are shown in Table 58. The X-ray diffraction analyses of these products are shown in Table 59.

These experiments indicate another important variable in hydrothermal growth, i.e., pH. The solubility of some sulphides varies with the pH of the reaction solution.

Pyrite appears to be unattacked in 0.2N sulphuric acid, see Expt. #755. Since the product in Expt. #437B was pyrite, it is uncertain whether pyrite was unattacked by 9.0N HCl or whether there was some pyrite grown. However, it is certain that no marcasite was formed. In Expts. #521, #522, #825, #826, #830, and #848, an oxidation had occurred to produce growth products which contained more sulphur than the nutrient; this was possible because the bulk of the nutrient had dissolved and was still in solution at the end of the experiment and the growth product weighed only a few milligrams.

(vi) Ferrous Iron and Nickelous Nickel Salts with Na_2S in Neutral or Acidic Solutions

Six attempts to prepare bravoite, $(Fe_{0.5}Ni_{0.5})\ S_2$, were undertaken. The conditions of these hydrothermal growth experiments are given in Table 60. The X-ray diffraction analyses are shown in Table 61.

In this series of experiments, the usually-used thick-walled Pyrex tubing was replaced by Pyrex tubing having a wall thickness of approximately 1 mm. This change was permissible because the experimental temperatures and pressures were within the safety limit of this thin-walled tubing. The advantage of this change

(Continued on page 104)

TABLE 52

Conditions Used for Hydrothermal Growth Involving Ferric Iron and Na_2S in 0.2N H_2SO_4

Expt. No.	Fe^{+++} (a) (moles)	$S^{=}$ (b) (moles)	0.2N H_2SO_4 (ml)	Fe:S	Temperature (°C)	Time (hr)
477	0.0018	0.0012	12.0	1:0.67	195	24
491A	0.0018	0.0012	12.0	1:0.67	190	216
491B	0.0018	0.0012	12.0	1:0.67	190	216
504A	0.0018	0.0011	11.5	1:0.61	190	240
504B	0.0018	0.0012	12.0	1:0.67	190	240
504C	0.0018	0.0013	12.5	1:0.72	190	240
589A (c)	0.00135	0.0018	18.0	1:1.33	190	60
589B (c)	0.00143	0.0017	18.0	1:1.19	190	60

(a) = The salt $Fe_2(SO_4)_3 \cdot 7.6\ H_2O$ was used.

(b) = The salt $Na_2S \cdot 9H_2O$ was used.

(c) = The tubes used were 30 cm long.

TABLE 53

X-Ray Diffraction Analyses of Hydrothermal Growth Involving Ferric Iron and Na_2S in 0.2N H_2SO_4

Expt. No.	Phases Present	X-Ray Diffraction Report No.
477	Marcasite	68-1229
491A	Black material = Pyrite, Marcasite, and Sulphur	69-27
	White material = $FeSO_4 \cdot H_2O$	69-26
491B	$FeSO_4 \cdot H_2O$, and Marcasite	69-28
504A	Not analysed, but appeared to be similar to 504C	---
504B	Not analysed, but appeared to be similar to 504C	---
504C	Metallic material = Marcasite	69-150
	Black fines = Marcasite, Pyrite, and Sulphur	69-151
589A	Marcasite and Sulphur	69-553
589B	Marcasite and Pyrite	69-554

Note: The products are recorded in order of abundance.

TABLE 54

Conditions Used for Hydrothermal Growth Involving Ferrous and Ferric Iron and Na_2S in 0.2N H_2SO_4

Expt. No.	Fe^{++} (a) (moles)	Fe^{++} (b) (moles)	Fe^{+++} (c) (moles)	$S^{=}$ (d) (moles)	0.2N H_2SO_4 (ml)	Fe:S	Temperature (°C)	Time (hr)
482A	0.00026	---	0.00024	0.0005	5.0	1:1	R.T.	336
482B	0.00026	---	0.00024	0.0005	5.0	1:1	190	4
482C	0.00026	---	0.00024	0.0005	5.0	1:1	190	336
482D	0.0006	---	0.0006	0.0012	12.0	1:1	190	336
590	---	0.0009	0.0009	0.0018	18.0	1:1	190	60
591	---	0.00026	0.00024	0.0007	6.0	1:1.4	190	5
592	---	0.00035	0.00036	0.0005	6.0	1:0.7	190	5

(a) = The salt $Fe(NH_4)_2(SO_4)_2 \cdot 6H_2O$ was used.

(b) = The salt $FeSO_4 \cdot 7H_2O$ was used.

(c) = The salt $Fe_2(SO_4)_3 \cdot 7.6\ H_2O$ was used.

(d) = The salt $Na_2S \cdot 9\ H_2O$ was used.

TABLE 55

X-Ray Diffraction Analyses of Hydrothermal Growth Involving Ferrous and Ferric Iron and Na_2S in 0.2N H_2SO_4

Expt. No.	Phases Present	X-Ray Diffraction Report No.
482A	Marcasite, Pyrite, and some amorphous material	69-04
482B	Pyrite, Pyrrhotite, and Marcasite	69-05
482C	Pyrite, Pyrrhotite, and Marcasite	69-06
482D	Pyrite, Pyrrhotite, and Marcasite	69-07
590	Pyrite, Pyrrhotite, and an unidentified material	69-555
591	Pyrite, Unidentified material, and Pyrrhotite	69-549
592	Pyrite, Pyrrhotite, and Greigite	69-550

Note: The products are recorded in order of abundance.

TABLE 56

Conditions Used for Hydrothermal Growth Involving Ferrous and/or Ferric Iron and Na_2S in 3N H_2SO_4

Expt. No.	Fe^{++} (a) (moles)	Fe^{+++} (b) (moles)	$S^{=}$ (c) (moles)	3N H_2SO_4 (ml)	Fe:S	Temperature (°C)	Time (hr)
468	---	0.00075	0.0005	5.0	1:0.66	190	18
469	0.00038	---	0.0005	5.0	1:1.3	190	18
470	0.0003	0.0003	0.0006	6.0	1:1	190	2

(a) = The salt $Fe(NH_4)_2(SO_4)_2 \cdot 6\ H_2O$ was used.

(b) = The salt $Fe_2(SO_4)_3 \cdot 7.6\ H_2O$ was used.

(c) = The salt $Na_2S \cdot 9\ H_2O$ was used.

TABLE 57

X-Ray Diffraction Analyses of Hydrothermal Growth Products Involving Ferrous and/or Ferric Iron and Na_2S in 3N H_2SO_4

Expt. No.	Phases Present	X-Ray Diffraction Report No.
468	Sulphur	68-1192
469	Sulphur	68-1193
470	The tube blew up	---

TABLE 58

Conditions Used for Hydrothermal Growth of Iron or Nickel Sulphides in an Acid Medium

Expt. No.	Nutrient	Acid Medium			Temperature (°C)	Time (hr)
		Acid	Normality	ml		
755	0.2198g Pyrite (from Expt. #679)	H_2SO_4	0.2	5.0	190	144
830	0.3722g Troilite (from Expt. #341c)	H_2SO_4	0.2	5.0	190	96
848	0.1575g $Fe_{0.91}S$ (from Expt. #449)	HCl	0.6	5.0	190	168
522	0.5104g $Fe_{0.91}S$ (from Expt. #449)	HCl	3.0	5.0	190	72
437B	0.1138g Pyrite (from Expt. #332)	HCl	6.0	3.5	150	120
826	0.4036g Troilite (from Expt. #341c)	HCl	6.0	5.0	190	72
437A	0.0899g Pyrite (from Expt. #396)	HCl	9.0	4.5	275	1
521	0.4450g $Ni_{1.04}S$ (from Expt. #501)	HCl	3.0	5.0	190	72
825	0.4138g $Ni_{0.93}S$ (from Expt. #684)	HCl	3.0	5.0	190	96
827	0.6673g Ni_7S_6 (from Expt. #362)	HCl	3.0	5.0	190	144
824	0.3059g $Ni_{0.93}S$ (from Expt. #684)	HCl	6.0	5.0	190	96
518	0.6104g $Ni_{6.96}S_6$ (from Expt. #362)	HCl	6.0	5.0	190	24
828	0.2290g NiS_2 (from Expt. #404)	HCl	6.0	5.0	190	144

TABLE 59

X-Ray Diffraction Analyses of Hydrothermal-Growth Products of Iron and Nickel Sulphides in an Acid Medium

Expt. No.	Phases Present	X-Ray Diffraction Report No.
755	No evidence of solution or growth	---
830	Pyrite, Pyrrhotite and Marcasite	71-836
848	Pyrite and a small minor amount of Marcasite	71-916
522	Pyrite	69-194
437B	Pyrite	68-1089
826	Pyrite and Marcasite	71-834
437A	Tube blew up	---
521	Vaesite	69-193
825	Polydymite	71-818
827	Millerite and Vaesite	71-841
824	Polydymite and α-NiS	71-823
518	Millerite	69-172
828	No evidence of solution or growth	---

TABLE 60

Conditions Used for Attempted Preparation of Bravoite by Hydrothermal Growth

Expt. No.	Fe^{++} (a) (moles)	Ni^{++} (b) (moles)	$S^{=}$ (c) (moles)	H_2O (ml)	0.2N H_2SO_4 (ml)	Fe:Ni:S	Temperature (°C)	Time (hr)
601	0.00300	0.00300	0.00300	35	--	1:1:1	137	66
602	0.00302	0.00303	0.01557	35	--	1:1:5	137	168
856	0.00100	0.00104	0.00524	--	10	1:1:5	120	96
857	0.00010	0.00011	0.00054	--	10	1:1:5	120	72
866	0.00100	0.00103	0.00532	10	--	1:1:5	120	336
873	0.00108	0.00102	0.00539	10 (d)	--	1:1:5	120	120

(a) = The salt $Fe(NH_4)_2(SO_4)_2 \cdot 6\ H_2O$ was used.

(b) = The salt $NiCl_2 \cdot 6\ H_2O$ was used.

(c) = The salt $Na_2S \cdot 9\ H_2O$ was used.

(d) = Dilute HCl was added dropwise to achieve a pH of 2-4.

TABLE 61

X-Ray Diffraction Analyses of Products of Attempts to Prepare Bravoite by Hydrothermal Growth

Expt. No.	Phases Present	X-Ray Diffraction Report No.
601	α-NiS type ?	69-753
602	Dark material = Millerite and an unidentified substance	69-761
	Light material = Amorphous substance	69-762
856	α-NiS, Violarite, and a trace of Bravoite	71-949
857	Violarite and Pyrite	71-956
866	Violarite and Vaesite	72-069
873	Bravoite type : a = 5.66 Å	72-101

was that larger-capacity tubes could be used without increasing the outside diameter. Protective iron-pipe jackets were employed.

It is observed that, only in Expt. #856, was any bravoite formed, and then only as a trace constituent. The reason for the low yield may be due to a slow reaction rate for the formation of crystalline bravoite. Clark and Kullerud (6) found that, in order to obtain a good crystalline bravoite, a heating period of 12 or more days was required. The results obtained from Expts. #856, #866, and #873 indicate that an acidic medium is necessary; the conditions used in Expt. #873 provide the basis for further investigations.

SUMMARY OF CRYSTAL-GROWTH ACTIVITIES

The scope of the crystal-growing investigation, in terms of success in obtaining good crystalline material, is shown in Table 62. A successful growth (S) indicates that the growth product was a single component of the desired phase. A partly successful growth (P) indicates that the growth product was a mixture of the desired crystal with one or more other crystalline compounds. In cases of failure (F), the growth product (if there was one) did not contain the sought-after crystalline material. To complete Table 62, a dash (——) is used to show those systems that have not been attempted.

The two main goals were, firstly, to explore the total field of the sulphides of cobalt, iron, and nickel so as to be prepared to supply quickly any of these compounds that the Divisional sulphide research group had expressed interest in at various times and, secondly, to grow the crystals as large as possible and, eventually, to produce them in the cubic-centimetre size-range. However, none of the successes (S) indicated in Table 62 represent crystals as large as this. Photographs of some of the better crystal products are shown on pages 107 to 112.

TABLE 62

Scope of Crystal-Growth Activities

Compound	Mineral Name	Success or Otherwise of Crystal-Growth Technique						
		Direct Combination	Vapour Transport	Chemical Vapour Transport	Hydrothermal	Flux	Melt	Melt- and Anneal
$Co_{1-x}S$	Jaipurite	S	-	P	-	-	-	-
Co_9S_8	Cobaltian-Pentlandite	S	-	-	-	-	-	-
Co_3S_4	Linnaeite	-	-	F	-	P	-	S
CoS_2	Cattierite	P	S	S	-	S	-	-
FeS	Mackinawite	-	-	-	P	-	-	-
FeS	Troilite	F	F	F	P	F	S	P
$Fe_{1-x}S$	Pyrrhotite	S	S	S	S	S	S	P
Fe_3S_4	Greigite	F	-	-	S	-	-	-
Fe_3S_4	Smythite	F	-	-	P	-	-	-
FeS_2	Marcasite	F	-	-	S	-	-	-
FeS_2	Pyrite	S	S	S	P→S	S	P	-
α-$Ni_{1-x}S$	High-temperature Millerite	S	F	P	-	-	F	S
β-$Ni_{1-x}S$	Millerite	-	-	-	S	-	-	S
Ni_3S_4	Polydymite	P	-	F	S	-	-	P

(Continued on next page)

TABLE 62 (Concluded)

Compound	Mineral Name	Success or Otherwise of Crystal-Growth Technique						
		Direct Combination	Vapour Transport	Chemical Vapour Transport	Hydrothermal	Flux	Melt	Melt-and-Anneal
NiS_2	Vaesite	P	S	S	S	S	-	-
α-Ni_2S_6	High-temperature Godlevskite	F	-	-	-	F	-	S
β-Ni_7S_6	Godlevskite	-	-	-	-	F	-	S
$(Ni_{1-x}Fe_x)S$	Ferrous Millerite	-	-	-	-	-	F	S
$(Ni,Fe)_9S_8$	Pentlandite	P	-	-	-	-	P	S
$(Fe,Ni)S_2$	Nickelian-Bravoite	-	-	-	S	P	F	-
$(Fe,Co)S_2$	Cobaltian-Bravoite	-	-	-	-	F	-	-
$FeNi_2S_4$	Violarite	P	-	-	P	-	-	-

SIZE OF THE CRYSTALS

Photographs of representative crystals of the seven most successfully grown sulphides are shown in Figures 15 to 24, inclusive. The growth details can be located in the Tables indicated in the captions. The scale divisions, shown underneath the crystals in Figures 15 to 23 inclusive, represent 1 mm. In Figure 24, the scale of 1 cm = 100 μ is shown on the photograph.

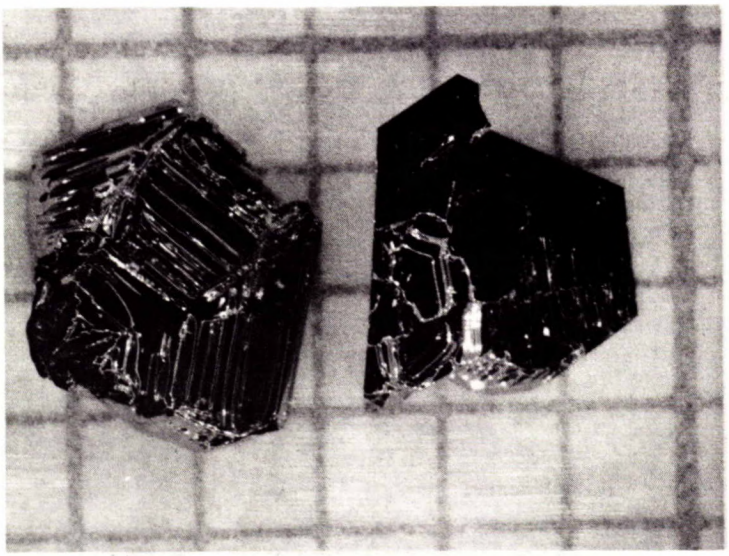

Figure 15. - Crystals of Hexagonal Pyrrhotite, $Fe_{0.92}S$, grown by Chemical Vapour Transport (Iodine) Technique (Expt. #646, see Tables 25 and 26).

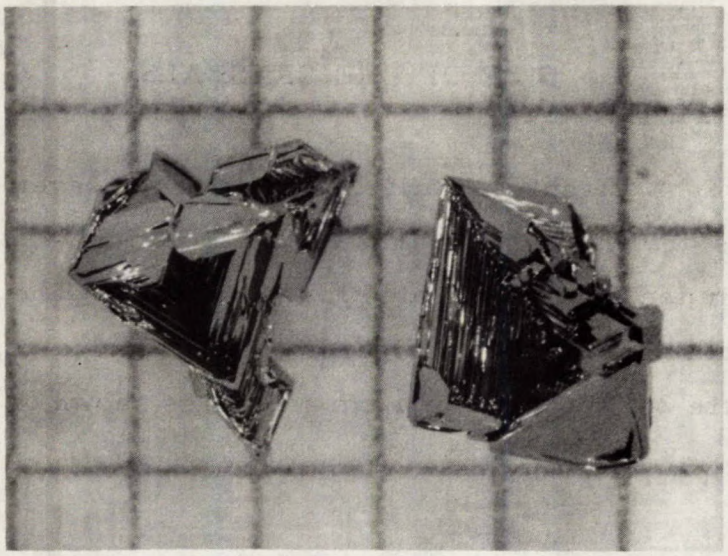

Figure 16. - Crystals of Cattierite, CoS_2, grown by Chemical Vapour Transport (Iodine) Technique (Expt. #606, see Tables 29 and 30).

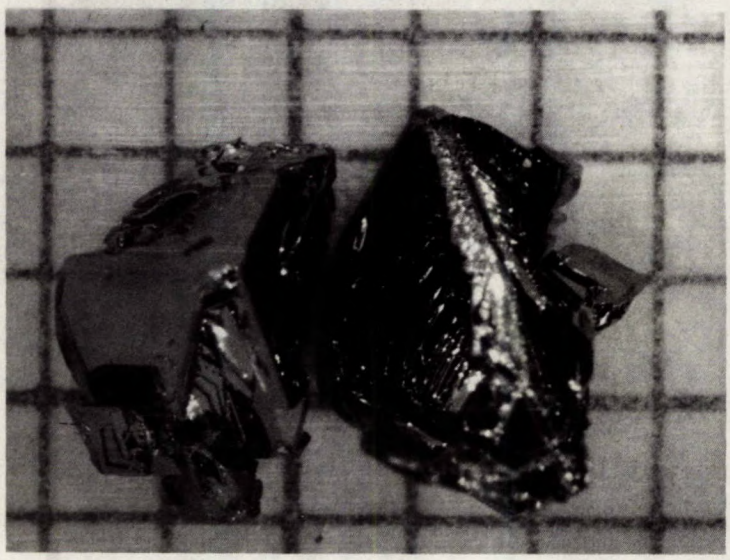

Figure 17. - Crystals of Vaesite, NiS_2, grown by Chemical Vapour Transport (Iodine) Technique (Expt. #605, see Tables 33 and 34).

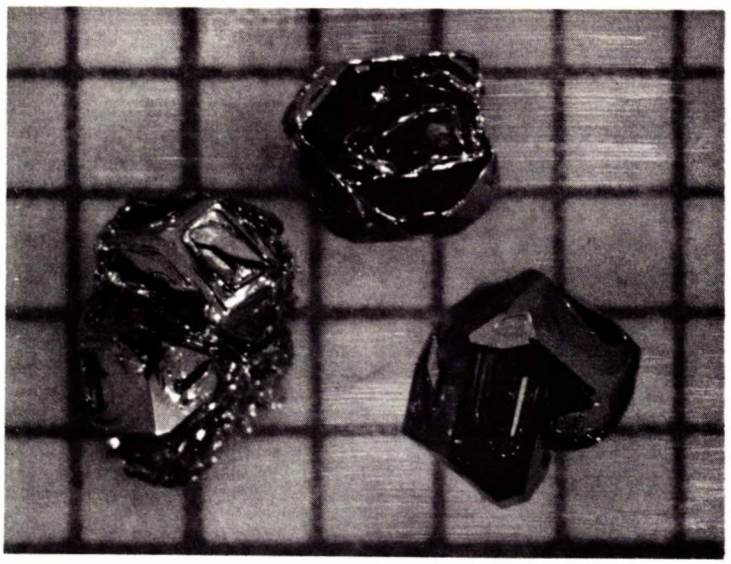

Figure 18. - Crystals of Pyrite, FeS_2, grown by Chemical Vapour Transport (Iodine) Technique (Expt. #611, see Tables 31 and 32).

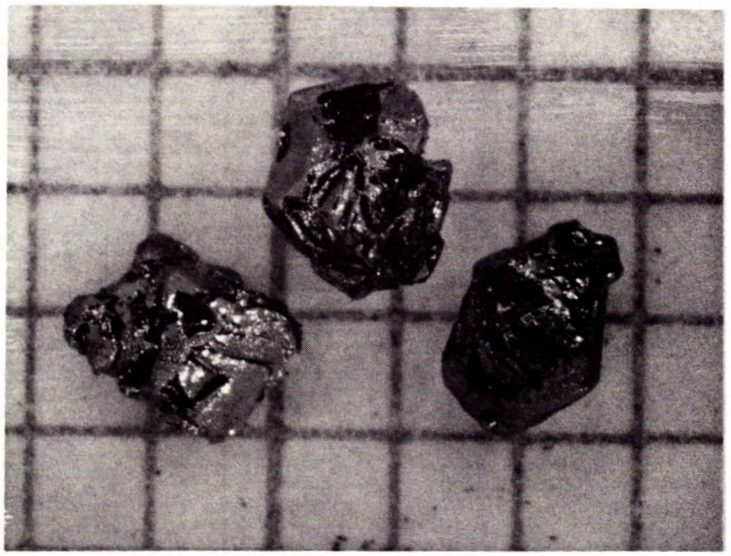

Figure 19. - Crystals of Cattierite, CoS_2, grown by Flux ($PbCl_2$) Technique (Expt. #754, see Tables 35 and 36).

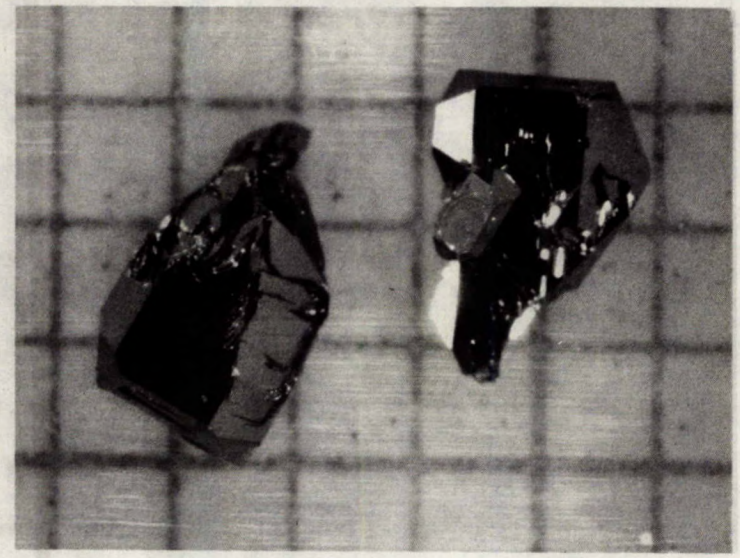

Figure 20. - Crystals of Vaesite, NiS_2, grown by Flux ($PbCl_2$) Technique (Expt. #753, see Tables 39 and 40).

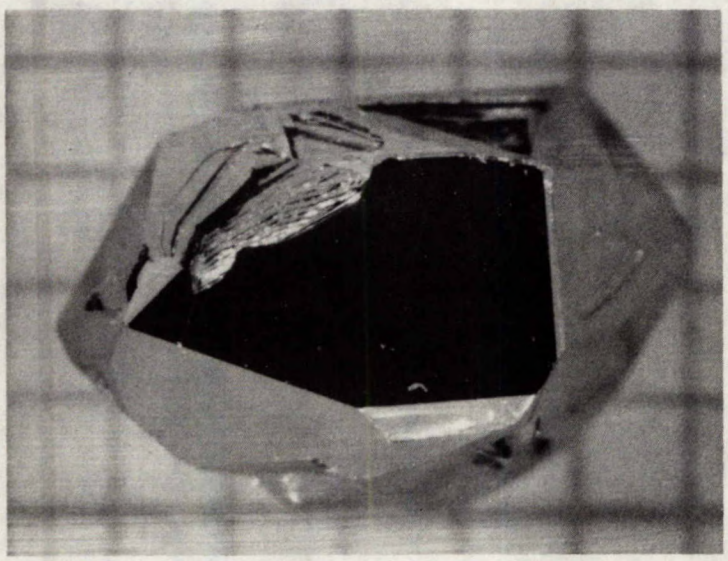

Figure 21. - Crystal of Pyrite, FeS_2, grown by Flux ($PbCl_2$) Technique (Expt. #679, see Tables 37 and 38).

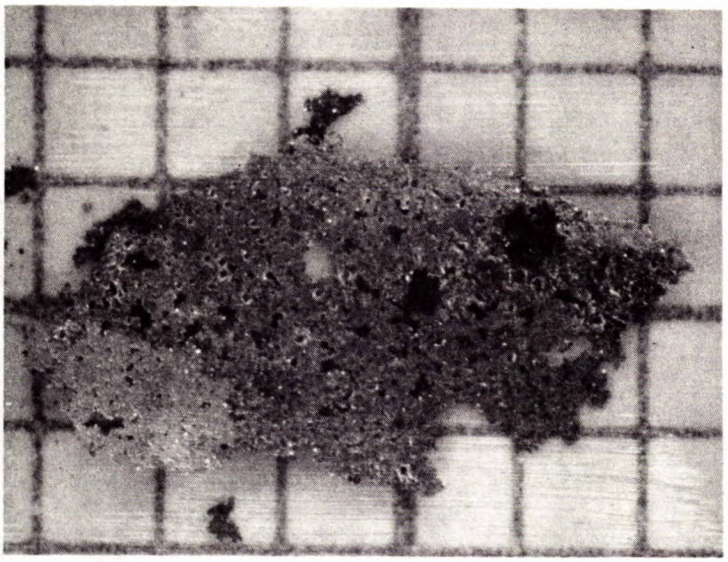

Figure 22. - Crystals of Marcasite, FeS_2, grown by Hydrothermal Technique (Expt. #504C, see Tables 52 and 53).

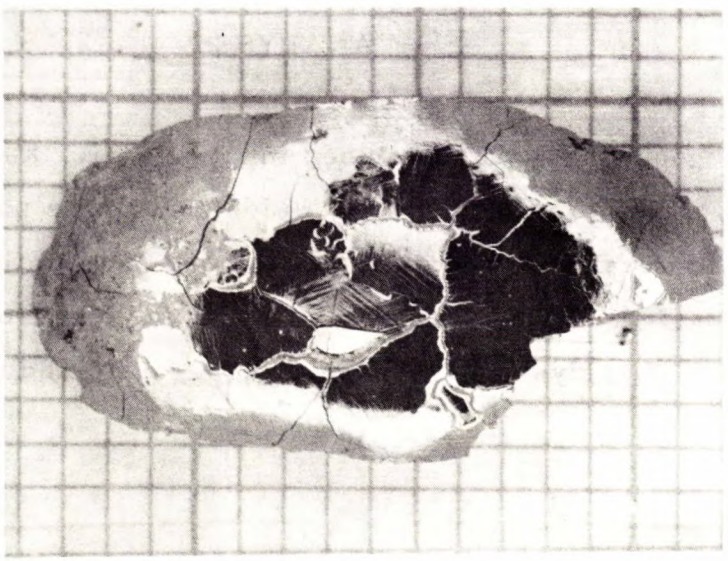

Figure 23. - Crystalline mass of Troilite, FeS, grown by Melt Technique (Expt. #451, see Tables 15 and 16).

Figure 24. - Cross-section of Crystalline High-temperature Millerite, α-$Ni_{1-x}S$, grown by Melt-and-Anneal Technique (Expt. #793, see Tables 17 and 18).

ANALYSES

Throughout the work described in this report, X-ray diffraction analysis has played a prominent role in identifying the phases obtained. However, it is equally important to know more quantitatively the exact concentrations of the elements present in the various growth products. Other methods of analysis have, therefore, been adopted to achieve this objective.

(a) Chemical Analyses

In the previous Research Report of this series (2), a method was described whereby the zinc concentration in zinc sulphide was determined by an oxidation to the oxide. The same procedure has been applied to the analyses of cobalt, iron, and nickel sulphides.

The main problem involved is the oxidation of the sulphides CoS_x, FeS_x, and NiS_x to a stable oxide. In the case of cobalt, CoO is stable at

900°C, but, on cooling in air, Co_3O_4 is formed, (see Expt. #768, Table 63). However, if CoO is quenched from 900°C, the oxidation of CoO is prevented (24). Iron is oxidized to approximately Fe_2O_3; the use of moist air or oxygen increases the rate of oxidation and permits the achieving of stoichiometric Fe_2O_3 in a shorter time. Nickel forms a monoxide that is essentially stoichiometric except for a small departure on the oxygen-rich side. Therefore, in order to provide a confirmatory figure, the resulting oxides of cobalt, iron, and nickel, were reduced to the metallic state with hydrogen.

To check the reliability of these procedures, standard samples were prepared. Pure cobalt or nickel wire was heated in hydrogen sulphide to form the monosulphide, whose formula was calculated from the gain in weight. In addition, $NiS_{1.07}$ and Fe_2S_3 were prepared by direct combination of the elements.

The results of the oxidation and reduction methods, when applied to the standard samples and to the sulphides of cobalt, iron and nickel, are shown in Tables 63, 64, and 65, respectively. It is obvious that the methods are reliable and that there is good agreement between the two methods, except for cobalt oxide cooled in air.

The iodine-transported products of CoS_2 (Expts. #405 and #606), FeS_2, (Expts. #396), and NiS_2 (Expt. #605) are essentially stoichiometric, while the FeS_2, (Expt. #611) is sulphur-deficient. The untransported products of CoS_2 (Expt. #606), and NiS_2 (Expt. #605) are very sulphur-deficient, indicating a mixture of MS and MS_2; this is in agreement with the X-ray diffraction analysis. Unreliable results could be expected from the two flux-grown materials, CoS_2 (Expt. #609) and FeS_2 (Expt. #679), because of the known $PbCl_2$ inclusions. In the case of the latter sample, fumes of a lead compound condensed along the walls of the combustion tube. The discrepancy in the analysis of the nickel monosulphides, Expt. #621 and #635, may well be due to segregation, as only part of the sample was analysed.

The limitation of these chemical procedures lies in the size of sample required for analysis; usually, 200-300 mg of crushed sulphide was oxidized.

TABLE 63

Chemical Analyses of Cobalt Sulphides

Expt. No.	Description of the Samples
768	Cobalt wire heated in H_2S to give $CoS_{0.98}$, used as a standard
620	CoS_2, Flux ($PbCl_2$)-grown in Expt. #609 (see Table 35)
716	CoS_2, Transported product of I_2 transport in Expt. #606 (see Table 29)
715	CoS_2, Untransported product of I_2 transport in Expt. #606 (see Table 29)
769	CoS_2, Transported product of I_2 transport in Expt. #405 (see Table 29)

Expt. No.	Analytical Results					
	Oxidation Method			Reduction Method		
	Temperature (°C)	Time (hr)	Formula (Calc.)	Temperature (°C)	Time (hr)	Formula (Calc.)
768	900 (a)	1	$CoS_{0.81}$	900 (b)	1	$CoS_{0.98}$
620	900 (b)	2	$CoS_{2.00}$	---	-	---
716	1000 (b)	3	$CoS_{2.00}$	---	-	---
715	1000 (b)	3	$CoS_{1.33}$	---	-	---
769	900 (b)	1	$CoS_{1.94}$	900 (b)	2	$CoS_{1.99}$

Note: Samples from Expts. #620, #716, #715, and #769, were leached with CS_2 to remove excess elemental sulphur prior to analysis.

(a) = Cooled in air (b) = Cooled in helium

However, in spite of this limitation, these procedures have confirmed the chemical compositions of the above sulphides.

(b) Semi-Quantitative Spectrochemical Analyses

Several samples of CoS_2, FeS_2, and NiS_2 (prepared by the following techniques: FeS_2 by direct combination; CoS_2, FeS_2, and NiS_2 by iodine vapour transport; and CoS_2 and FeS_2 by flux ($PbCl_2$)), have been analysed by the semi-quantitative spectrochemical method. The results of the analyses are recorded in Tables 66, 67, and 68, respectively.

The levels of the impurities in Tables 66 and 67, are of the same order of magnitude as was experienced with ZnS (2). The two main impurities are silica and iron (in the CoS_2 and NiS_2), while, in Table 68, the quantity of lead is partly in agreement with the amounts reported by the atomic-absorption spectrophotometric procedure (see Table 41) and is due to inclusions of the flux ($PbCl_2$) in the crystals of the disulphides.

(c) Electron-Microprobe Analyses

Electron-microprobe analysis has been very informative. It has supplied spot counts (analyses) across the specimens; in this way, the uniformity of distribution in the matrix of impurities and inclusions have been determined. Four groups of sulphides have been examined:

(1) The first group of sulphides examined was the monosulphides of cobalt, iron, and nickel. The analyses of two cobalt monosulphides, Expts. #823 and #836, that were prepared as shown in Table 12 are given in Table 69. The results indicate that the sample from Expt. #836 had disproportionated on cooling, but that the sample from Expt. #823 was homogeneous. The reason for this difference is observed in Figure 1, where the boundary of the $Co_{1-x}S$ thermal stability field is both temperature- and composition-dependent. The data in Figure 1 indicate that the sample from Expt. #836 would have started to disproportionate after being cooled to 700°C, whereas that from Expt. #823 would not have started to disproportionate until cooled to 460°C. These results confirm that a very rapid quench would be necessary for cobalt monosulphides with compositions approaching CoS to avoid disproportionation.

(Continued on page 123)

TABLE 64

Chemical Analyses of Iron Sulphides

Expt. No.	Description of the Samples
719	FeS_2, Transported product of I_2 transport in Expt. #611 (see Table 31)
721	FeS_2, Flux ($PbCl_2$) grown in Expt. #679 (see Table 37)
762	FeS_2, Transported product of I_2 transport in Expt. #396 (see Table 31)
759, 760 and 761	Fe_2S_3, Prepared by direct combination in Expt. #258 (see Table 12)
874	FeS_2, Naturally-occurring pyrite that had been isolated from the ore by a heavy-liquid separation.
875	FeS_2, Naturally-occurring marcasite that had been isolated from the ore by a heavy-liquid separation.

TABLE 64 (Concluded)

Expt. No.	Analytical Results					
	Oxidation Method			Reduction Method		
	Temperature (°C)	Time (hr)	Formula (Calc.)	Temperature (°C)	Time (hr)	Formula (Calc.)
719	1000	3	$FeS_{1.89}$	--	--	--
721	1000	3	$FeS_{2.10}$	--	--	--
762	950	1	$FeS_{1.99}$	900	1	$FeS_{1.99}$
759	1000	2.5	$Fe_2S_{3.06}$	900	1	$Fe_2S_{3.06}$
760	--	--	--	900 (a)	1	$Fe_2S_{2.98}$
761	1000	1.5	$Fe_2S_{3.06}$	900	1.5	$Fe_2S_{3.02}$
				900 (b)	+1	$Fe_2S_{3.04}$
874	1050	1	$FeS_{2.00}$	--	--	--
875	1050	1	$FeS_{1.92}$	--	--	--

Note: Samples from Expts. #719, #721, and #762, were leached with CS_2 to remove excess elemental sulphur prior to analysis.

(a) = This sulphide was reduced directly without going through the oxide stage.
(b) = Additional heating of this reduction product.

TABLE 65

Chemical Analyses of Nickel Sulphides

Expt. No.	Description of the Samples
622	Nickel powder heated in H_2S to give $Ni_{0.97}S$ in Expt. #621
767	Nickel wire heated in H_2S to give $NiS_{0.73}$ used as a standard.
709	$Ni_{0.975}S$, Prepared by Melt-and-Anneal in Expt. #635 (see Table 17)
763	$NiS_{1.07}$, Prepared by direct combination in Expt. #684, used as standard.
710	NiS_2, Transported product of I_2 transport in Expt. #605 (a) (see Table 33)
712, and 764	NiS_2, Transported product of I_2 transport in Expt. #605 (b) (see Table 33)
713	NiS_2, Untransported product of I_2 transport in Expt. #605 (b)(see Table 33)

(a) = This sample was not leached with CS_2 to remove excess elemental sulphur.
(b) = These samples were leached with CS_2 to remove excess elemental sulphur prior to analysis.

TABLE 65 (Concluded)

Expt. No.	Analytical Results					
	Oxidation Method			Reduction Method		
	Temperature (°C)	Time (hr)	Formula (Calc.)	Temperature (°C)	Time (hr)	Formula (Calc.)
622	900	2	$Ni_{0.96}S$	--	--	--
767	900	1	$NiS_{0.72}$	900	1	$NiS_{0.73}$
709 (a)	1000	2	$Ni_{0.95}S$	--	--	--
763	900	1	$NiS_{1.08}$	850	1	$NiS_{1.08}$
710	1000	3.5	$NiS_{2.11}$	--	--	--
712	1000	3.25	$NiS_{2.02}$	--	--	--
764	900	2	$NiS_{2.00}$	900	1	$NiS_{2.02}$
713	1000	3	Ni_4S_5	--	--	--

(a) = In Report MS-AC 70-803, Miss E. Mark gives a sulphur value of 35.63%, (an average of four determinations), which would correspond to $Ni_{0.987}S$, based only on the sulphur value.

TABLE 66

Semi-Quantitative Spectrochemical Analyses of Direct-Combination Iron Disulphides
(% by weight)

Expt. No.	Sample	Mn	Mg	Si	Fe	Cu	Ti	Ni	Co
444	FeS_2	0.01	0.002	0.2	PC	0.05	0.006	0.02	N.D. (a)
463	FeS_2	0.01	0.0004	0.2	PC	0.01	0.005	0.01	N.D. (a)

(a) = Report No. MS-AC 69-13; in addition to the above elements, the following elements were not detectable by spectrographic means: Ba, Sb, Mo, Pb, Sn, Cr, Bi, Al, V, Ca, Zr, Ag, Zn, Sr.

PC = Principal constituent
N.D. = Not detectable

Note: Samples from Expts. #444 and #463 were prepared as shown in Table 12.

TABLE 67

Semi-Quantitative Spectrochemical Analyses of C. V. T.-Grown Cobalt, Iron, and Nickel Disulphides
(% by weight)

Expt. No.	Sample	Mn	Mg	Cr	Si	Fe	Al	Zr	Cu	Ni	Co
405	CoS_2	0.03	0.05	N.D.	0.5	0.2	0.008	0.03	0.04	N.D.	PC (a)
606	CoS_2	0.006	0.03	N.D.	0.1	0.05	0.02	N.D.	N.D.	N.D.	PC (b)
396	FeS_2	0.01	0.03	N.D.	0.5	PC	0.005	0.02	0.01	0.07	0.05 (a)
404	NiS_2	0.01	0.03	0.15	0.4	0.2	0.008	0.03	0.03	PC	0.07 (a)
605	NiS_2	N.D.	0.05	0.007	0.08	0.04	0.02	N.D.	0.04	PC	N.D. (c)

(a) = Report No. MS-AC 68-632; in addition to the above elements, the following elements were not detectable by spectrographic means: Ba, Sb, Mo, Sn, Bi, Ag, Zn, Sr, Ti, V, Pb.

(b) = Report No. MS-AC 69-105; in addition to the above elements, the following elements were not detectable by spectrographic means: Ba, B, Sb, Ge, As, Mo, W, Nb, Ta, Ca, Sr, In, Ag, Na, Zn, Ti, V, Pb.

(c) = Report No. MS-AC 69-669; in addition to the above elements, the following elements were not detectable by spectrographic means: Ba, B, Sb, As, W, Sn, Nb, Ta, Ge, In, Be, Mo, Ag, Na, Zn, Sr, Ti, V, Pb.

PC = Principal constituent.

N.D. = Not detectable.

Note: Samples from Expts. #405 and #606 were prepared as shown in Table 29.
Sample from Expts. #396 was prepared as shown in Table 31.
Samples from Expts. #404 and #605 were prepared as shown in Table 33.

TABLE 68

Semi-Quantitative Spectrochemical Analyses of Flux ($PbCl_2$)-Grown Cobalt, and Iron Disulphides
(% by weight)

Expt. No.	Sample	Si	Fe	Mg	Pb	Sn	Mo	Cu	Co
609	CoS_2	0.4	0.06	N.D.	0.4	N.D.	N.D.	0.02	PC (a)
679	FeS_2	0.06	PC	0.2	0.25	0.01	0.02	0.01	N.D. (b)

(a) = Report MS-AC 69-658; in addition to the above elements, the following elements were not detectable by spectrographic means; Ba, Sb, As, W, Cr, Mn, Nb, Ta, Bi, Al, V, Ca, In, Zr, Ag, Na, Zn, Ti, Ni, Ge, Sr.

(b) = Report MS-AC 71-88; in addition to the above elements, the following elements were not detectable by spectrographic means: Ba, B, P, Mn, Sb, Ge, As, W, Cr, Ga, Nb, Ta, Bi, V, Be, Al, Ca, In, Ag, Na, Zn, Ti, Ni, Zr, Sr.

PC = Principal constituent.

N.D. = Not detectable.

Note: Samples from Expts. #609 and #679 were prepared as shown in Tables 35 and 37, respectively.

The analysis of an iron monosulphide, Expt. #803, which was prepared as shown in Table 17, is given in Table 70. The results indicate that this material was of the target composition and that the homogeneity was good.

The analyses of nine nickel monosulphides, prepared as shown in Tables 17 and 15, were analysed and the results are shown in Tables 71 and 72. The surface of the product from Expt. #684, which has a composition of $NiS_{1.07}$, was scanned at thirty individual points for nickel and sulphur; the counts were found to be constant over the length of the specimen, i.e., it is apparently homogeneous. The microprobe analysis of the product of Expt. #631, $NiS_{0.975}$, showed the presence of three distinct phases. The larger area was NiS and was not a single crystal, but a smaller area, at the tip of the specimen, consisted of an intergrowth of Ni_3S_2 and Ni_7S_6. A further feature was that the iron impurity was present to a different extent in each of the three phases. The specimen from Expt. #793, $NiS_{1.00}$, gave a similar analysis. The larger fragment, when scanned at thirty locations across the sample, showed the material to be homogeneous with the analysis as shown in Table 71. However, a small fragment of sample that had lodged at the warm end of the main specimen during the annealing step, was found to contain two or three of three phases: NiS, Ni_7S_6, and Ni_3S_2; the intergrowth was too intimate to determine all phases by the electron microprobe. In the sample from Expt. # 676, $NiS_{0.954}$, two phases, showing optical differences in their colour, were detected and analysed. These analyses indicated that the phases $Ni_{0.98}S$ and $Ni_7S_{6.25}$ were present.

These results show that the bulk of each sample is high-temperature millerite ($Ni_{0.99}S$ to $Ni_{0.98}S$), which is homogeneous, and that the excess nickel is present in two other sulphides: Ni_7S_6 and Ni_3S_2, which had condensed as intergrowths at the warm end of the billet during the annealing step. These results are in agreement with the phase diagram shown in Figure 3.

(2) The second group of sulphides examined with the microprobe were some of the iodine-grown disulphides of cobalt, iron, and nickel; the details of the preparation of these compounds were shown in Tables 29, 31, and 33, respectively.

(Continued on page 127)

TABLE 69

Electron-Microprobe Analyses of Cobalt Monosulphides

Expt. No.	Target Formula	Microprobe Analysis % Co	Microprobe Analysis % S	Calculated Formula	Microprobe Report No.	Comment
823	$Co_{0.885}S$	62.17	37.46	$Co_{0.90}S$	EP 71-94	(a)
836	$Co_{0.95}S$	Major 66.18	32.87	$Co_{9.0}S_{8.2}$	EP 71-113	(b)
		Minor 63.29	37.04	$Co_{0.93}S$	EP 71-113	

(a) = The homogeneity of the sample was good.
(b) = This sample was not homogeneous; the major phase was buff-coloured, and the minor phase was more yellow.

Note: Samples from Expts. #823 and #836 were prepared as shown in Table 12.

TABLE 70

Electron-Microprobe Analysis of Iron Monosulphide

Expt. No.	Target	Microprobe Analysis %Fe	Microprobe Analysis %S	Calculated Formula	Microprobe Report No.	Comment
803	$Fe_{0.99}S$	63.29	37.15	$Fe_{0.98}S$	EP 71-82	(a)

(a) = The homogeneity of the sample was good.

Note: Sample from Expt. #803 was prepared as shown in Table 17.

TABLE 71

Electron-Microprobe Analyses of Nickel Monosulphides

Expt. No.	Target Formula	Microprobe Analysis %Ni	Microprobe Analysis %S	Calculated Formula	Microprobe Report No.	Comments
684	$NiS_{1.07}$	62.83	36.94	$NiS_{1.08}$	EP 70-185	(a)
631	$NiS_{0.975}$	64.90	35.83	$Ni_{0.989}S$		(b)
632	$NiS_{0.99}$	64.56	35.87	$Ni_{0.983}S$		
633	$Ni_{1.00}S$	64.83	35.80	$Ni_{0.989}S$	EP 70-13	
634	$Ni_{0.99}S$	64.84	35.45	$Ni_{0.999}S$		
635	$Ni_{0.975}S$	64.83	36.40	$Ni_{0.972}S$		(c)
635 (d)	$Ni_{0.975}S$	63.81	35.03	$Ni_{0.996}S$	EP 70-01	(e)
793	$Ni_{1.00}S$	65.01	35.70	$Ni_{0.995}S$	EP 71-22	(f)

(a) = Sample is homogeneous.
(b) = See text for comment.
(c) = Iron is evenly distributed at $\sim 0.11\%$. This iron was present as an impurity in the nickel powder used to prepare these sulphides.
(d) = Analysis on a different portion of the same sample.
(e) = Sample is homogeneous in two directions of traverse.
(f) = Sample is homogeneous; see text for additional comment.

Note: All of the above samples were prepared as shown in Table 17.

TABLE 72

Detailed Electron-Microprobe Analyses of Nickel Monosulphides

Expt. No.	Target Formula	Phase	Microprobe Analyses %Fe	%S	%Ni	Ratio Ni:S	Calculated Formula
631	$NiS_{0.975}$	1	0.11 (a)	35.3 (b)	63.7 (b)	1:1.015	$Ni_{0.986}S$
631	$NiS_{0.975}$	2	0.23 (a)	31.99 (b)	69.03 (b)	1:1.849	Ni_7S_6
631	$NiS_{0.975}$	3	0.06 (a)	26.37 (b)	74.64 (b)	1:0.647	Ni_3S_2
676	$NiS_{0.954}$	1	---	36.56 (c)	65.48 (c)	1:1.02	$Ni_{0.98}S$
676	$NiS_{0.954}$	2	---	32.34 (c)	66.36 (c)	1:0.892	$Ni_7S_{6.25}$
676	$NiS_{0.954}$	3	---	35.85 (c)	64.54 (c)	1:1.02	$Ni_{0.98}S$

(a) = Microprobe Report EP-70-35. The origin of this iron is explained in footnote (c) in Table 71.
(b) = Microprobe Report EP-69-128.
(c) = Microprobe Report EP-70-49.

Note: Sample from Expts. #631 and #676 were prepared as shown in Tables 17 and 15, respectively.

The main application of the microprobe was to determine whether iodine had been entrapped in the crystals. The results, as shown in Table 73, gave no evidence that iodine was present in any form.

The second application was to determine the metal-to-sulphur ratio; the results, in Table 73, for NiS_2, Expt. #605, and for CoS_2, Expt. #606, showed these samples to be uniform but slightly sulphur-deficient.

(3) The third group of sulphides examined were some of the flux ($PbCl_2$)-grown disulphides of cobalt and iron; the details of their preparation were shown in Tables 35 and 37, respectively.

The main application of the microprobe here was to determine whether any of the flux, $PbCl_2$, was entrapped in the crystals. The results, as shown in Table 74, indicate that $PbCl_2$ is present in the FeS_2, Expts. #332, 438, and 679, as large inclusions, but is rarely present as inclusions in CoS_2, Expt. #609.

The second application was to determine the metal-to-sulphur ratio; the results, in Table 74, showed these samples to be uniform and, in Expt. #679, the composition to be $FeS_{1.988}$.

(4) The fourth group of sulphides examined by the microprobe included six of the three-component systems. The description of the samples and the analyses are presented in Table 75; the copious footnotes makes it necessary to present Table 75 in two sections.

Two of the samples, from Expts. #598 and #603, had been prepared by a flux growth, as shown in Table 42. The results showed that the iron:nickel ratio in Expt. #598, and the cobalt:iron ratio in Expt. #603, varied across the samples and that there were inclusions of $PbCl_2$ in both samples; see the footnotes below Table 75.

The other four samples, from Expts. #673, #674, #799, and #822, were prepared by the melt-and-anneal method, as shown in Table 19. The microprobe analysis of the sample from Expt. #673 showed it to consist of a homogeneous matrix containing a few small areas of two other intergrown phases, which were similar to the phases found in Expt. #631 (see Table 72), except for varying amounts of iron being present in all the phases. The

(Continued on page 132)

TABLE 73

Electron-Microprobe Analyses of C.V.T.-Grown Cobalt, Iron, and Nickel Disulphides

Expt. No.	Sample	Microprobe Analysis		Calculated Formula	Microprobe Report No.	Comments
		Metal	% S			
396	FeS_2	---	---	---	EP 68-19	(a)
404	NiS_2	---	---	---	EP 68-19	(a)
405	CoS_2	---	---	---	EP 68-19	(a)
605	NiS_2	49.2% Ni	51.9	$NiS_{1.93}$	EP 69-113	(b)
606	CoS_2	48.25% Co	51.81	$CoS_{1.973}$	EP 69-127	(c)

(a) = No impurities were detectable; this includes iodine.
(b) = Sample is uniform and no iodine was detectable.
(c) = No silica or iodine were detectable.

Notes: Samples from Expts. #405 and #606 were prepared as shown in Table 29.
Sample from Expts. #396 was prepared as shown in Table 31.
Samples from Expts. #404 and #605 were prepared as shown in Table 33.

TABLE 74

Electron-Microprobe Analyses of Flux ($PbCl_2$)-Grown Cobalt, and Iron Disulphides

Expt. No.	Sample	Microprobe Analysis		Calculated Formula	Microprobe Report No.	Comments
		Metal	% S			
332	FeS_2	---	---	---	EP 68-19	(a)
438	FeS_2	---	---	---	EP 68-30	(b)
679	FeS_2	46.72% Fe	53.35	$FeS_{1.988}$	EP 71-13	(c)
609	CoS_2	---	---	---	EP 69-110	(d)

(a) = Large inclusions of $PbCl_2$, but FeS_2 itself appears to be free from Pb and Cl_2; FeS_2 is uniform.

(b) = Large inclusions of $PbCl_2$, but neither Pb nor Cl_2 was detectable in the FeS_2 grains.

(c) = Specimen is uniform; neither Pb nor Cl_2 was detectable within the FeS_2, or as $PbCl_2$.

(d) = The ratio of cobalt to sulphur is constant; the $PbCl_2$ inclusions were rare.

Note: Samples from Expts. #332, #438, and #679, were prepared as shown in Table 37.

Sample from Expt. #609 was prepared as shown in Table 35.

TABLE 75

Electron-Microprobe Analyses of Three-Component Systems

Expt. No.	Sample	Phase	Microprobe Analysis %Fe	%Co	%Ni	%S	Calculated Formula
598	$(Fe_{1-y}Ni_y)S_x$	Matrix	-	-	2	-	$(Fe_{0.98}Ni_{0.02})S_x$ (a)
		Grey	7.0-11.5	-	-	-	$(Fe_{0.10}Ni_{0.90})S_x$ (a)
603	$(Fe_{1-y}Co_y)S_x$	Yellow	46.6	-	-	53.4	FeS_2 (b)
		Purple	23.9	28.0	-	51.9	$(Co_{0.59}Fe_{0.52})S_2$ (b)
673	$(Ni_{0.99}Fe_{0.01})S$	Matrix	0.74	-	64.72	36.05	$(Ni_{0.99}Fe_{0.01})_{0.99}S$ (c)
		Yellow	0.5	-	67.34	31.73	$(Ni_{0.99}Fe_{0.01})_{7.02}S_6$ (c)
		White	0.1	-	70.26	24.89	$(Ni_{0.998}Fe_{0.002})_{3.2}S_2$ (c)
674	$(Ni_{0.5}Fe_{0.5})S$	Matrix	31.87	-	31.62	37.05	$(Fe_{0.51}Ni_{0.49})_{0.96}S$ (d)
		Interstitial "A"	21.36	-	47.33	33.01	$(Ni_{0.68}Fe_{0.32})_{9.24}S_8$ (d)
		Interstitial "B"	27.71	-	40.56	33.19	$(Ni_{0.58}Fe_{0.42})_{9.17}S_8$ (d)

(a) = Microprobe Report EP 69-91; Fe:Ni variable across sample, $PbCl_2$ inclusions present.
(b) = Microprobe Report EP 69-102; sample not homogeneous; $PbCl_2$ inclusions present.
(c) = Microprobe Report EP 70-74; millerite, Ni_7S_6, and Ni_3S_2 in the three phases, respectively.
(d) = Microprobe Report EP 70-75; interstitials "A" and "B" are ~pentlandites.

Notes: Total analyses in product from Expt. #673, white phase, do not add up to 100% due to intergrowth with the yellow phase.
Samples from Expts. #598 and #603 were prepared as shown in Table 42.
Samples from Expts. #673 and #674 were prepared as shown in Table 19.

TABLE 75 (Concluded)

Expt. No.	Sample	Phase	Microprobe Analysis %Fe	%Ni	%S	Calculated Formula
799	$(Ni_{0.96}Fe_{0.04})S$	(i) (a)	2.52	62.11	34.37	$(Ni_{0.959}Fe_{0.041})_{1.029}S$
		(ii) (a)	1.29	66.84	31.81	$(Ni_{0.98}Fe_{0.02})_{7.02}S_6$
		(iii) (a)	1.38	66.56	31.82	$(Ni_{0.978}Fe_{0.022})_{7.0}S_6$
		(iv) (a)	0.19	72.42	26.69	$(Ni_{0.997}Fe_{0.003})_{2.93}S_2$
822	$(Fe_{0.5}Ni_{0.5})_9S_8$	Major (b)	31.59	35.12	32.60	$(Ni_{0.514}Fe_{0.486})_{9.16}S_8$
		Minor (b)	46.83	15.76	36.60	$(Ni_{0.24}Fe_{0.76})_{0.97}S$

(a) = Microprobe Report EP 71-82; approximately one half of the specimen is composed of quite homogeneous millerite (i), while the other consists of a mixture of godlevskite (ii) and (iii) and heazlewoodite (iv). The millerite area (i) is homogeneous, and no variation in Fe:Ni was noted. The second half consists of grains of godlevskite in relief (ii), surrounded by a fine-grained intergrowth of both godlevskite and heazlewoodite. The areas of godlevskite, in relief to the surrounding intergrowth, are homogeneous, with constant Fe:Ni (ii). However, counts from the fine-grained intergrowth showed variations in Fe from 0.19% to 3.79% (iii).

(b) = Microprobe Report EP 71-98; Microscopic examination showed the presence of very small inclusions (30 microns) in the matrix. These differ from the matrix in that they are highly anisotropic and are similar in colour to pyrrhotite.

Note: Samples from Expts. #799 and #822 were prepared as shown in Table 19.

analysis of the product from Expt. #674 showed this sample to consist largely of a coarse, granular matrix containing numerous small exsolutions. Also present, separating the grains of the matrix, are much smaller, interstitial grains of a phase similar to pentlandite, $(Ni,Fe)_9S_8$, except that the iron:nickel ratio varies from phase to phase. The analysis of these interstitial phases A and B are given for the lowest and for the highest iron:nickel ratios detectable. The analysis of the product of Expt. #799 showed this sample to be similar to that from Expts. #631 and #673, except for the differing amounts of iron being present in all the phases. The analysis of the product of Expt. #822 showed this sample to be predominantly pentlandite with very small inclusions (30 microns) of pyrrhotite, which have been estimated at much less than 1% in amount.

(d) X-Ray Fluorescence Analyses

The first products obtained by the flux growth, using $PbCl_2$, were analysed qualitatively by X-ray fluorescence for the presence of lead, as shown in Table 76.

TABLE 76

X-Ray Fluorescence Analyses of Flux ($PbCl_2$)-Grown Cobalt, Iron and Nickel Disulphides

Expt. No.	Sample	X-Ray Fluorescence Analysis (a)
350 (see Table 34)	CoS_2	Very little lead present
319 (see Table 36)	FeS_2	No lead detectable
332 (see Table 36)	FeS_2	Some lead present
342 (see Table 38)	NiS_2	Some lead present

(a) = Private communication from Mrs. D. J. Reed, Spectrochemistry Group, Mineral Sciences Division

These results were the first indication that some lead was being entrapped in the growth products. Subsequently, the level of lead was quantitatively determined by other methods of analysis, which have been recorded above.

CHARACTERISTICS OF SOME OF THE SULPHIDES

The two most successfully grown groups of sulphides covered by this report are: nickel monosulphide, and the disulphides of cobalt, iron, and nickel. Therefore, in addition to the results of the several analyses previously described herein, a brief account of three other related studies involving several of the synthetic sulphide crystals grown in this study will now be given.

(a) Electrical Measurements

The nickel monosulphide compositions, $Ni_{(1-x)}S$, where x = 0, 0.01, 0.025, have been prepared, (see Table 17), and made available for electrical studies including thermoelectric power, conductivity, Hall, and magnetic susceptibility measurements. The results have been published in various journals (36), (37), and (38). The metallic character of pentlandite, $(Fe,Ni)_9S_8$, has been published (39).

Resistivity measurements were made on two iodine-transported pyrites, Expts. #396 and #611 (see Table 31), and on one flux-grown pyrite, Expt. #438 (see Table 37). One such measurement determined the total number of electrical carriers present in the product from Expt. #396; the results indicated the equivalent of either an iron:sulphur ratio of $FeS_{1.98}$ or a maximum of 10 ppm of impurities. Realistically, the situation is assumed to be a blend of these two possibilities, i.e., the iron:sulphur ratio lies between $FeS_{1.98}$ and $FeS_{2.00}$ and the impurities lie between 0 and 10 ppm. Unfortunately, the smallness of the crystals from Expts. #438 and #611 (1-2 mm^3) precluded other planned resistivity measurements.

(b) Microhardness, Infrared Absorption, and Bond Energy Studies

Crystals of CoS_2, FeS_2, and NiS_2, obtained by the iodine vapour transport see Tables 29, 31, and 33 , and by a flux ($PbCl_2$)-growth see Tables 35, 37, and 39 , were submitted for these studies. The results of these investigations have been published (45, 46).

(c) X-ray Precession Camera Studies

This procedure gives a measure of the degree of perfection within the crystal.

Only one sample of pyrite, that from Expt. #319 (see Table 37), was submitted for such examination, and was coded as X.R.D. Single-Crystal sample No. 125. The report of this examination concluded that this sample consisted of good single-crystals of pyrite, although the actual composition was not determined.

(d) Stability of the Monosulphides at Room Temperature

Kullerud and Yund (14) reported that, while α-NiS was stored at 25°C, whether in a vacuum or in an atmosphere, it was partly inverted to β-NiS after a new months.

Some of the monosulphides made in the present study were re-analysed after specified periods of storage time, as shown in Table 77. The results showed that cobalt and iron monosulphides samples did not change during the short period of time between analyses. However, more information was obtained on the nickel monosulphides. It was apparent that α-NiS was slowly changing to β-NiS after storage times of approximately one year, and was almost all inverted after 30 months. In the two samples in which 2-3% iron was present, the inversion had not occurred during the storage time specified.

Additional re-analysis of the cobalt and iron monosulphides after longer storage-times will be necessary before their stabilities can be determined.

TABLE 77

Stability of the Monosulphides of Cobalt, Iron, and Nickel at Room Temperature

Expt. No.	Composition of the Sulphides	Analysis at time of Preparation (a)	Delayed Analysis (a)	Time Elapsed (months)	X-Ray Diffraction Report No.
823	$Co_{0.885}S$	$Co_{1-x}S$ (several)	No change	5	72-078
836	$Co_{0.95}S$	Co_9S_8 and β-$Co_{0.96}S$	No change	4	72-077
803	$Fe_{0.99}S$	Monoclinic pyrrhotite and troilite ?	No change	7	72-080
835	$FeS_{1.27}$	Orthorhombic pyrrhotite and pyrite	No change	3	72-081
597	$Ni_{1.00}S$	α-NiS	Major β-NiS Minor α-NiS	30	72-058
631	$NiS_{0.975}$	Not Analysed	α-NiS	18	71-488
			Major α-NiS Minor β-NiS	24	72-064
635	$Ni_{0.975}S$	Not Analysed	α-NiS	18	71-489
793	$Ni_{1.00}S$	α-NiS	Major α-NiS sl. Minor β-NiS	12	72-063
751	$Ni_{0.98}Fe^{57}_{0.02}S_{1.0}$	Not Analysed	Major α-NiS Trace-pyrrhotite	14	72-068
699	$Ni_{0.97}Fe_{0.03}S_{1.0}$	Not Analysed	α-NiS	13	71-532
			α-NiS	20	72-065

(a) = By X-ray diffraction analysis.

SUMMARY

During the course of the present investigation much progress has been achieved in understanding the crystal-growth problems associated with the sulphides of cobalt, iron, and nickel.

Of the twenty-two sulphides listed in Table 1, seven have been obtained as good single crystals, see Figures 15 to 24.
All of the remaining sulphides (15 compounds) were obtained, but as intimate mixtures of two or more sulphides, existing as extremely small particles or as solid solutions.

To grow these crystals, five different growth techniques were employed. Although, in a few cases, two different methods were successful, it was generally found that one procedure only would yield the desired product for a given compound.

In all cases, a future goal should be to grow larger crystals of all the sulphides listed in this report.

ACKNOWLEDGEMENTS

The author wishes to thank Mr. E. J. Murray for the many X-ray diffraction analyses performed during the course of this project.

In addition, he wishes to thank all the personnel of the Mineral Sciences Division (see Table 2) who have provided various physical analyses, those who have fed back information concerning the crystals, and those who have helped with the preparation of this report.

Dr. A. H. Webster is also thanked for many useful discussions concerning various aspects of the programme and for providing the photographs of the crystals.

The above-mentioned personnel were all members of the staff of the Mineral Sciences Division, Mines Branch, Department of Energy, Mines and Resources, at the time of their involvement with this project.

REFERENCES

1. L.G. Ripley, "Crystal Growth, Part I: Background to Crystal Growth", Mines Branch Research Report R235, (1971).
2. L.G. Ripley, "Crystal Growth, Part II: The Growth of Zinc Sulphide Crystals", Mines Branch Research Report R236, (1971).
3. "New Mineral Names", Am. Mineralogist, 55, 317, (1970).
4. T. Rosenqvist, "A Thermodynamic Study of the Iron, Cobalt, and Nickel Sulphides", Journ. Iron and Steel Inst., 176, 37, (1954).
5. N. Hansen and K. Anderko, "Constitution of Binary Alloys", 2nd Ed., Published by McGraw-Hill Book Co. Inc., New York (1958).
6. L.A. Clark and G. Kullerud, "The Sulphur-Rich Portion of the Fe-Ni-S System", Econ. Geol., 58, 853 (1963).
7. R.P. Elliott, "Constitution of Binary Alloys, First Supplement", published by McGraw-Hill Book Co., Inc., New York (1965).
8. D.D. Klemm, "Untersuchungen über die Mischkristallbildung im Dreieckdiagramm FeS_2 - CoS_2 - NiS_2 und ihre Beziehungen zum Aufbau der naturlichen 'Bravoite'", Neues Jahrb. Mineral. Monatsh., page 76, (1962).
9. D.D. Klemm, "Synthesen und Analysen in dem Dreiecksdiagrammen FeAsS - CoAsS - NiAsS und FeS_2 - CoS_2 - NiS_2", Neues Jahrb. Mineral. Abh., Band 103, 205 (1965).
10. A.J. Naldrett, J.R. Craig, and G. Kullerud, "The Central Portion of the Fe-Ni-S system and its Bearing on Pentlandite Exsolution in Iron-Nickel Sulphide Ores", Econ. Geol., 62, 826, (1967).
11. M. Uda, "The Structure of Synthetic Fe_3S_4 and the Nature of Transition to FeS", Zeitschrift für anorg. und allgemeine Chemie., Band 350, 105 (1967).
12. L.A. Taylor, "Smythite, $Fe_{3-x}S_4$, and Associated Minerals from the Silverfields Mines, Cobalt, Ontario", Am. Mineralogist, 55, 1650 (1970).

13. R.W. Shewman and L.A. Clark, "Pentlandite Phase Relations in the Fe-Ni-S System and Notes on the Monosulphide Solid Solution", Canad. Journ., Earth Sci., 7, 67 (1970).

14. G. Kullerud and R.A. Yund, "The Ni-S System and Related Minerals", Journ. Petrology, 3, Part 1, 126 (1962).

15. V.G. Kuznetsov, M.A. Sokolova, K.K. Palkina, and Z.V. Popova, "The Cobalt-Sulphur System", Inorganic Materials, 1, 617-632, (1965), Translated from Izvestiya Akademii Nauk SSSR, Neorganicheskie Materialy, 1, No. 5, pp 675-689, May 1965.

16. G. Hägg and I. Sucksdorff, "Die Kristallstruktur von Troilit und Magnetkies", Zeit. physik. Chem., B22, 444-452, (1933).

17. N. Morimoto, H. Nakazawa, K. Nishiguchi, and M. Tokonami, "Pyrrhotites: Stoichiometric Compounds with Composition $Fe_{n-1}S_n$ ($n \geq 8$)", Science, 168, 964 (1970).

18. B.J. Skinner, R.C. Erd, and F.S. Grimaldi, "Greigite, The Thio-Spinel of Iron: A New Mineral", Am. Mineralogist, 49, 543 (1964).

19. R.C. Erd, H.T. Evans Jr., and D.H. Richter, "Smythite, A New Iron Sulphide and Associated Pyrrhotite from Indiana", Am. Mineralogist, 42, 309 (1957).

20. E.T. Allen, J.L. Crenshaw, J. Johnston, and E.S. Larsen, "The Mineral Sulphides of Iron", Am. Journ. Sci., 33, No. 195, 169 (1912).

21. R.C. Weast, Editor-in-chief, "Handbook of Chemistry and Physics", 48th Ed., p. B-185, published by The Chemical Rubber Co., Cleveland, U.S.A. (1967).

22. G. Kullerud, "Thermal Stability of Pentlandite", Canad. Mineralogist, 7, 353 (1962-3).

23. J.R. Craig, "Violarite Stability Relations", Am. Mineralogist, 56, 1303 (1971).

24. B. Morris, V. Johnson, and A. Wold, "Preparation and Magnetic Properties of Cobalt Disulphide", Journ. Phys. Chem. Solids, 28, 1565 (1967).

25. P.K. Gallagher, J.B. MacChesney, and R.S. Sherwood, "Mössbauer Effect in the System $Co_{1-x}Fe_xS_2$", Journ. Chem. Phys., 50, 4417 (1969).

26. R. J. Bouchard, "The Preparation of Pyrite Solid Solutions of the Type $Fe_xCo_{1-x}S_2$, $Co_xNi_{1-x}S_2$, and $Cu_xNi_{1-x}S_2$", Mat. Res. Bull., 3, 563 (1968).

27. J. P. Gamondes and M. Laffitte, "Préparation de monocristaux de sulfure de nickel", Revue de Chimie minérale, 6, 755 (1969).

28. R. J. Bouchard, "The Preparation of Single Crystals of FeS_2, CoS_2, and NiS_2 Pyrites by Chlorine Transport", Journ. Crystal Growth, 2, 40 (1968).

29. T. Kamigaichi, T. Hihara, H. Tazaki, and E. Hirahara, "Electrical Conductivity of Iron Sulphide Single Crystals at the Temperature Range of α-transformation", Journ. Phys. Soc. Japan, 11, 606 (1956).

30. E. Hirahara and M. Murakami, "Magnetic and Electrical Anisotropies of Iron Sulphide Single Crystals", Journ. Phys. Chem. Solids, 7, 281 (1958).

31. I. Tsubokawa, "On the Magnetic Properties of Nickel Sulphide", Journ. Phys. Soc. Japan, 13, 1432 (1958).

32. K.-Th. Wilke, D. Schultze, and K. Töpfer, "Kristallisation von Disulfiden aus Schmelzlösungen", Journ. Crystal Growth, 1, 41 (1967).

33. O. Knop, C.-H. Huang, and F. W. D. Woodhams, "Chalcogenides of the Transition Elements, VII-A Mössbauer Study of Pentlandite", Am. Mineralogist, 55, 1115 (1970).

34. P. W. Bridgman, "Certain Physical Properties of Single Crystals of Tungsten, Antimony, Bismuth, Tellurium, Cadmium, Zinc, and Tin", Proc. Amer. Acad. Arts and Sci., 60, 305 (1925).

35. J. B. Mullin, R. J. Heritage, C. H. Holliday and B. W. Straughan, "Liquid Encapsulation Crystal-Pulling at High Pressure", Journ. Crystal Growth, 3 and 4, 281 (1968).

36. J. L. Horwood and M. G. Townsend, "Magnetic Susceptibility of Single-Crystal Hexagonal Nickel Sulphide", Solid-State Communications, 9, 41-43 (1971).

37. M. G. Townsend, R. J. Tremblay, J. L. Horwood, and L. G. Ripley, "Metal-Semiconductor Transition in Single-Crystal Hexagonal Nickel Sulphide", J. Phys., C: Solid State Phys., 4, 598 (1971).

38. J.L. Horwood, L.G. Ripley, M.G. Townsend and R.J. Tremblay, "Electrical and Magnetic Properties of Single-Crystal Hexagonal Nickel Sulphide", Journ. Appl. Phys., 42, 1476 (1971).

39. M.G. Townsend, J.L. Horwood, R.J. Tremblay, and L.G. Ripley, "On the Metallic Character of Co_9S_8 and $(Fe,Ni)_9S_8$", Physica Status Solidi (A) 9, K137 (1972).

40. R.S. Boorman, "Subsolidus Studies in the ZnS-FeS-FeS_2 System", Econ. Geol., 62, 614 (1967).

41. G. Delarue, "Properties chimiques dans l'eutectique LiCl-KCl fondu. II; Soufre, sulfures, sulfites, sulfates", Bull. Soc. Chem. France, 906 (1960).

42. W.M. Barnard, "Synthesis of Pyrite from Chloride-Bearing Solutions", Econ. Geol., 62, 138 (1967).

43. H.T. Evans Jr., C. Milton, E.C.T. Chao, I. Adler, C. Mead, B. Ingram, and R.A. Berner, "Valleriite and the New Iron Sulphide, Mackinawite", Article 133 in U.S. Geol. Survey Prof. Paper 475-D, pages D64-D69 (1964).

44. R.A. Berner, "Iron Sulphides Formed from Aqueous Solutions at Low Temperatures and Atmospheric Pressures", Journ. Geol., 72, 293 (1964).

45. E.H. Nickel, A.H. Gillieson and L.G. Ripley, "Microhardness, Infrared Absorption and Bond Energies of FeS_2, CoS_2 and NiS_2", Mineral Sciences Division, Report MS-PP 69-48.

46. E.H. Nickel, A.H. Webster, and L.G. Ripley, "Bond Strengths in the Disulphides of Iron, Cobalt, and Nickel", Canadian Mineralogist, 10, 773 (1969-71).

47. H. Nakazawa and N. Morimoto, "Phase Relations and Superstructures of Pyrrhotite, $Fe_{1-x}S$", Mat. Res. Bull., 6, 345 (1971).

48. D.T. Richard, "Synthesis of Smythite-Rhombohedral Fe_3S_4", Nature, 218, 356 (1968).

49. J.C. Ward, "The Structure and Properties of some Iron Sulphides", Rev. Pure and Appl. Chem., 20, 175 (1970).

50. M. J. Buerger, "The Pyrite-Marcasite Relation", Am. Mineralogist, 19, 37 (1934).

51. L. A. Taylor, "Low-Temperature Phase Relations in the Fe-S System", Annual Report of the Director, Carnegie Institution, Geophysical Laboratory, Year Book for July 1, 1968 - June 30, 1969.

52. G. Kullerud, "The Fe-Ni-S System", Annual Report of the Director, Carnegie Institution, Geophysical Laboratory, Year Book for July 1, 1962-June 30, 1963.

- - -

LGR/pg